STUDIES ON CELLULOSE ACETATE/POLY(ETHYLENE TEREPHTHALATE) BLENDS

By

Ajay Gupta

A THESIS

Submitted to
Michigan State University
in partial fulfillment of the requirements
for the degree of

MASTER OF SCIENCE

DEPARTMENT OF CHEMICAL ENGINEERING

1994

ABSTRACT

STUDIES ON CELLULOSE ACETATE/POLY(ETHYLENE TEREPHTHALATE) BLENDS

By
Ajay Gupta

Blends of Cellulose Acetate (CA) and poly(ethylene terphthalate) (PET) have been prepared and compatibilized by reactive extrusion. The effect of composition, extent of transesterification, method of extrusion and addition of plasticizer on the morphology was studied. In the first part ot the work, viscosity of unplasticized CA has been estimated to be of the order of 10^{11} Pa.s. Isothermal crystallization studies were done on CA blends with PET bottle recycle to determine optimum processing conditions. Blends of CA and glycol modified PET were compatibilized via traneseterification reaction and the extent of reaction was characterized by Soxhlet extraction and electron microscopy. Optimum particle size for impact resistance was concluded to be ~ 1 micron. Fibrillar morphology was found desirable for high tensile properties. Maximium tensile strength of 12,000 psi, tensile modulus of 0.55 Mpsi, and Izod impact strength of 1.27 ft.lb/inch were obtained.

... to my parents

ACKNOWLEDGEMENTS

I wish to thank my advisor, Dr. Ramani Narayan, for creating this project for me, for his excellent guidance and support, and for giving me the freedom to learn. I also wish to thank my colleagues, friends and staff at Composite Materials and Structures Center, Chemical Engineering Department, Department of Packaging, Electron Optics Center and Michigan Biotechnology Institute for helping me in their own ways and for making my stay at MSU rewarding and enjoyable.

TABLE OF CONTENTS

LIST OF TABLES

LIST OF FIGURES

ABBREVIATIONS

CA	Cellulose Acetate.
DEP	Diethyl pthalate.
DMA	Dynamic mechanical analysis.
DMAP	4-dimethylaminopyridine.
DS	Degree of substitution.
DSC	Differential scanning calorimetry.
EKX	"Transpet EKX-105" grade glycol modified PET.
FTIR	Fourier transform infra-red.
PET	Poly(ethylene terephthalate).
rpm	Revolutions per minute.
SEM	Scanning electron microscope.
St. Oc.	Stannous 2-ethyl hexanoate.
TEM	Transmission electron microscope.
TGA	Thermo-gravimetric analysis.
$TiBuO_4$	Titanium Butoxide.

Introduction

The large increase in the consumption of plastics in the past few decades has resulted in a dramatic solid waste problem. The plastic waste in the municipal solid waste (MSW) is projected to be 9.8% by the year 2000 from 7.2% in 1987 which was about 50% of the total plastics sold in the U.S. (Michigan DNR, 1987) Out of this plastic waste stream, it is estimated that only about 1% is recycled [Narayan, 1990]. This has brought about severe shortage of landfill sites and pollution. In 1988, 180 million tons of MSW was produced out of which 70% was landfilled. Two thirds of the usable landfill sites in the U.S. have closed in the last 11 years and one third of the remainder will close by 1995 (Recycling Source Book, 1993). Since recycling is still quite expensive, there is an increasing interest in the use of renewable resources to make plastic materials. The main reasons for this interest are [Narayan, 1991]:

- Environmental Concerns.
- Alternate feedstocks to non-renewable imported petroleum feedstocks.
- The need to utilize the nation's abundant agricultural feedstocks.
- Legislation and public opinion.

Natural polymers such as starch, polyhydroxy butyrate valerate and cellulose and their derivatives such as poly(lactic acid), cellulose acetate, cellulose propionate etc are

being increasingly used as a replacement (partially or in full) for synthetic polymers derived from petroleum. Moreover, these polymers have the advantage that they are chemically or biologically degradable and thus can be recycled back to earth instead of being reused in low grade applications.

These natural polymers are relatively more difficult to process and may be more expensive than synthetic polymers. Therefore, it is of interest to find new methods of modifying these materials to make them easier to process and improve the properties.

At the same time, new applications are being sought for the reclaimed polymers for which the demand is outstripped by the supply. Very often, it is not possible to clean and purify the collected plastic waste products and they have be utilized in lower grade uses rather than being used in the original application.

Blending of two or more polymers to make a material with desirable properties is becoming increasingly popular. Alloys and blends represent inexpensive routes to satisfy both end-user requirements and suppliers desires for product differentiation. Tailoring of properties, the use of existing equipment and the low cost of developing of new products have made polymer blends demand outstrip that for engineering base polymers.

This thesis deals with the study of a renewable polymer, Cellulose Acetate and it's blends with a synthetic polymer, poly(ethylene terephthalate) to create a new material with superior properties that could possibly be commercially viable as an engineering grade composite.

Terminology

Many of the terms used in the field of polymer blends have subtle differences in the implied meaning of the terms. The following is the description of some of the terms used in this text:

- Polymer blend: A mixture of two or more polymers. This is different from a block or graft copolymer in the sense that there are no chemical bonds between the polymers.
- Polymer alloy: A blend with properties superior than the component polymers.
- Miscible blend: A blend which forms a single thermodynamically compatible phase.
- Immiscible blend: A polymer blend in which the component polymers exist as distinct phases.
- Compatible polymers: The term "compatibility" is used for polymers when a desired or beneficial result occurs when they are mixed. It does not imply miscibility or immiscibility.
- Compatibilized blend: An immiscible polymer blend which has been compatibilized by some method such as surface modification, grafting, addition of a compatibilizing agent etc.
- Polymer composite: A combination of a polymer with a reinforcing agent or a filler.

Structure of the thesis: Problems and Solutions

Cellulose Acetate (CA) is a derivative of the natural polymer cellulose in which some or all the hydroxyl groups are replaced with acetate groups to reduce hydrogen bonding and make the polymer easier to process. However even with this chemical modification, it is necessary to use a plasticizer to aid in processing. The plasticizers used impart qualities like clarity and impact resistance but result in a decrease in strength and modulus. Also, the plasticizers that are being currently used are low molecular weight plasticizers, which have a tendency to leach out with time and leave behind a brittle polymer. It was sought to avoid the use of a monomeric plasticizer by blending CA with a synthetic polymer which could act as a processing aid. The polymer selected to blend with CA was poly(ethylene terephthalate) (PET) which is widely used in consumer product such as bottles, fibers, films etc. and thus large quantities of post-consumer wastes are being collected and is available in the market at prices much lower than that of virgin PET. Other reasons for selecting PET were:

- Due to it's high crystallinity, it could probably act as a reinforcing phase for the amorphous CA matrix.
- Low melt viscosity as compared to unplasticized CA.
- The presence of ester groups in the backbone presented an opportunity to compatibilize the blend easily via a trans-esterification reaction.
- Hydrogen bonding between CA and PET could help in compatibilizing the blend.

A description of all the materials used for this work is given in Chapter 3.

Most mixtures of polymers are not miscible [Paul, 1978 (a)]. Indeed, incompatibility is it often desirable as provides the opportunity to achieve a synergistic combination of properties in which the properties of the blend are superior to the properties of the component homopolymers. To achieve this effect it is necessary to control the morphology of the blend. It is also necessary to compatibilize the blend so as to reduce interfacial tension between the phases. Both these issues were investigated in this thesis.

The most important factors in controlling the morphology of a blend are viscosity and volume ratios, processing conditions, compatibilization etc. Since CA has always been processed with a monomeric plasticizer, available literature on the viscosity and properties of CA do not contain data on unplasticized CA. To study the blend of CA and PET, it was necessary to know the viscosity of unplasticized CA. This proved to be a challenging problem as the viscosity of unplasticized CA could not be measured by conventional methods. Chapter 6 is devoted to the estimation of viscosity of unplasticized CA.

The next step was to blend CA and PET without any effort at compatibilization. Chapter 4 describes the method of preparing the blends. Extrusion was the process of choice because the operations of melting, mixing, compatibilization and processing can be integrated in one step. Chapter 5 discusses in detail the methods and instruments used for the characterization of the blends. Chapter 7 contains data, results and discussion for the uncompatibilized CA/PET blends. An effort has also been made to compare the values for modulus and strength obtained to various theoretical models in order to

evaluate the scope for further improvement through better control of morphology and/or compatibilization.

Chapter 7 also contains a section on crystallization kinetics of CA/PET blends. This was found necessary as processing of CA/PET blends was difficult due to the crystallization of PET in the extruder. Isothermal crystallization kinetics were studied in order to better understand and solve the problem.

By blending CA with PET, large improvements in strength and modulus were obtained. These compared well with theoretical predictions for a compatibilized blend. However, low impact strength and morphological studies suggested that better adhesion could result in better properties.

The presence of ester groups in both CA and PET offered the possibility of modifying the polymers via a transesterifiaction reaction. It was sought to catalyze this reaction during the extrusion process to provide an "in situ" compatibilizer. Reactive extrusion in a single or twin-screw extruder is an economical method to produce and process polymer blends. Various catalysts were investigated and the extent of the reaction was characterized by solvent extraction. The trans-esterification reaction and the results for the compatibilized blends are presented and discussed in Chapter 8.

To study the effect of viscosity and volume ratios on the morphology of the blend, a novel method was investigated. Instead of using polymers of different molecular weights to vary the viscosity of the polymers in the blends as has been traditionally done, the viscosity of CA and PET was varied by using as plasticizer which was compatible with both the polymers. A redistribution of the plasticizer between the two phases

occurred and the glass transition temperature was used as the measure of plasticizer in the phase. This viscosity of the phase could thus be calculated. The results of the study are described and discussed in Chapter 9.

Finally, Chapter 10 contains the conclusions from the thesis and some recommendation for further work.

The background and literature survey for each topic has been presented as it has come up in the thesis. However, Chapter 2 contains some background on the subjects of polymer blends, their thermodynamics, morphology and rheology, reactive extrusion, compatibilization and viscoelasticity so as to give an overview of the field of polymer blends and the goals that have been sought to accomplish by this work.

Background

2.1 Polymer Blends

Polymer blends are finding increased acceptance by the industry due to many advantages over component homopolymers. Alloys and blends represent fast and inexpensive routes to satisfy both end-user requirements and suppliers' desires for product differentiation. Tailoring of properties, the use of existing equipment and the low cost of developing of new products have made polymer blends demand outstrip that for engineering base polymers. Some other advantages that may be obtained by blending are [Kulshreshtha, 1993].

- Extending the performance of expensive resins.
- Reuse of plastic scrap.
- Increase in toughness, flame retardance, modulus, crack resistance etc.
- Improved dimensional stability, processibility and ozone resistance.

Polymer blends may be miscible, partially miscible or immiscible. The miscible and partially miscible blends are characterized by a single glass transition temperature, exhibit homogeneity under magnification in an electron or phase contrast microscope and have physical properties intermediate between those of blend components. Films of

miscible blends tend to be transparent. However films of immiscible polymer blends can also be transparent if the components have the same refractive index, form a two layered film or the phase size of one of the phases is smaller than the wavelength of light [Paul, 1978 (a)].

Blends of immiscible polymers have a high interfacial tension and poor adhesion between the two phases. This interfacial tension contributes to higher viscosities, difficulty in imparting desired degree of dispersion to random mixtures and to their subsequent lack of stability to phase separation during use. However, sometimes immiscibility is desirable to achieve a synergistic combination of the two polymers to form a polymer alloy.

The miscibility or immiscibility of two polymers is dictated by the thermodyanmics of the mixture. The free energy of mixing ΔG_{mix} is given by

$$\Delta G_{mix} = \Delta H_{mix} - T\Delta S_{mix} \qquad (2.1)$$

This quantity, consisting of enthalpic (ΔH) and entropic (ΔS) parts, is a function of composition and temperature T. For miscibility, ΔG_{mix} must be negative. Because of the small number of moles of each polymer in the blend, the entropy of mixing is very small and so for most of the polymer blends, the free energy of mixing is positive. Specific interactions, like hydrogen bonding, dipole-dipole interactions or intramolecular repulsion effects can also lead to some degree of miscibility. This may explain the partial miscibility among hologenated polymers and those containing oxygen (e.g. ester groups) [Paul, 1978 (a)].

Polymer blends are currently formulated by many methods including solvent

casting, extrusion in a single or twin screw extruder etc. Reactive extrusion in a single or twin-screw extruder is an economical method to produce and process polymer blends as the operations of melting, mixing, compatibilization and processing can be integrated in one step.

2.2 Blend Morphology

Blends of immiscible polymers can be organized into a variety of morphologies. The properties and therefore the subsequent use of an immiscible blend are strongly dependent on this arrangement of the two phases. If one phase is dispersed in another, the matrix component dominates the properties. A parallel arrangement as in fiber composites allow both the phases to contribute to the mechanical properties. Both phases can be continuous to form an "interpenetrating network". These structures are structurally isotropic and adhesion between the two phases is not as critical as in the other morphologies. The advantage of having a two phase structure over a homogenous structure is that the two phases can combine synergistically to give mechanical properties which are greater than those of the homopolymers. Unique properties may be imparted to the blend by the control of rheological factors during the processing of the blend. [Paul, 1978 (a)]. The effect of processing parameters, rheology, volume fractions etc. on the morphology of the blend and the effect of morphology on the properties of the blend have been investigated by a number of authors [Kuleznev, 1978; Utracki, 1991; Favis, 1991; Willis, 1991; Tsebrenko, 1984]. Tanaka [Tanaka, 1992] has investigated

the effect of trans-esterification reaction on the morphology of binary blends of polyesters.

Under the appropriate flow fields and viscoelastic conditions, droplets of the dispersed phase deform and break up as shown in Figure 2.1 [Han, 1981; Torza, 1972].

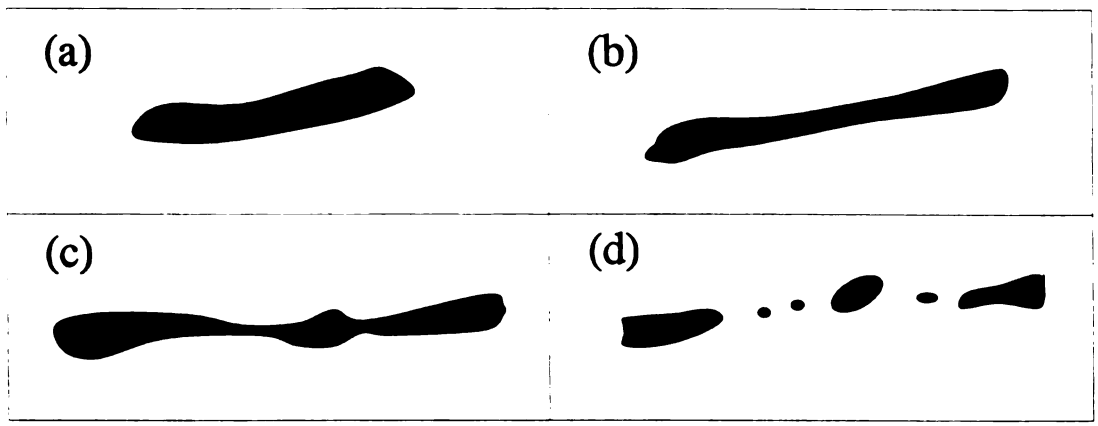

Figure 2.1: Droplet deformation and break-up in shear flow field.

Taylor [Taylor, 1934] was the first to study droplet breakup in Newtonian fluids. Rumscheidt & Mason [Rumscheidt, 1961] studied the deformation of newtonian droplets over a wide range of viscosity ratios in uniform shear flow and hyperbolic flow. Two phase flow in nonuniform shear flow (poiseuille flow) has also been investigated [Goldsmith, 1962; Gauthier, 1971; Chaffey 1965; Hetsroni, 1972]. However, polymers exhibit viscoelastic behavior specially at high shear rates. According to Van Oene, the component with the larger normal stress function will form droplets in the other component, and difference in viscosity, shear rate (or shear stress), extrusion temperature and residence time spent in mixing influence only the homogeneity of the dispersion and not the mode of dispersion [Van Oene, 1972]. Tavgac [Tavgac, 1972] studied the effect

of fluid elasticity on the extent of the deformation of the droplets in uniform shear and extensional flow fields. Lee noted that the deformation of viscoelastic droplets in hyperbolic flow appears to be the same as that of Newtonian droplets having a viscosity equal to the zero-shear viscosity of the viscoelastic droplet [Lee, 1972].

2.3 Compatibilization

Ideally, two or more polymers may be blended together to form a wide variety blends with desired morphologies and properties. But most polymers are thermodynamically immiscible and do not give a homogeneous product upon blending. However in many cases it is desirable to have a two phase morphology, for example, the rubber microphase in polystyrene acts as inhibitors to crack propagation and thus increase the impact strength of polystyrene. In such cases property enhancement is achieved by the synergy of the two phases to give "alloys" rather than simple blends with properties in between those of the homopolymers. However, the high interfacial tension and poor adhesion between the phases would be undesirable. High interfacial tension results in high viscosities, phase separation and poor dispersion while processing of the blend. Poor adhesion may lead to very weak and brittle mechanical behavior and may make the generation of highly structures morphologies (in coextrusion, fibers etc.) impossible. Thus it is highly desirable to add a "compatibilizer" (interfacial agents) which can alleviate to some degree the problems mentioned above [Paul, 1978 (a)].

Compatibilization is accomplished generally by two routes:

1. Addition of a third ingredient as a co-compatibilizing agent. Block or graft copolymers are often chosen as compatibilizing agents and may be added as a third component or be produced "in situ" through reactive blending.
2. By modification of the matrix, or dispersed phase, or both to form a co-reactive alloy. The co-reactive technique is, for instance, used for toughening of nylon through reaction of amine end groups of nylon with anhydride grafted modifier. Some of the other modified polymers which have been used in such co-reactive alloys are isocynate terminated polycaprolactone, oxazoline functionalized polystyrene, acrylic acid functionalized polyethylene etc [Curry, 1990].

The addition of a compatibilizer can be expected to (1) reduce the interfacial tension between the phases, (2) permit finer dispersion during mixing, (3) decrease the tendency of phase separation and (4) improve interfacial adhesion. These factors usually result in an increase in mechanical properties such as impact strength, ductility, toughness, dimensional stability and thus these properties can also be used as an indirect measure of compatibilization. Direct methods to monitor the extent of interfacial activity or reaction would be FTIR spectroscopy, NMR, separation of phases by extraction, electron microcopy etc.

2.4 Reactive Extrusion

Reactive extrusion is the use of chemical reactions during polymer extrusion to form desired products. Free radical initiators, cross-linking agents and other reactive additives can be injected into the extruder to cause these reactions [Cheung, 1990] Reactive extrusion has been receiving considerable attention as a commercial process because of the following advantages [Hyun, 1988]:

1. The extruder takes advantage of the high viscosity to transfer through drag flow.
2. The extruder allows for good control of the reaction temperature.
3. The improved surface/volume ratio leads to higher reaction rates throughout the entire extruder channel.
4. Reactive extrusion can eliminate several solidification-remelting stages, resulting in significant economic advantages as well as minimizing polymer degradation during processing. Even ultra-high molecular weight polymers can be processed by an extruder.

The use of twin screw extruders for reactively compatibilizing polymer blends is arguably the most economical means of polymer blend processing as it integrates the operations of melting, mixing, compatibilization and processing in one step.

The extruder being used for reactive extrusion should have the following characteristics [Tucker, 1987]:

1. Good temperature control for the barrel, preferably fluid heated barrels for uniform heat distribution. The barrel temperature will influence specific energy consumption to some extent, and shear stress at the wall of the extruder bore.

2. Good distributive mixing at low shear rates. Thermal homogeneity in the melt must be maintained by continual distributive mixing, because the low thermal conductivity of polymers in general permits large temperature gradients to exist in the absence of good mixing. Distributive mixing also brings the compatibilizer in contact with the phase boundary.
3. Screws designed to give good dispersive mixing. This refers to the reduction in domain size of the dispersed phase (for immiscible polymers). This type of mixing is directly related to the shear stress applied to the polymer and material properties of the blend components.
4. Convenient and accurate feeding of the raw materials, compatibilizing agents, low molecular weight additives etc. It may be necessary to keep the polymer(s) dry before feeding or one or more of them may need to be fed at some distance downstream from the first feed port.
5. Venting ports may be necessary to remove byproducts of the reaction or for maintaining an inert atmosphere inside the barrel.

The reactions that are usually carried out in extruders are [Tucker, 1987]:

1. Controlled degradation: This is done by exposing the polymer to high temperatures, shear and usually a free radical generator such as oxygen or an organic peroxide. Narrow molecular weight distribution and high concentration of reactive sites for grafting can be achieved by this method. This type of reaction is generally carried out on polyolefins.

2. In-situ polymerization: This includes both addition and condensation reactions. Reactions requiring high residence times may not be possible by this method. Examples of commercially viable in-situ extrusion processes are production of polyurethane elastomers, the condensation reaction of polyether imides, and the anionic polymerization of nylon 6 from caprolactum.

3. Graft reactions: Graft reactions can be used to make two-phase dispersion products in which grafting is done to promote better mechanical properties, for instance, a rubber phase dispersed in a brittle thermoplastic and modified polymer products with the grafting of monomers or additives onto the polymer backbone. Polyolefins are often modified with maleic anhydride, acrylic acid, methacrylic acid etc. to improve mechanical properties and to promote adhesion to non-polymer surfaces such as glass, ink and fillers. Halogenation of butyl rubber is done to enhance chemical resistance and improve mechanical properties.

4. Functionalization: Functionalization of end groups in polymers usually provides improved chemical or thermal stability, mechanical and optical properties and may alter the morphology of the material. For example, ethylene-acrylic acid ionomer is modified with an amine to improve mechanical and optical properties in thick extruded sheets used as glazing laminates.

Shear Rate in Extruder

In the extruder, the materials are subjected to complex shear and elongational deformations and complex temperature profiles along the various cross-sections of the extruder barrel.. Therefore, it is difficult to characterize the type and magnitude of the strain rate in the extruder by a single number [Wu, 1987]. However, an effective strain rate may be determined and used as a crude but convenient parameter. The shear rate in a co-rotating twin screw extruder has been analyzed by Burkhardt and coworkers [Burkhardt, 1978]. The shear rates usually encountered in twin screw extruders are of the order of a few hundred s^{-1}. For this work, an arbitrary value of 100 rad/s has been chosen for all calculations as this was the highest rate at which viscosity could be measured conveniently. Since a constant screw speed was used throughout this work, any error in using this shear rate would only cause a systematic error.

2.5 Viscoelastic properties

In viscoelastic studies of polymeric materials the method of sinusoidal excitation and response is very useful. In this case the applied force and the resulting deformation both vary sinusoidally with time, the rate being specified by the frequency in cycles/second. For linear viscoelastic behavior, the strain is out of phase with the stress. This results from the time necessary for molecular rearrangements and is associated with relaxing phenomena.

The stress σ and the strain ϵ can be expressed as follows :

$$\sigma = \sigma_o \sin(\omega t + \delta) \tag{2.2}$$

$$\epsilon = \epsilon_o \sin(\omega t) \tag{2.3}$$

where ω is the angular frequency and δ is the phase angle. Then

$$\sigma = \sigma_o \sin(\omega t)\cos\delta + \sigma_o \cos(\omega t)\sin\delta \tag{2.4}$$

The stresses can be considered to consist of two components, one in phase with the strain ($\sigma_o \cos \delta$) and the other 90° out of phase ($\sigma_o \sin \delta$). When these are divided by the strain, we can separate the modulus into an in-phase (real) and out-of-phase (imaginary) component. These relationships are

$$\sigma = \epsilon_o E' \sin(\omega t) + \epsilon_o E'' \cos(\omega t) \tag{2.5}$$

$$E' = \frac{\sigma_o}{\epsilon_o}\cos\delta \quad \textit{and} \quad E'' = \frac{\sigma_o}{\epsilon_o}\sin\delta \tag{2.6}$$

where E' is the real part of the modulus and E'' is the imaginary part. The complex representation of the modulus can be expressed as :

$$E^* = E' + iE'' \tag{2.7}$$

For the other deformation types, for example, the ratio of the peak stress to peak strain for shear, the relationships are similar

$$|G^*| = G'^2 + G''^2 \tag{2.8}$$

where G^* is the shear complex modulus, G' is the real part, also called the storage

modulus and G'' the imaginary part, also called the loss modulus. The storage modulus is related to the storage of energy as potential energy and its release in the periodic deformation. The loss modulus is associated with the dissipation of energy as heat when the material is deformed. The phase angle δ is given by

$$\tan\delta = \frac{G''}{G'} \qquad (2.9)$$

The loss tangent *tan* δ is called internal friction or damping, and is the ratio of energy dissipated per cycle to the maximum potential energy stored during the cycle.

The Cox-Merz rule allows a direct correlation to be made between the steady shear viscosity and the complex viscosity. The two viscosities are equal when the shear rate (in reciprocal seconds) equals the frequency (in radians/second).

Materials

3.1 Poly(ethylene terephthalate)

PET or poly(oxyethylene oxy terephthaloyl) is a thermoplastic polyester produced by melt condensation polymerization from terephthalic acid or dimethyl terephthalate and ethylene glycol [Figure 3.1].

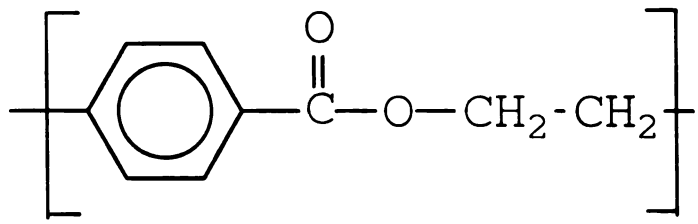

Figure 3.1: Poly(Ethylene Terephthalate).

The ester (-COO-) link influences the properties of the polymer in the following ways [Brydson, 1989, pp 653-654]:

1 It is, chemically, a point of weakness being susceptible to hydrolysis, ammonolysis and ester interchange, the first two reactions leading to chain scission. In some cases the reactivity is influenced by the nature of the adjacent groupings.

2 As a polar group it can adversely affect high frequency electrical insulation properties.

3 The polar ester group may act as a proton acceptor allowing interactions with other grouping either of an inter- or an intramolecular nature.

4 The ester link appears to enhance chain flexibility of an otherwise polymethylenic chain. At the same time it generally increases interchain interactions and in terms of the effects on melting points and rigidity the effects appear largely self-cancelling.

Engineering grade PET resins have excellent melt flow characteristics and close mold tolerances. PET is hygroscopic and to prevent excessive hydrolysis while processing, the moisture content of the resin entering the machine should not be more than 0.02%. To achieve maximum crystallinity, high surface gloss and minimize warpage, the mold temperature should be high (210°F-250°F) [Modern Plastics Encyclopedia, 1990]. PET copolyesters are available with slower rates of crystallization, lower T_m and T_g, which permit a broader range of processing conditions. The use of isopthalic acid as a partial replacement for terephthalic acid also retards crystallinity and this has been used commercially with 1,4-cyclohexylene glycol instead of ethylene glycol [Brydson, 1989, pp 680]. Use of higher homologous component instead of ethylene glycol also reduced the melting points of the polymer e.g. PBT has a melting point of 224°C. PET has wide applications in automotive parts, electrical/electronic components, small appliances, bottles, furniture etc.

3.1.1 PET bottle regrind

The used blow molded PET bottles are sorted, ground and cleaned for a variety of end uses such as fiberfill for pillows and sleeping bags, carpet fiber, injection molded parts, and film and sheet. Eastman Kodak and Wellman are the major suppliers of PET recyclate in the U.S. Some data for PET bottle regrind is given in Table 3.1.

Table 3.1: Data for PET bottle regrind.

Molecular weight		M_w ~ 40,000
Density (unoriented crystalline polymer)		~1.45 g/cm^3
Glass transition temperature		T_g = 78°C
Melting Temperature		T_m ~ 249°C
Enthalpy of Melting		H_m = 51.43 J/g
Maximum rate of crystallization - at		125°C
Solubility parameter [Brandrup, 1989]		21.7 - 22.7(MPa)$^{1/2}$
Cost (bulk)	recycled flake	$0.36-$0.40/lb
	pelletized	$0.44-$0.50/lb
	plant scrap	$0.40-$0.45/lb

3.1.2 Transpet "EKX"-105

EKX grade of PET is a copolymer of PET and neo-pentyl glycol (2,2 Dimethyl -1,3 propanediol), was supplied by Hoechst Celanese in pellet form. The inclusion of neo-pentyl glycol in the polymer backbone reduces the rate and extent of crystallinity permitting the use of a broader range of processing conditions. The molded parts are clear and can be used in cosmetic applications such as bottles, vials, toothbrushes and

display boards. EKX can be sterilized by gamma radiation and has medical applications such as tubing, bottles etc. EKX is also currently being thermoformed into trays. Table 3.2 lists some data for EKX.

Table 3.2: Data for EKX-105 grade PET.

Molecular weight	$M_w \sim 50{,}000$
Density	1.30 gm/cm^3
Glass transition temperature	$T_g = 78.5°C$
Melting temperature	$T_m = 220°C$
Enthalpy of melting	$H_m = 17.8$ J/g
Maximum rate of crystallization - at	159°C
Solubility parameter [Brandrup, 1989]	21.7 - 22.7(MPa)$^{1/2}$
Cost (bulk)	\$1.05/lb

3.2 Cellulose Acetate

Cellulose Acetate is derived by chemical modifying Cellulose (a polysaccharide consisting of β-D-glucopyronosyl units). Due to strong hydrogen bonding of hydroxy groups, cellulose is not thermoplastic. Replacing hydroxyl groups with acetate groups reduces the hydrogen bonding, increases the interchain separation and makes the polymer less polar [Brydson, 1989]. The number of acetate groups per anhydroglucose unit is called the degree of substitution (DS). The CA unit has got a $^4C_1$ chair configuration with maximum number of groups in the equatorial plane (Figure 3.2). The C(3) carbon is less reactive, perhaps due to Hydrogen bonding with O(5) pyranose ring atom.

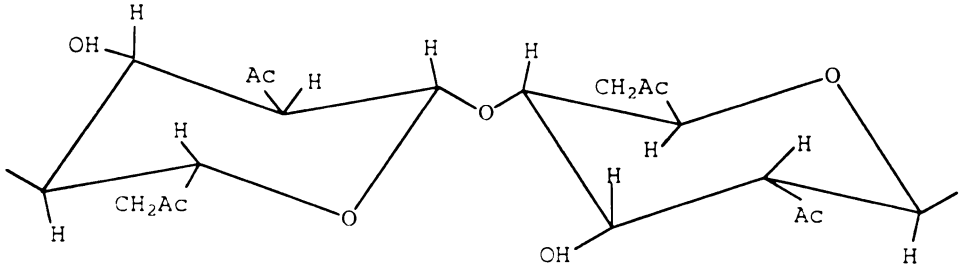

Figure 3.2: Dimer of CA (DS = 2).

Steric hindrance by a substituent already attached to the C(2) position may also play a role towards the subdued reactivity [Bikales, 1971]. CA has the advantage that it is derived from a renewable resource (cellulose) obtained from wood pulp or cotton linters.

The processibility of pure CA is poor and plasticizers such as dioctyl pthalate or diethyl pthalate are generally used. Plasticized CA has got excellent clarity, high gloss, colorability, machinability, toughness and hardness. For molding and extrusion, CA with 19%-37% plasticizer is used (flow grades "H5" to "S"). Figure 3.1 shows the flow designation of commercially available CA formulations.

CA is widely used in tool handles, playing cards, optical applications-opthalmic frames and face shields, cosmetic and personal care items, tubing, store fixtures and displays, sporting goods, writing instruments, sheeting and furniture profiles, extruded tape, audio tape, and electrical items.

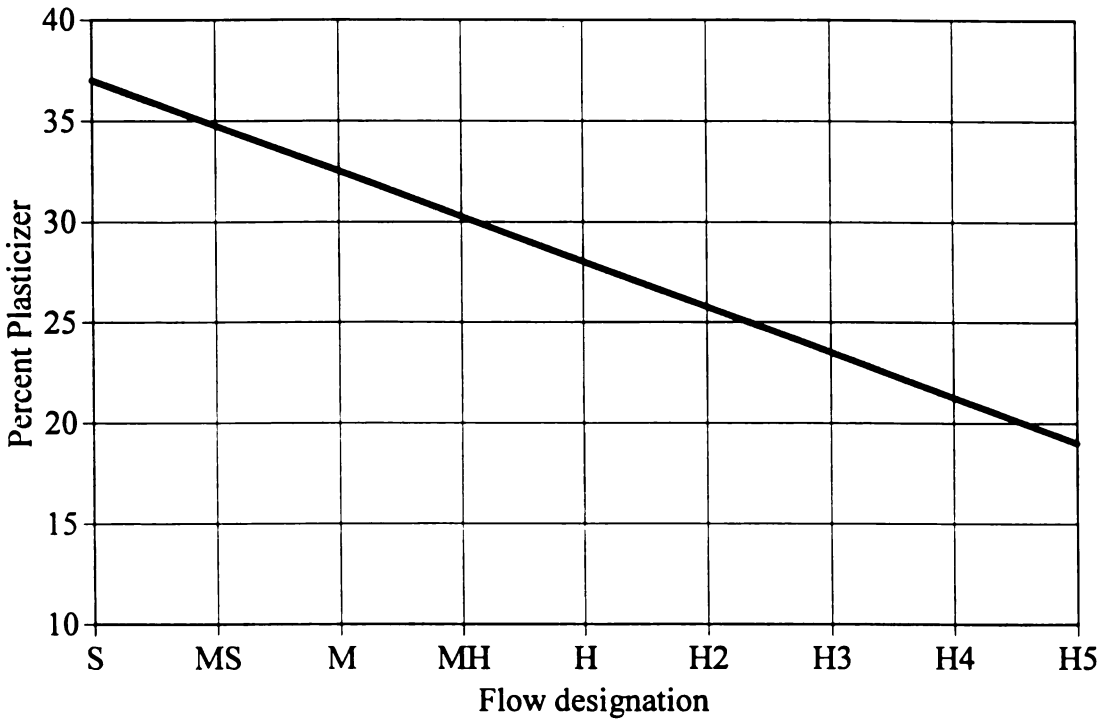

Figure 3.3: Flow designation of CA/plasticizer formulations.

CA (unplasticized) grade JLF-68 was supplied by Hoechst Celanese in flake form. Plasticized CA samples (made from JLF-68) were supplied by Rotuba Extruders in pellet form. Table 3.3 gives some data for CA.

Table 3.3: Data for CA.

Molecular weight		M_w = 55,100 M_n = 11,800
Density		1.30 g/cm^3
Degree of substitution		2.45
Glass transition temperature		T_g = 191.5°C
Melting temperature		T_m = 230°C
Enthalpy of melting		H_m = 12.1 J/g
Maximum rate of crystallization - at		
Solubility parameter [Brandrup, 1989]		22.7-26.0 (MPa)$^{1/2}$
Cost (bulk)	CA flakes	$1.35/lb
	plasticized CA	$1.3-$1.5/lb

3.3 Catalysts

Catalysts were used to catalyze the trans-esterification reaction between the ester groups of PET and CA. Tin and Titanium compounds are increasingly used as trans-esterification catalysts. The Tin-Carbon bond is quite stable to heat. Also, the Tin-Carbon bond does not add to the carbonyl group, nor does it react with alcohols. Triorganotins and tetraorganotins are toxic, specially the lower triorganotin compounds. Diorganotin compounds are substantially less toxic than the analogous triorganotins. Mono-organotins compounds present no special toxological problems. In general, they show decreasing toxicity with increasing alkyl chain length, but of lower order of toxicity than diorganotins [Kirk-Othmer, 1983 (pg 52-57)].

3.3.1 Dibutyltin dilaurate

$[CH_3(CH_2)_{10}CO_2]_2Sn[(CH_2)_3CH_3]_2$ (CAS # 77-58-7) FW = 631.83

Dibutyltin dilaurate (FASCAT 4202, Atochem) is an off-yellow liquid. Diorganotins are often used as trans-esterification catalyst at 200°C - 230°C. Dibutyltin dilaurate is used for polycondensation of dimethyl terephthalate to PET. It has been used as a catalyst for reaction injection molding of poly(urethane-urea)s [Ryan, 1991]. It is also used as a stabilizer for PVC to prevent degradation by heat and sunlight. [Kirk-Othmer, 1983, pg 64]. It has a tin content of 18.8 % by weight (elemental analysis).

3.3.2 4-Dimethylaminopyridine

$[C_7H_{10}N_2]$ (CAS # 1122-58-3) FW = 122.17

DMAP (Aldrich Chemical Company) is a widely used and versatile catalyst. It is a colorless, crystalline solid with a melting point of 114°C. It is a highly efficient catalyst for a variety of acylation reaction and is many times used on an industrial scale.

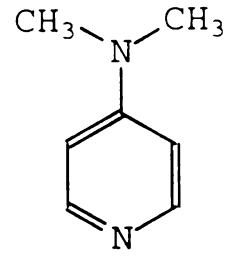

Figure 3.4: DMAP molecule.

3.3.3 Dibutyltin oxide

$[Sn[(CH_2)_3CH_3]_2O]$ (CAS # 818-08-6) FW = 248.92

Dibutyltin oxide (FASCAT 4201, Atochem) is an infusible and insoluble solid. This catalyst is used at 220°C - 240°C. It has a tin content of 47.7 % by weight (elemental analysis).

3.3.4 Stannous 2-ethylhexanoate

$[C_{16}H_{30}O_4Sn]$ (CAS # 301-10-0) FW = 405.1

Stannous 2-ethylhexanoate (SIGMA Chemical Company), sometimes referred to as stannous octanoate is a clear, very light yellow and somewhat viscous liquid. The primary use of stannous octanoate is as a catalyst with certain amines for the manufacture of polyester urethane foams. Other industrial applications include its use as a catalyst in silicones, including room temperature vulcanizing, silicone rubbers and silicone-oil emulsions, in epoxy formulations and in various urethane coatings and sealants [Kirk-Othmer, 983, pg 68]. it has a tin content of 29.3 % by weight (elemental analysis).

3.3.5 Titanium(IV) Butoxide

$[Ti[O(CH_2)_3CH_3]_4]$ (CAS # 5593-70-4) FW = 340.36

Titanium Butoxide (Aldrich Chemical company) is a colorless combustible liquid. Titanium Butoxide has been used to catalyze trans-esterification reaction of Polycarbonate and PET at 275°C [Pilati, 1984] where some discoloration and gas evolution were observed due to side reactions. Titaniun Butoxide has a Titanium content of 14.7% by weight (elemental analysis).

3.4 Plasticizer

Plasticizers are additives that soften and flexibilize rigid polymer chains. Processing temperature is lowered by a reduction in glass transition temperature and due to internal lubrication. To study the morphology of CA/EKX blends as a function of volume fraction and viscosity, it is found convenient to vary the viscosity of both CA and EKX by adding a plasticizer which is distributed between the two phases during extrusion. The samples of CA supplied by Rotuba extruders were plasticized by diethyl pthalate (DEP). DEP was also found compatible with EKX (only one T_g was observed for EKX/DEP blends). Table 3.4 shows some data for DEP.

Table 3.4: Data for DEP.

Melting Point	-3°C
Boiling Point	298°C
Glass transition temperature	~ - 65°C
Density	1.118 gm/cm^3
Solubility index [Brandrup, 1989]	20.5 (MPa)$^{1/2}$
Cost (bulk)	$0.76/lb

Blend Preparation

Preparation of blends in the twin screw extruder was the first step in the experimental protocol. The raw materials - Cellulose Acetate and PET had to be of the right particle size before they could be fed to the extruder. Where necessary, they had to be mixed with catalysts, plasticizer etc. before being fed to the extruder. In many experiments, the plasticizer was fed to the extruder directly with a syringe along with the CA/PET feed. The extrudate was collected and further processed by compression molding or injection molding for further characterization. Figure 4.1 shows the main steps involved in the experimental procedure followed.

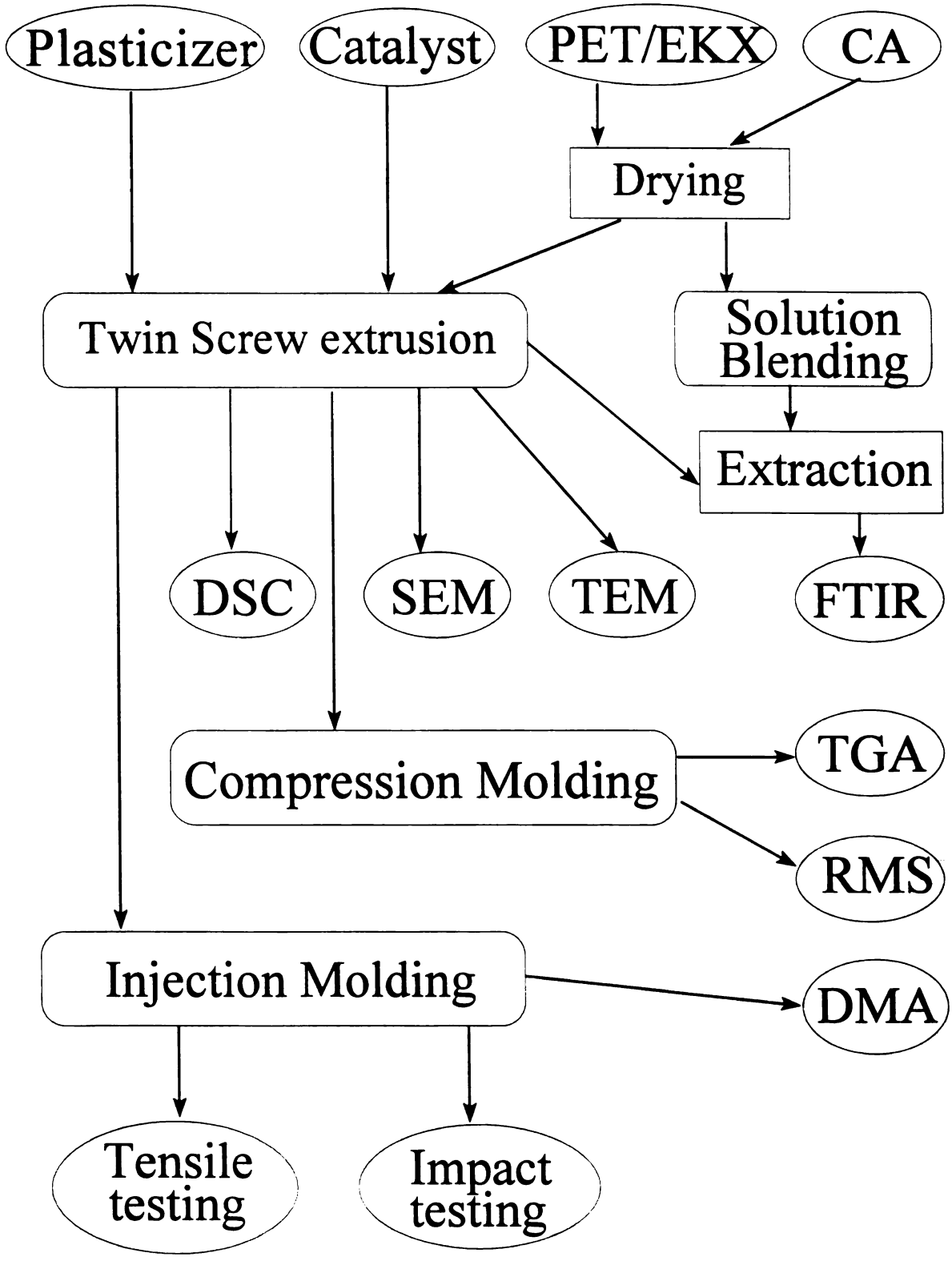

Figure 4.1: Experimental Procedure

4.1 Grinding and Sieving

Before processing and drying of the raw materials and blends, it was found necessary to grind/sieve the blend components. The extruder that was used had only one feeder and having the blend components of about the same particle size helped in proper feeding and mixing of the blend in the proper ratio. The larger pellets were transported faster than the fine particles and so the feed to the extruder was not homogenous. Besides, not all the fine particles were fed because of the design of the feeder. Drying was also more efficient after grinding. Figure 4.2 shows the feed rates obtained with the feeder for "EKX" pellets.

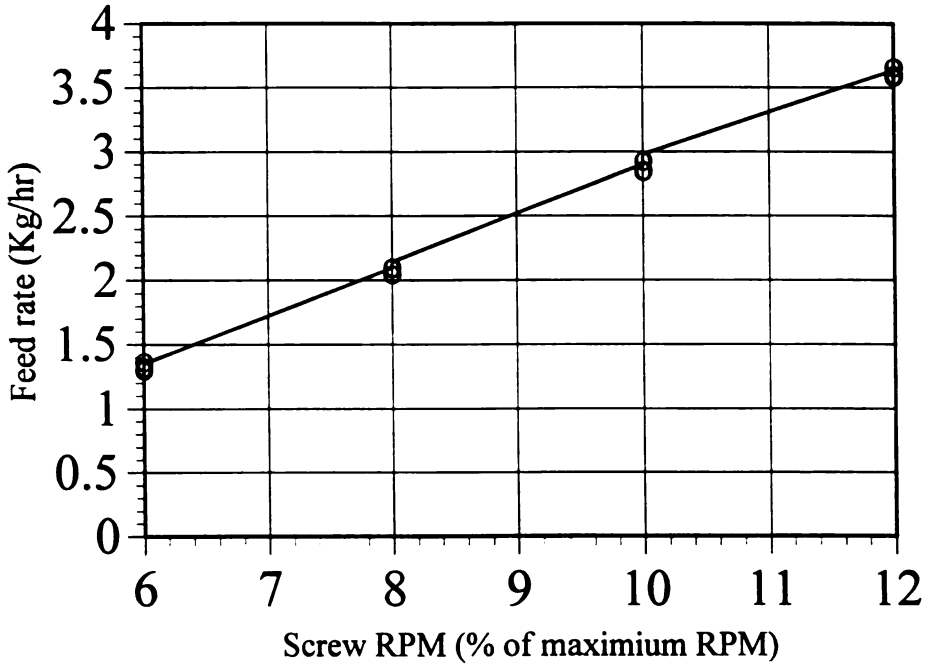

Figure 4.2: Calibration of feeder for EKX pellets.

Cellulose Acetate was supplied by Hoechst Celanese in flake form though there were about 20% by weight of fine particles which the feeder of the extruder could not feed

efficiently. So these were removed with a 1 mm sieve. These fine particles were utilized to make blends of Cellulose Acetate and plasticizer, for extrusion in the microtruder and for characterization of CA with DSC etc.

"EKX" was supplied by Hoechst Celanese in pellet form. These had to be ground before mixing with Cellulose Acetate flakes or drying. A granulator for plastic materials available in the department of Packaging, MSU was used for this purpose. The granulator had a 2 mm classification sieve which was cleaned before grinding each batch of material. This granulator was able to grind even large pieces (about 5 cm diameter and 10 cm long) of the extrudate obtained when blends were made without using a die.

4.2 Drying

The Cellulose Acetate, PET (or EKX) and the blends obtained by extrusion were always dried before extrusion or injection molding to minimize degradation of the material. Improper drying of the feed could also result in poor injection molded samples. The materials were dried in a convective oven at 70°C for at least 8 hours before processing. Plasticized samples of Cellulose Acetate were always dried at 60°C to minimize loss of the plasticizer. The materials to be dried were kept in aluminum trays such that the thickness of the layer was not more than 5 cm. To minimize reabsorption of water during processing, about 300 grams of material was removed from the oven at one time and put into the feeder of the extruder or injection molder. Thus whenever blends needed to be extruded, the blend components were mixed in the proper ratio before drying.

4.3 Extrusion

Extrusion was one of the most important steps of the experiments. This is where the blend materials were mixed and the "in-situ" compatibilization was done through trans-esterification reaction.

The extruder used was a Baker-Perkins co-rotating intermeshing twin screw extruder. Figure 4.3 shows a schematic diagram of the extruder). The diameter of each of the screw was 3 cm, the length was 42 cm. There were two feed ports on the barrel, two barrel valves and a venting port. The materials were fed through the first port and the other feed port and venting port were kept closed. Each screw had two sets of six mixing paddles and a Camel back discharge screw at the end. The die that was used had two holes of 3 mm diameter. This die could be easily removed and was not used whenever there was too much dieswell or the extra residence time if the material in the die resulted in unacceptable degradation. The temperature was measured at three points on the barrel, at one point in the die and at four points inside the barrel (melt temperature), defining the conditions in zone 1, zone 2, zone 3 and the die. The barrel was cooled by water whose flow could be controlled manually by four valves. There was no cooling water provided to the die.

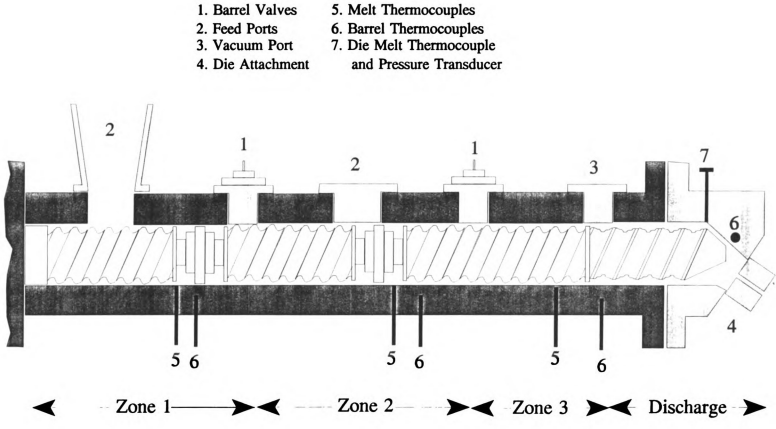

Figure 4.3: Schematic of the Baker-Perkins Twin Screw Extruder, CMSC, MSU

The extruder shafts were composed of slip-on screws, kneading paddles and orifice plug segments. In all the experiments the configuration of these elements was kept as depicted in Figure 4.4. The transversely neighboring paddles are always kept at 90 degrees to each other, while axially kneading paddles can take a number of orientations depending on the amount of forwarding action desired in each mixing zone. Barrel valves are used in conjunction with orifice plugs to control the amount of cross-sectional area available for axial flow. The orifice plugs are discs of diameter close to that of the barrel, and the barrel valve is a triangular-shaped vane positioned directly over the orifice plugs [Nichols, 1991]. The barrel valves were kept open 12% to provide some backmixing.

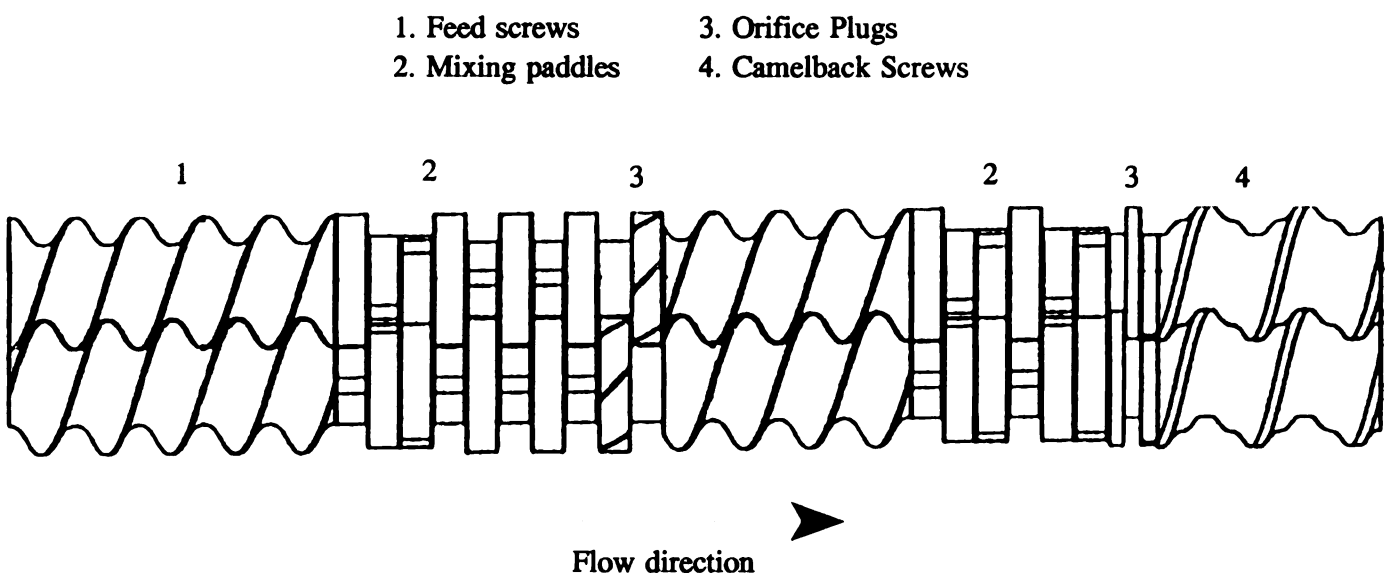

Figure 4.4: Configuration of the co-rotating twin screws

The extruder was purged (cleaned) with Polystyrene before and after each run. the temperature of the barrel and the die was kept at 200°C (and screw RPM = 200) for purging before the run and then the temperature was increased to the required temperature. This was done because the extruder could be cleaned better when the PS was relatively more viscous and could push out the less viscous polymer already in the extruder. When PS coming out of the extruder was clear, it was assumed that no other material (except PS) was in the extruder. This generally took about 300-500 grams of PS. Now the screw was stopped, the temperature was raised if required and the feeder was cleaned by a vacuum cleaner. The dried material was fed in batches of about 300 grams straight out of the dryer to prevent reabsorption of atmospheric water vapor. In the beginning, the extrudate was a mixture of the material and PS and the first 400 gram was discarded. Since injection molding required about 1000 gram of material, about 1500 g of material were fed to the extruder. Collection of the material was stopped when the load (torque) of the extruder which was kept constant during extrusion (about 85% for most blends) started decreasing. Although there was still some material left in the extruder, this was subjected to an extended residence time in the hot extruder and could thus have been degraded. After the run was complete, the feeder was cleaned and PS added to purge the extruder again. If another blend of similar ratios was to be extruded after the previous run, the extruder was not purged with PS. The material was added after cleaning the feeder and again the first 400 gram of extrudate was discarded.

Materials which had enough melt strength and less die swell were extruded with the die. The strands could be pulled and continuously pelletized by a pelletizer. Since

the pelletizer was not able to pinch or cut soft material, the strands had to be cooled by using a fan (a water tank was available but was not used to minimize water absorption by the material). Materials which had to much die swell and/or were highly viscous were extruded without the die to avoid unnecessarily high residence times. These extrudates could not be pelletized and so had to be ground in a grinder before further processing. Some extruded strand was always saved to prepare samples for Electron Microscopy.

The melt temperatures in zone 1 and zone 3 ran lower than the set points whereas the temperature in zone 2 ran higher than the set point. The discharge temperature ran quite close ($\pm 2^{\circ}C$) to the set point. Typical extrusion temperatures are shown in Table 4.1. The temperature in the first zone is kept lower as the materials are to be conveyed ahead without melting in this zone. A RPM of 200 was used for all materials.

Table 4.1: Temperatures used for extrusion.

Zone	Set temperature (°C)	Melt temperature (°C)
feed zone	210	170
1	210	230-235
2	250	230-238
Die	220-240	220-242

Materials Characterization

After preparing the blends in the extruder, the blends were further processed (injection molded, or compression molded) if necessary and characterized by thermal analysis equipment (TGA, DMA, and DSC), mechanical tests (Tensile and Impact), the viscoelastic properties were measured with a dynamic mechanical spectrometer and the morphology was studied by electron microscopy (SEM and TEM). The trans-esterification reaction was characterized by DSC, SEM and Soxhlet extraction.

5.1 Injection Molding

A New Britain (model 75) injection molder was used for molding the materials into ASTM D638 type I specimens (Figure 5.1). Before injection molding, the materials were ground to a 2 mm sieve size and dried (the same conditions as those for extrusion). Before each run the injection molder was purged with Polystyrene till a few clear dogbones were obtained. If two runs with only slightly different samples were injection molded, the injection molder was not purged with PS but rather the first 400 g (about 20 dogbones) after adding the new material were discarded. It was found necessary to spray a release agent on the mold after 10 dogbones that were molded. The cooling time was

kept high enough to allow solidification and some shrinkage of the material but short enough to keep the sprue soft enough to be easily separated of the injected part when the old was opened. The injection time was typically 4-7 seconds. The time of injection should allow the mold to be completely filled but if the pressure is maintained for longer times, the material cannot shrink and the injected part cannot be pushed out from the mold. When the injected part was not ejected from the mold, it had to be removed by hand and sometimes the sprue stuck in the runner had to be forced out with a brass rod. This took about a minute and so the material in the barrel which by then was subjected to a long exposure to high temperature, were discarded by running the screw for a few seconds. Table 5.1 shows some typical temperatures used for injection molding.

Table 5.1: Typical temperatures used for injection molding.

Zone	Temperature (°C)
1	215
2	240
nozzle	240

5.2 Compression Molding

When less number of samples were required as for DMA and RMS, compression molding was used to conserve material. However, compression molding has got the

disadvantages that the blend is not homogenous and the dispersed phase will not get aligned as in injection molding. So compression molding was only used to mold pellets of plasticized CA and extruded blends for DMA and RMS. About 2 inches of the material extruded without the die used in 4 inch X 6 inch X 2 mm mold gave good void-free sheets suitable for characterization work.

5.3 Tensile and Izod Impact Tests

The samples for these tests were conditioned for 40 hours at room temperature and 50% humidity prior to testing.

Tensile tests for strength, elongation and Young's modulus were conducted on a UTS machine SFM-20 (ASTM D638M). A laser extensometer was used to measure the strain. The speed of testing was kept constant at 0.2% for all the tests. At least 5 good readings were obtained for each sample.

The injection molded specimens (type I) were also used for Izod impact tests. With a diamond saw, a section with length 63.5 mm was cut from the injection molded dogbone as shown in Figure 5.1 confirming with ASTM D256 (these cut sections could also be used for DMA). A TMI notch cutter and impact tester were then used to notch and test the specimens. At least 10 good readings were obtained for each sample. A thin specimen (under 6.36 mm thick) generally absorbs more energy due to crushing, bending and twisting than do wider specimens. Therefore, specimens 6.36 mm or over are recommended (Note 10, ASTM D256 - 90b).

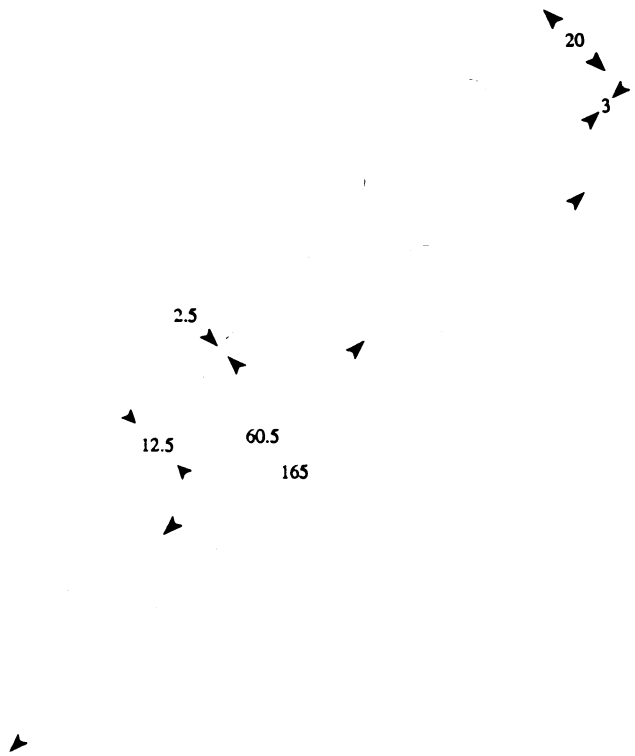

Figure 5.1: ASTM D638 type I injection molded specimen (all dimensions in mm). The cuts and notch for Izod impact test and DMA specimens are also shown.

5.4 Rheometrics Mechanical Spectrometer (RMS)

A Rheometrics Mechanical Spectrometer Model RMS-800 was used to characterize the rheological properties of the pure polymers, their blends and plasticized polymers. The main parts of the rheometer are

a. Pneumatics: Pressurized air is used for the air bearings of the motor and of the transducer. Gas is used for the environmental chamber where the sample is heated. The

computer functions as the heart of the system, controlling the test sequence, making measurements and reducing the resulting data. The test sequence parameters are programmed via the computer keyboard and from the panel of the instrument.

b. Environment Chamber: This is a computer controlled, forced gas convection oven in which the sample and the test fixtures are placed. The sample and test fixtures can be heated or cooled before the start of the test. The environmental chamber uses a platinum resistance thermometer as the control sensor in the control loop. Figure 5.2 shows a schematic of the environment chamber with the test fixtures and the sample.

c. Transducer Linear Drive: When the temperature is equilibrated in the environmental chamber, the test sample is loaded between the test fixtures. This is done by moving the transducer assembly until the test fixtures are separated sufficiently to allow sample insertion. The transducer assembly is connected to a motor driven platform that can be raised or lowered. The output from the transducer is coupled to a linear force scaling and stepper cutout card. this scaled axial force is input to the computer through an analogue to digital converter.

Modes of Operation:

The RMS-800 can be operated in various modes like the rate sweep, temperature sweep, frequency-temperature sweep, strain sweep, time sweep etc. In this work the strain sweep, temperature sweep and the frequency-temperature sweep modes were used. All measurements were taken under dynamic strain so that complex viscosities, real and imaginary modulii etc could be calculated.

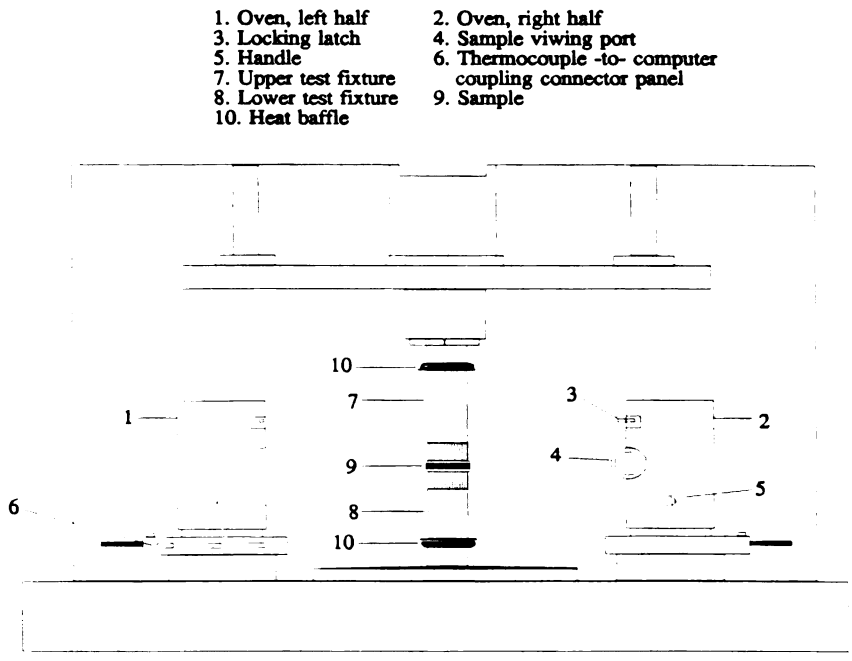

Figure 5.2: Environment chamber of the RMS-800.

Sample Preparation: Samples in the form of discs 2 mm thick and 25 mm diameter were required for the RMS. Pellets were compression molded to give a sheet 2 mm thick. The temperature was kept such that a sheet free of voids was obtained. Circular samples were then cut from this sheet using a die. Sometimes it was found necessary to grind the pellets to obtain void free samples.

5.5 Differential Scanning Calorimetry (DSC)

DSC is a technique of non-equilibrium calorimetry in which the heat flow into or a the sample and a reference is measured as a function of time or temperature. The

sample and the reference are kept at the same temperature by changing a current passing through the heaters under the two pans. This is an accurate and easy method to use and is very useful to measure temperatures and heats of transition, specific heat, thermal emissivity, rate and degree of crystallinity, purity, rate of decomposition, the rate of reactions etc. Since the heating is controlled with a computer, it is possible to follow complex heating algorithms. The experiment can be followed in real time. This is useful when large temperature changes have to done manually at a particular point in the heating program (like quenching or suddenly cooling to study rate of crystallinity).

A DuPont 910 DSC module was used with a DuPont 9900 Computer/Thermal Analyzer for all the experiments. The sample size was always kept 10 - 20 mg.

5.6 Dynamic Mechanical Analysis (DMA)

DMA involves the determination of the dynamic mechanical properties of polymers and their assemblies. As a result of this analysis, the relationships between the dynamic properties and structural parameters (crystallinity, molecular orientation, molecular weight, crosslinking, copolymerization, and plasticization, etc.) and environmental or external variables (temperature, pressure, time, frequency, type of deformation, surrounding atmosphere, humidity, etc.) can be explained [Murayama, (pg. 2)].

The commonly used frequency range in DMA of polymeric materials is from 10^{-2} Hz to 10^{6} Hz.. However when low frequencies are used , the results of DMA can be

compared with those of other thermal analysis techniques. A frequency of 1 Hz has been used for the all the experiments in this thesis.

Glass Transition (T_g) and Melting Point (T_m):

The properties of polymers change with temperature. In particular, the properties like thermal expansion coefficients, modulii undergo an abrupt change in the region of glass transition. The temperature of this abrupt change is defined as the glass transition temperature. In dynamic mechanical studies, the dynamic modulus (storage modulus) decreases rapidly, and the loss modulus and tan δ exhibit maxima. The glass temperature can also be determined by DSC, TMA, NMR studies, change in dielectric constant, refractive index etc. Since so many different methods exist for the determination of T_g, different values are often obtained. Even the same method will often yield different results depending on the conditions used. The T_g obtained by DMA is dependent on the rate of heating, frequency, crystallinity, phase size, etc. Throughout this work the maxima of loss modulus peak was taken as the T_g as this was found to give unambiguous results as compared to the maxima of tan δ or the inflexion point of storage modulus. The tan δ peak at a frequency of one cycle per second is at a temperature of about 5°C to 15°C above the glass temperature as measured by dilatometry or DSC. The maximum in the loss modulus at low frequencies is very close to the T_g [Nielson, 1974]. The rate of heating and thermal history was kept the same whenever comparisons of the results was required.

Sample preparation: The samples for DMA were either cut from the injection molded dogbones (as for Impact test specimens) or from compression molded sheets (the same sheets could be used for both DMA and RMS).

5.7 Thermo-Gravimetric Analysis (TGA)

In TGA the weight of a sample is measured as a function of time or temperature. This is a relatively simple technique giving useful information about the moisture content, plasticizer content, degradation temperature etc. The results obtained may depend on the sample size, atmospheric conditions, type of pan and heating rate. The same heating profile was used whenever comparison of data was required. The sample was heated under nitrogen, covered or uncovered. Care was taken not to touch the sample pans or pan covers by hand.

To find plasticizer content (Chapter 6), in the case when the rate of weight loss did not fall to zero, the final weight was calculated by a second order deferential equation. To find the degradation temperature of polymers, a high resolution "HiRes" mode was used. Here the heating rate is automatically reduced whenever there is a large change in sample weight. This gave sharper peaks at the degradation temperature.

DuPont TGA modules 951 and HiRes 2950 were used with a DuPont 9900 Computer/Thermal analyzer for all the experiments. The sample weight was always $\sim$ 20 mg.

5.8 Scanning Electron Microscopy (SEM)

Image formation: The SEM is employed to observe the surface morphology of a sample. The normal SEM image is formed when secondary electrons from the atoms of the sample are given out as a result of inelastic scattering by the electron beam. These secondary electrons are then detected by an Everhart-Thornley detector. The production of secondary electrons is very sensitive to the changes in topography of the sample. The projecting areas of the samples giving out a large number of these electrons and thus appear brighter. The electrons cannot escape from low lying areas like crevices and thus these areas appear dark in the final image. A resolution of 4 to 6 nm is possible with this technique.

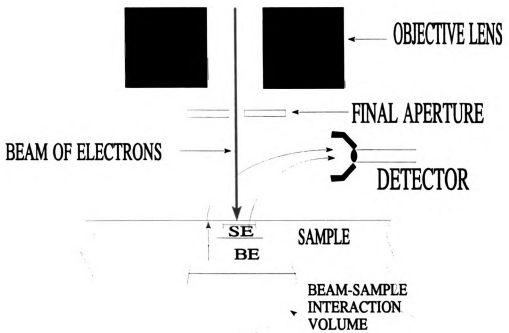

Figure 5.3: Image formation in the SEM.

Sample Preparation: The samples for SEM are typically 2 to 4 mm size.The samples are fractured after freezing under liquid nitrogen. This "freezes in" the actual morphology of the sample and minimizes the artifacts introduced by fracturing. Surfaces obtained by room temperature fracturing were also used for the mica and talc samples. These were then mounted on Aluminum stubs and coated with gold in a sputter coater. When a backscattered electron image (BEI) is desired, the sample has to be coated with Carbon. A coating of about 20 nm thickness and the use of graphite paint was found to be sufficient to prevent charging of the sample with a 15 kV accelerating voltage. Any staining, critical point drying or etching of the samples was done before the coating step.

5.10 Transmission Electron Microscopy (TEM)

Image Formation: Transmission Electron Microscopy (TEM) is used to give information about the composite morphology. The image is formed by the electrons transmitted through a very thin section of the sample. The amount of secondary electrons produced depends on both density and thickness of the sample. This difference in scattering of the electrons between different portions of the sample gives the contrast necessary to form the TEM image. The areas which are thinner and/or have less atomic number are "electron transparent", i.e., they allow more electrons to pass through and thus appear as bright areas in the image. The "electron dense" areas scatter more electrons as well as absorb electrons and appear as darker areas in the image. A resolution of up to 0.2 nm is possible with the TEM.

Sample Preparation: Sample preparation for TEM is a difficult step and that is why this technique is used only where some information is required that is not available by SEM or when a higher resolution is required. A cuboid is cut from the sample of dimensions approximately 4x6x10 mm and one of its edges is trimmed to a trapezoid using a razor blade. (Fig 5.4) Thin sections of 60-150 nm are then be cut by a microtome using either a glass or a diamond knife. The size and thickness of the sections have to be adjusted to give the best image in the TEM. The sections are collected on copper grids, coated with carbon or stained as required (Osmium tetraoxide staining was required for CA/EKX samples).

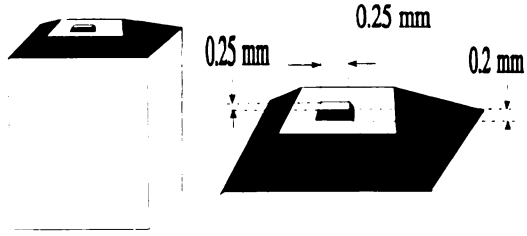

Figure 5.4: Sample preparation for TEM.

5.10 Extraction

The Extraction apparatus consisted of a Soxhlet extracton tube, an Allihn condensor, a 500 ml round bottom flask and cellulose extraction thimbles (Figure 5.5). With the Soxhlet apparatus, one phase can be extracted from the blend by using a suitable solvent. To extract CA, Acetone was used since PET is insoluble in Acetone. The sample is kept in a cellulose thimble and about 300 ml of Acetone is allowed to boil in the flask. The condensed acetone vapors drip into the thimble dissolving CA . When the Acetone in the Soxhlet tube reaches a certain height, it is automatically siphoned back into the flask. Thus, a closed system is set up and the blend can be continuously refluxed with fresh solvent. The blend was extracted for 24 hours. The thimble was weighed before and after the extraction to calculate the weight of the residue.

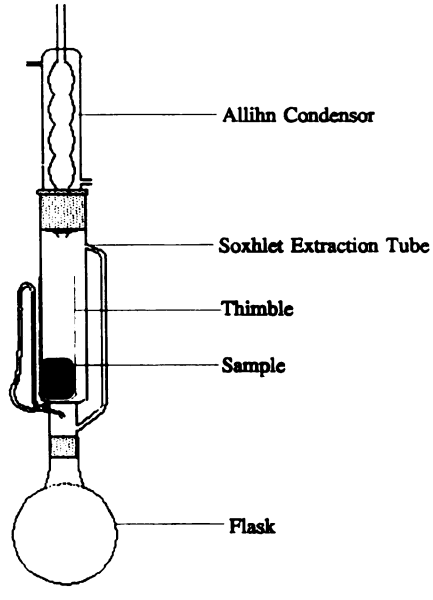

Figure 5.5: Apparatus used for extraction.

The viscosity of concentrated polymer solutions

The modeling of concentrated polymer solution viscosity is interesting both from the theoretical and practical points of view. On a fundamental level, attempts are made to model polymer viscosities with molecular parameters like branching, friction factor, free volume etc. Many empirical and semi-empirical relations have also been found useful. In chapter 7, the morphology of CA/PET systems with and without plasticizer is studied as a function of viscosity and volume ratios. Thus it is necessary to know the volume and viscosity of the two phases. The usefulness of several strategies and correlations was investigated by using data available in literature. It was also found necessary to understand the underlying theory and assumptions before selecting the methods to use. The equations by Kelly and Bueche were found to give satisfactory results.

6.1 Background

The rheological and thermodynamic properties of dilute polymer solutions are fairy well characterized both experimentally and theoretically. The purpose of these theories and equations was to provide a rational extrapolation of viscosity data to infinite

dilution. However, the viscosity behavior of polymer solutions at high concentrations, especially in the region approaching pure polymer, has not yet been investigated extensively. The effect of high concentrations on rheological properties has not yet been fully understood. The problem of the viscosity of concentrated solutions of high molecular weight polymers is a very complicated one from both the theoretical and experimental point of view because in fairly concentrated solutions one encounters viscoelastic behavior. The effect of crystallinity has not been addressed at all by any of the authors.

Various attempts have been made to reach a better understanding of concentrated polymer solutions and establish analytically the relation between viscosity and concentration of the solution. The approaches commonly used are assumptions of an effective viscosity [Peterlin, 1954], application of Network theory [Lodge, 1958], reduced variables [Simha & Zakin, 1960, 1962; Ultracki & Simha, 1963], derivations of theoretical equations based on free volume concepts [Fujita & Kushimoto, 1961; Kelly & Bueche, 1961], and calculation of concentration dependent intermolecular potentials from fluctuation theory [Fixman & Peterson, 1964]. The equations from these efforts have not been able to cover the entire range of concentrations successfully and have parameters which are often difficult to determine. An empirical equation for the entire concentration range in terms of Huggins Constant has been developed [Lyons & Tobolsky, 1970] but it is applicable only for low molecular weight polymers. The model due to Rouse also predicts the viscosity at lower molecular weights [Graessley W.W., 1984]. An excellent review on the subject has been published [Berry & Fox, 1968].

Another difficulty in the development of theories for the viscosity of concentrated polymer solutions has been the in obtaining accurate data at high concentration specially near the glass transition temperature. Published data covering a wide range of concentrations is available for only a limited number of systems. The data that have been used by the above authors have been obtained by capillary viscometer, falling cylinder viscometer and tensile creep apparatus. Viscosities at higher shear rates which would be of practical importance in processing equipment has not been investigated.

In the development of these theories, the viscosity of the pure polymer has often been used as a known parameter. Thus these theories and equations should prove useful in the interpolation of data at higher concentrations. However, in the case of Cellulose Acetate it is not possible to obtain the viscosity of the unplasticized polymer or even fairly concentrated solutions at higher shear rates and temperatures as it decomposes below it's processing temperature. Thus, the extrapolation of the available data to low levels of diluent concentration is therefore of interest in the case of Cellulose Acetate and other similar polymers. An attempt is made to fit the various equations to the available data [Bueche, 1955] and analyze which of them is suitable for this purpose.

6.2.1 Molecular theory for viscosity

The viscosity of polymers and their solutions is found to depend on various parameters like molecular weight or chain length, chain dimensions, temperature, chain branching, polydispersity, diluent, shear rate etc. To correlate the experimentally

observed values of viscosity with these variables the zero shear viscosity η_0 is considered to be a product of two factors, a structural sensitive factor F, dependent primarily on number of atoms (or groups) Z in the chain backbone and a temperature or density dependent friction factor *per chain atom* ζ. Thus the following empirical relation is obtained

$$\eta = F(Z)\zeta(\rho) \tag{6.1}$$

A relation similar in form to the Vogel equation has been used to give the temperature dependence of ζ as

$$\ln\zeta = \ln\zeta_o + \frac{1}{\alpha(T-T_o)} \tag{6.2}$$

The inherent friction factor ζ_0 is presumed to be constant, independent of molecular weight and temperature although this may not be entirely true. If the molecular weight dependence of α and T_0 are known, then we can calculate the viscosities at constant friction factor, ζ, from the isothermal viscosities according to

$$\ln\eta_\zeta = \ln\eta_T - \frac{1}{\alpha(T-T_o)} \tag{6.3}$$

with the values of α and T_0 appropriate to each Z to correct for the dependence of ζ on Z. The correction $1/\alpha(T\text{-}T_0)$ is typically independent of Z when Z > ca. 400.

It is found that the isothermal viscosity can be approximated by the relation

$$\eta_T = K_T Z^a \tag{6.4}$$

where

$$a = 3.4\,, \quad Z \geq Z_c\,;$$

$$2.5 \geq a \geq 3.4\,, \quad Z \leq Z_c$$

K_T depends on the material and Z_c represents a critical value of Z, above which a = 3.4. Equation 6.4 is found to be consistent with equation 6.1. [Berry & Fox, 1968] [Fox & Allen, 1962] noted that a parameter X given by

$$X = Z(|s^2|)_o / M)\ \phi_2 / v_2 \qquad \textbf{(6.5)}$$

is a more significant parameter than either M or Z. Here v_2 is the polymer specific volume, $|s^2|$ is the unperturbed radius of gyration and ϕ_2 is the volume fraction of the polymer. When the viscosity at constant friction factor is plotted against X it is noted that

$$\eta_\zeta \propto X, \quad for\ X \leq X_c \qquad \textbf{(6.6)}$$

$$\eta_\zeta \propto X^{3.4}, \quad for\ X \geq X_c$$

Moreover X_c is found to be nearly the same for all the polymers. This behavior has been observed to be followed by many systems. [Bueche, 1953, 1955; Fox and Allen, 1964; Johnson, 1952; Kelly & Bueche, 1961; Burke & Weiss, 1975] Thus, the effect of diluent can be accounted for by the inclusion of ϕ_2 in the definition of X.

6.2.2 The concept of free volume

The concept behind the free volume theory for viscosity is that the rate controlling step in viscous flow at low shear stresses is the formation of a void into which a chain segment can jump and hence produce flow. Doolittle [Doolittle, 1951] showed that the viscosity of liquid paraffins can be accurately defined as a simple function of relative free space except for values in the neighborhood of freezing points of each compound. Unfortunately there is no unique manner of defining this quantity. Doolittle considered this free space to arise due to the total thermal expansion of the liquid without change in phase. He defined a 'fractional free volume' as the fractional increase in the volume resulting from expansion

$$f = v_f / v_o = (v - v_o) / v_o \tag{6.7}$$

where v_f=volume of free space per gram of liquid at any temperature; v_o=volume of 1 gram of liquid extrapolated to absolute zero and v = volume of 1 gram of liquid at any temperature. The viscosity data could then be correlated by the expression

$$\ln \eta = A + B / f \tag{6.8}$$

where A and B are constants. Ferry modifies Doolittle's equation as follows:

$$\ln \eta = \ln A + B(v - v_f) / v_f \tag{6.9}$$

It is assumed that above the glass transition temperature, the fractional free volume increases linearly with temperature

$$f = f_g + \alpha_f(T - T_g) \qquad \textbf{(6.10)}$$

where f_g is the fractional free volume at an arbitrary reference T_g and α_f is the thermal coefficient of expansion of the fraction free volume. α_f has been approximated by the relations [Peticolas, 1963; Porter, 1966].

$$\alpha_f = \alpha_l - \alpha_o \quad for \quad T \geq T_g \qquad \textbf{(6.11)}$$

and

$$\alpha_f = \alpha_g - \alpha_o \quad for \quad T < T_g$$

Here α_l ,α_g and α_o are the expansion coefficients for the liquid, glass and occupied volume respectively.

6.2.3 Dependence of fractional free volume on diluent

The fractional free volume usually increases by the addition of the diluent. This dependence of f on ϕ is not simple as T_g and α_l are known to vary with ϕ. However some investigators [Wood, 1954] have suggested that simple additivity in the free volume might adequately give the dependence $f(\phi)$. Thus for a two component system

$$f^M = \phi_1 f_1 + \phi_2 f_2 \qquad \textbf{(6.12)}$$

Here subscript M, 1 and 2 refer to the mixture, diluent and polymer respectively. f_1 and f_2 follow similar relations as Equation 6.10

6.3 The Mixture Rule

Generally, the simplest method of estimating the viscosity of a solution at a temperature well above T_g is to use a mixture rule such as

$$\log\eta \cong \phi_p \log\eta_p + \phi_L \log\eta_L \qquad \textbf{(6.13)}$$

The viscosities of pure polymer and liquid are η_p and η_L, respectively, while ϕ_P and ϕ_L are the corresponding volume fractions.

The data of Fujita & Maekawa [Fujita & Maekawa, 1962] for diethyl phthalate viscosities for the temperatures 20°C to 110°C was used. The Arrhenius equation (Equation 6.14) was used to find the viscosity at other temperatures.

$$\eta = Ke^{(E/RT)} \qquad \textbf{(6.14)}$$

Here K is a constant characteristic of the material, E is the activation energy for the flow process, R is the gas constant and T is the temperature in degrees kelvin. Thus

$$\frac{\eta_{T_2}}{\eta_{T_1}} = e^{\frac{E}{R}\left(\frac{1}{T_2}-\frac{1}{T_1}\right)} \qquad \textbf{(6.15)}$$

Figures 6.1-6.3 show the PMMA/DEP data from Bueche at three temperatures. The dotted lines in each case refer to the prediction by Equation 6.13. However, treating the viscosity of pure polymer as an unknown and the fitting the equation to the remaining data we can determine how well the viscosity of pure polymer is predicted by the mixture rule. Table 6.1 shows the results obtained.

Table 6.1: Pure PMMA viscosities estimated by mixture rule.

TEMPERATURE (^{o}C)	PURE PMMA VISCOSITY (actual)	PURE PMMA VISCOSITY (estimated)
140	5.25×10^{7}	4.31×10^{3}

The prediction of pure PMMA viscosity is very poor at lower temperatures but gets better at high temperatures. Figure 6.4 shows the predicted viscosities of pure CA as a function of frequency at 240°C.

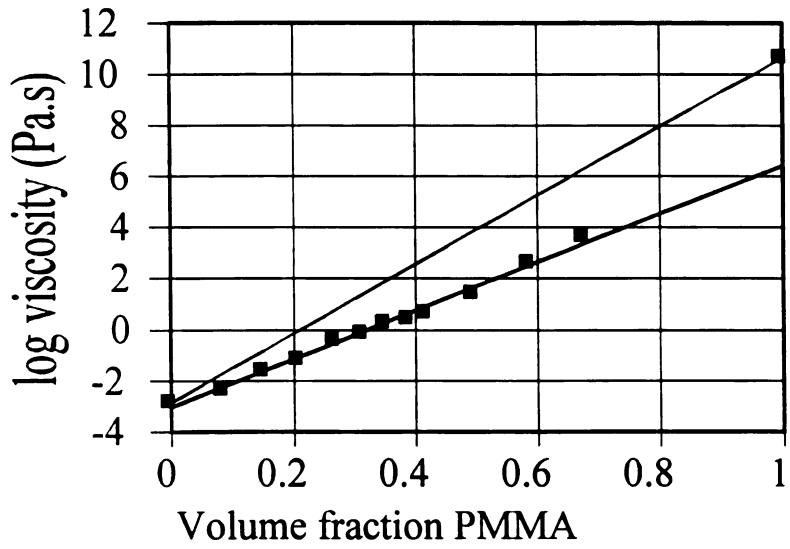

Figure 6.1: PMMA/DEP data for 120°C; '- -' mixture rule, '--' best fit not using data at $\phi = 1$.

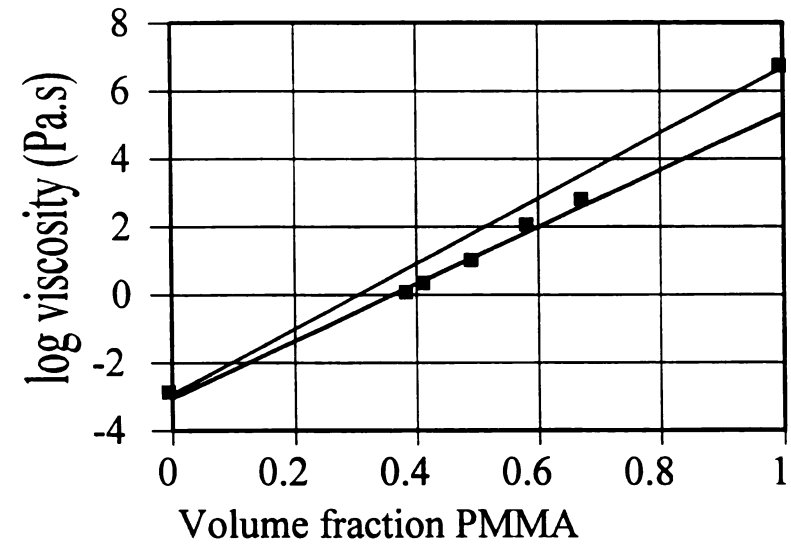

Figure 6.2: PMMA/DEP data for 140°C; '- -' mixture rule, '--' best fit not using data at $\phi = 1$.

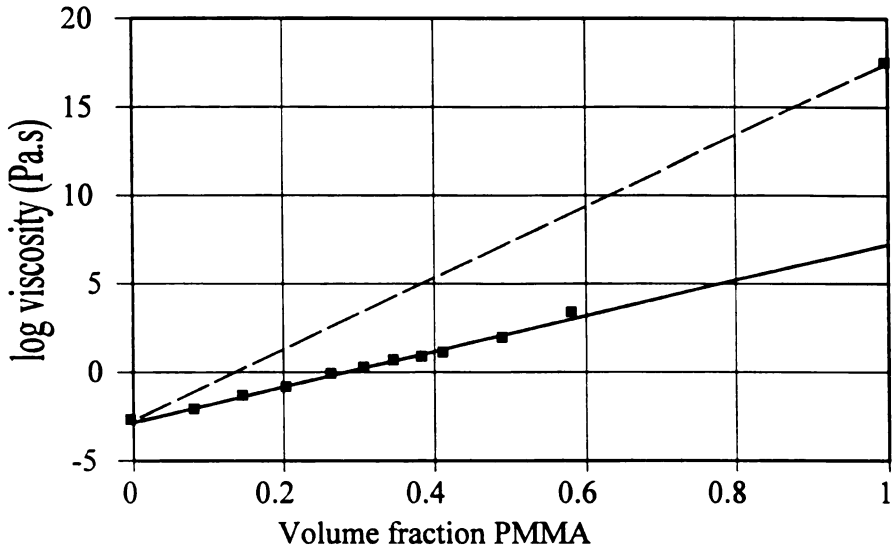

Figure 6.3: PMMA/DEP data for 100°C; '- -' mixture rule, '--' best fit not using data at $\phi = 1$.

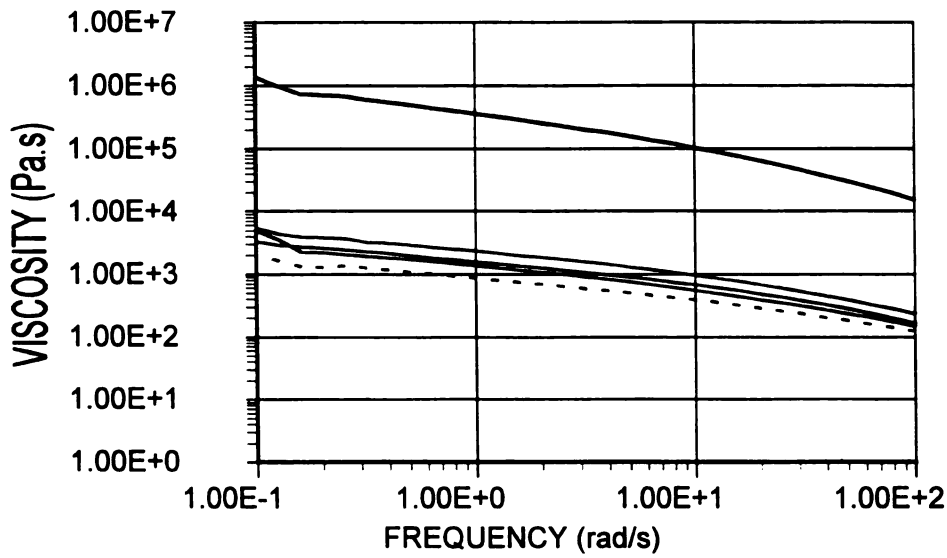

Figure 6.4: Viscosity of CA estimated by the mixture rule. Lower four curves are for CA/DEP blends.

6.4 Reduced Variable Treatment [Kraus & Gruver, 1965]

This method allows the superposition of the viscosity-shear rate curve for any polymer containing a diluent on the viscosity curve of a pure polymer. The Newtonian viscosity according to the semi-empirical equation by [Fox & Allen, 1964] is

$$\eta_N = (N_a / 6X_c^{2.4})[|s_o^2| / M)\rho Z]^{3.4} f_o \qquad \textbf{(6.16)}$$

with

$$X_c = \rho Z_c(|s_o^2| / M)$$

where

η_N = Newtonian Viscosity

N = Avogadro's Number

$|s_o^2|$ = Mean square radius of gyration of the molecule

M = Molecular weight

ρ = density

f_o = segmental friction factor

Z = number of main chain atoms per molecule

Z_c = critical value of Z for entanglement

In a system containing diluent it appears generally true that [Bueche, 1956; Fox & Allen, 1964]

$$Z_c' c = Z_c \rho \qquad \textbf{(6.17)}$$

where Z_c' is the value of Z_c for the polymer-diluent system and c is the concentration of

the polymer. Thus the Newtonian viscosity of a plasticized polymer is

$$\eta_N = (N_a/6)(Z_c\rho)^{-2.4}(|s^2|/M)(Z_c)^{3.4}f \qquad \textbf{(6.18)}$$

Dividing Equation 6.18 by Equation 6.16 we obtain

$$\eta_N(\phi)/\eta_N(1) = \phi^{3.4}(f/f_o)(|s^2|/s_o^2|) \qquad \textbf{(6.19)}$$

where ϕ is the volume fraction of the polymer and the subscript "o" refers to pure polymer. To account for non-Newtonian behavior, the shear rate dependence of viscosity can be stated as [Bueche, 1959]

$$\eta/\eta_N = F(\eta_N\dot{s}) \qquad \textbf{(6.20)}$$

where η is the viscosity at shear rate s. The function F is independent of the molecular weight. Bueche [Bueche, 1959] suggests that this relation may be extended to solutions by introduction of the concentration as shown in the following equation

$$\eta/\eta_N = F(\eta_N\dot{s}/\phi) \qquad \textbf{(6.21)}$$

Recent studies [Markowitz & Brown, 1963] have shown that better concentration superposition might be obtained with ϕ^2 instead of ϕ.

$$\eta/\eta_N = F(\eta_N\dot{s}/\phi^2) \qquad \textbf{(6.22)}$$

The use of this method in its original form requires prior knowledge of the viscosity of unplasticized polymer. However, here the unplasticized polymer viscosity has been treated as an unknown and the best possible superposition of data is obtained on the calculated viscosity of the pure polymer.

The steps involved in this process are

1. Assume a Newtonian viscosity for the unplasticized polymer, $\eta_N(1)$.

2. Calculate the shift factor $a_\phi = \eta_N(\phi)/\eta_N(1)$.

3. Shift the data to give a curve of η/a_ϕ vs. $a_\phi s/\phi^2$.

4. When all the data is shifted, a curve is fitted to the data using an equation similar to the Cross Equation

$$\eta / a_\phi = C_1 + \frac{C_2 - C_1}{1 + C_3(\eta_N \dot{s}/\phi^2)^{C_4}} \qquad \textbf{(6.23)}$$

The deviation of the data from this curve is calculate and different values of $\eta_N(1)$ are chosen till this value is minimized.

Figure 6.5 shows the shifted data and the curve for the unplasticized Cellulose Acetate. The absicca shows $a_\phi s/\phi^2$ and the ordinate is η/a_ϕ. Unfortunately, due to the large value of $\eta_N(1)$ obtained, the shift factor is small and the shear rates for which the curve is obtained are much reduced which are not useful for processing equipment.

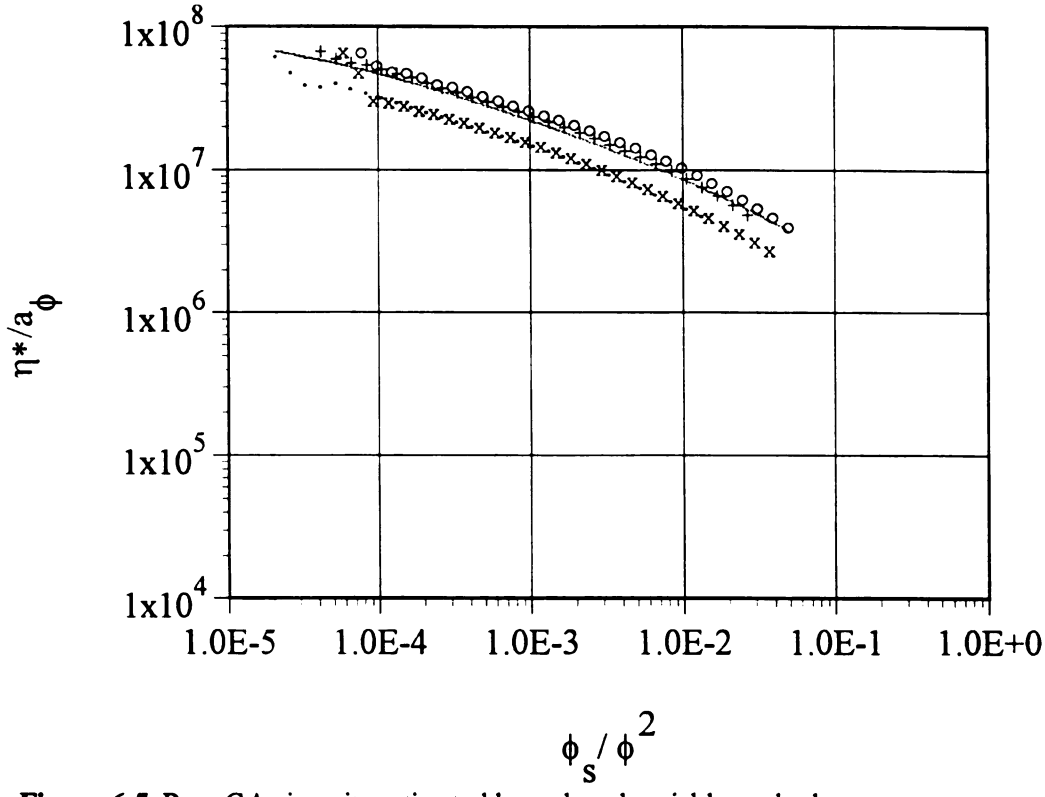

Figure 6.5: Pure CA viscosity estimated by reduced variable method.
"o" H2, "+" H, "x" MH and "." MS grade CA/DEP blend.

6.5 The use of equation 6.6

As mentioned earlier, the behavior predicted by Equation 6.6 has been observed to be followed by a number of systems. To use this correlation, the isothermal viscosities, η_T first have to be converted to viscosities at constant friction factor, η_ζ. The diluent affects both F(X) and $\zeta(\rho)$. The dependence of F(X) on the volume fraction of polymer is taken care of by the inclusion of ϕ in the definition of X. Thus only the effect of ϕ on ζ has to be investigated. A relation similar to Equation 6.2 can be used for plasticized polymers

$$\ln\zeta^M = \ln\zeta_o + \frac{1}{\alpha^M(T-T_o^M)} \qquad \textbf{(6.24)}$$

With the help of the W-L-F equation this can be recast as [Williams, Landel and Ferry, 1955]

$$\log\zeta^M = \log\zeta_o + \frac{K^M}{1 + (T - T_g^M)/\Delta^M} \qquad \textbf{(6.25)}$$

where

$$\Delta^M = T_g^M - T_o^M$$

and

$$1/K^M = 2.303\alpha^M(T_g^M - T_o^M)$$

Data on η(T) at constant diluent volume fraction may be analyzed to obtain parameters α^M and T_o^M as functions of composition since the temperature dependence of F(X) is small. Knowing these the parameters K^M and Δ^M can be determined as functions of ϕ if T_g^M is known as a function of ϕ. However, it is observed that K^M and Δ^M are only slightly dependent on ϕ

for $\phi > 0.5$. Treating these as constants we can rewrite Equation 6.25 as [Berry, 1966]

$$\ln\zeta^M = \ln\zeta_o + \frac{C_1}{(C_2 + T - T_g^M)} \qquad \textbf{(6.26)}$$

where C_1 and C_2 are constants with respect to ϕ. These constants can be used to compute η_ζ according to the relation [Berry, 1966]

$$\log\eta_\zeta(\phi_2) = \log\eta_T(\phi_2) - C \qquad \textbf{(6.27)}$$

with

$$C = \left[\frac{C_1}{C_2+T-T_g}\right]_{\phi_2} - \left[\frac{C_1}{C_2+T-T_g}\right]_{\phi_2=1}$$

The parameters C_1 and C_2 can be optimized by using the data for concentrated mixtures such that η_ζ is proportional to $\phi_2^{3.4}$. Figure 6.6 shows the viscosity of PMMA at 120°C as predicted with this scheme.

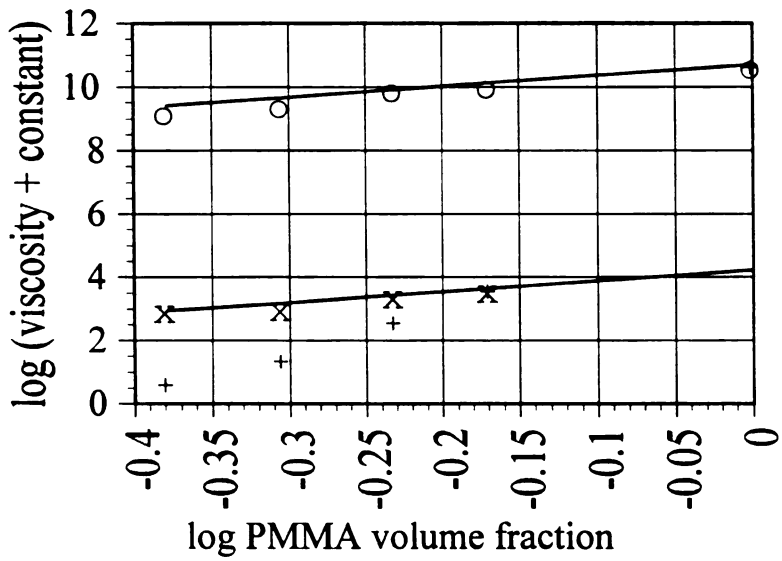

Figure 6.6: Prediction of pure PMMA viscosity with Equation 6.6 "+" actual data from Bueche, "o" data fitted to Equation 6.6, "x" data fitted to Equation 6.6 without the data at $\phi = 1$.

As can be seen from Figure 6.6, the data can be fitted to Equation 6.6 after the viscosities are corrected for constant friction factor, but this method cannot is not able to predict the large increase in viscosity at very high polymer concentration. It should be noted that at $\phi_1 = 0$, the constant = 0, so $\eta_\zeta = \eta_T$.

6.6 The Kelly and Bueche equation

The basis of the Kelly and Bueche theory is the free volume concept i.e. the effect of diluent on a polymeric system is pictured as a relative increase in free volume contributed by the diluent, thereby loosening the local liquid structure [Kelly & Bueche, 1961]. Cohen and Turnbull [Cohen & Turnbull,1959] derived an expression for the dependence of viscosity on a critical free volume v^* , required for the displacement of a flow unit and arrived at an equation similar to Equation 6.9. This theory has been combined with the W-L-F equation by Kelly and Bueche to arrive at a very useful equation for predicting the viscosity of concentrated polymer solutions. The W-L-F equation takes the free volume of the polymer to be [Williams, Landel & Ferry, 1955]

$$f = 0.025 + 4.8\ X\ 10^{-4}(T - T_g) \qquad \textbf{(6.28)}$$

In this relationship 0.025 represents the free volume at glass temperature, and the additional term expresses the increase in *free volume* due to the expansion of the polymer as the temperature is raised from T_g to T.

Kelly and Bueche make the assumption that the free volume contributed by the diluent

may be added to that of the polymer. Thus the free volume of the system for ϕ_2 volume fraction of the polymer is

$$f = \phi_2[0.025 + 4.8\ X\ 10^{-4}(T - T_g)] + (1 - \phi_2)[0.025 + \alpha_s(T - T_g')] \qquad \textbf{(6.29)}$$

where α_s and T_g' are the thermal expansion coefficient and glass temperature of the solvent respectively. Using this value of f, the following equation is obtained.

$$\eta = K\rho^4 \exp\{\phi[0.025 + 4.8\ X\ 10^{-4}(T - T_g)] + (1 - \phi)[0.025 + \alpha_s(T - T_g')]\}^{-1} \qquad \textbf{(6.30)}$$

where K is a combined constant including the molecular weight. The corresponding equation for $M < M_c$ is of the same form except for a first power concentration dependence.

This relation requires a knowledge of the glass temperature of polymer and solvent and α_s for the solvent. Since in practice, α_s and T_g' may be difficult to determine by direct measurements, several reasonable estimates might be tried until the best fit of the data is obtained. The coefficient α_s is usually of the order 10^{-3}. The value of glass temperature for Di Ethyl Phthalate is taken to be -65°C for fitting the data [Kelly & Bueche, 1961]. It should be noted that at higher polymer concentrations, the factor $(1-\phi)$ becomes small, so precise values of α_s and T_g' are not essential. Figures 6.7 and 6.8 show the PMMA/DEP data at 120°C and 140°C by Bueche fitted to Equation 6.30.

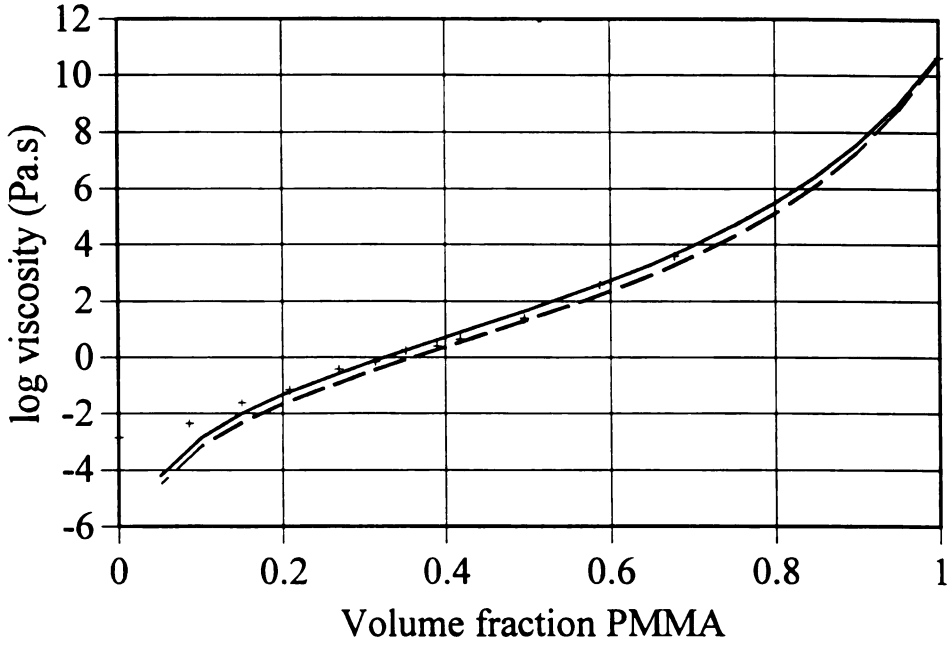

Figure 6.7: Prediction of PMMA viscosity using Kelly and Bueche equation at 120°C, "+" PMMA/DEP data from Bueche, "...." best fit, "__" best fit without using data at $\phi = 1$.

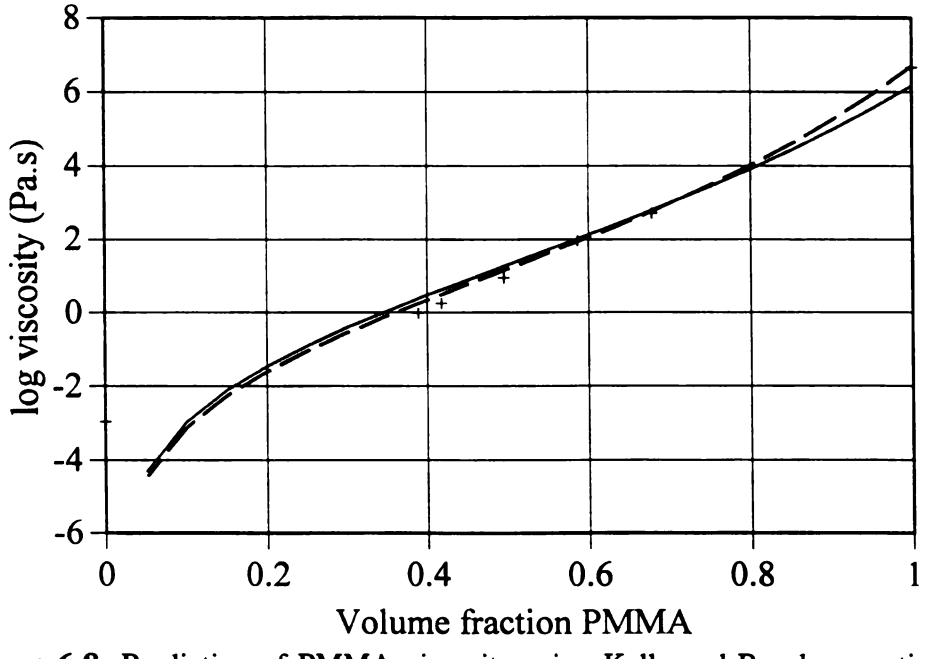

Figure 6.8: Prediction of PMMA viscosity using Kelly and Bueche equation at 140°C, "+" PMMA/DEP data from Bueche, "...." best fit, "__"best fit without using data at $\phi = 1$.

The Kelly & Bueche equation is seen to give a very good fit the PMMA/DEP data and is able to predict the large increase in viscosity at high polymer concentrations. Table 2 shows the actual and estimated values of viscosities.

Table 6.1: Pure PMMA viscosities extrapolated by the Kelly and Bueche equation.

TEMPERATURE (°C)	PURE PMMA VISCOSITY (Actual)	PURE PMMA VISCOSITY (estimated)	ERROR (%)
120	5.01×10^{11}	4.97×10^{11}	0.8
140	5.25×10^{7}	5.248×10^{7}	0.03

Fujita & Kushimoto [Fujita & Kushimoto, 1961] have tried to eliminate the parameter K in Equation by using a viscosity η^* (corresponding to volume fraction ϕ_1^*) and using viscosity ratios (shift factors). The final equation obtained is:

$$-\frac{1}{ln a_c} = f(T,\phi_1^*) + \frac{[f(T,\phi_1^*)]^2}{\beta(T)} \cdot \frac{1}{(\phi_1 - \phi_1^*)} \qquad \textbf{(6.31)}$$

where

$a_c = \eta(T,\phi_1)(1-\phi_1^*)/\eta(T,\phi_1^*)(1-\phi_1)$

$\beta(T)$ is a parameter relating the fractional free volume f to ϕ_1

The values of $\beta(T)$ and $f(T, \phi_1)$ can be evaluated by plotting data in the form of $-1/\ln a_c$ against $1/(\phi_1 - \phi_1^*)$. However there is considerable uncertainty in determining these from the intercept

and slope of the straight line obtained because in general the value of fractional free volume are small and in determining $\beta(T)$ these errors are squared.

6.7 Viscosity of Cellulose Acetate

The viscosity and volume fraction CA data from the four CA/DEP blends was fitted to Equation 6.30 and the parameters K and α_s were optimised. Figure 6.9 shows the fit obtained for the data at 10 rad/s.

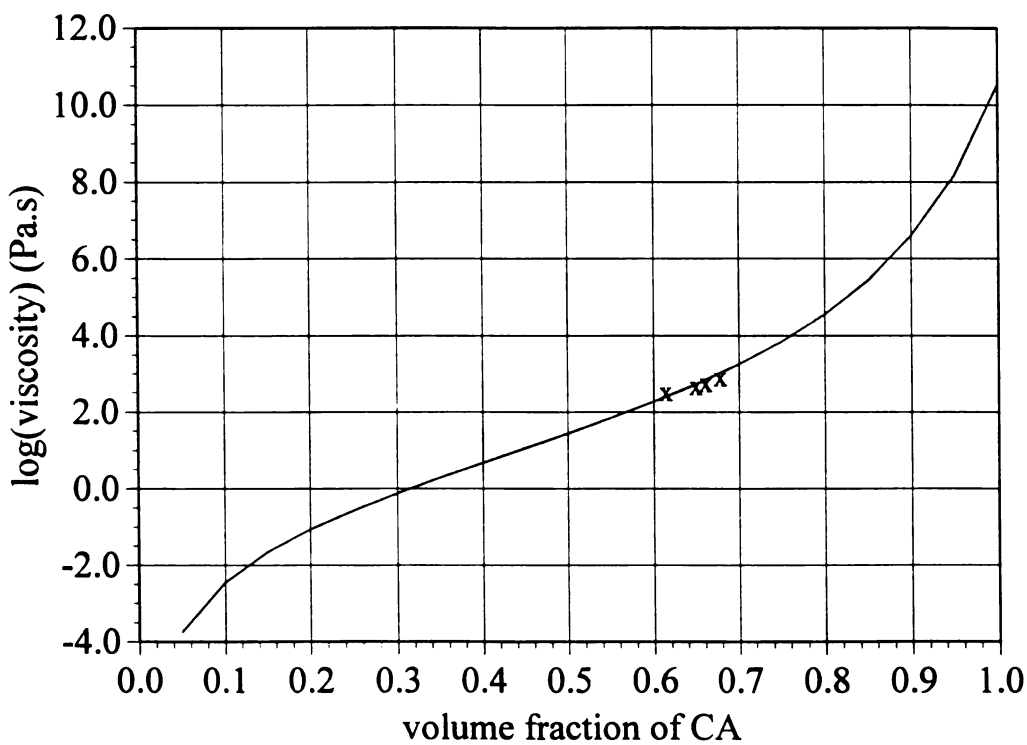

Figure 6.9: Kelly and Bueche Equation fit for CA/DEP data at 10 rad/s.

The value of Kand α_s used were 0.45 and 7.91 X 10^{-4} respectively. The same value of α_s was used for data at other frequencies, varying the value of K.

Figure 6.10 shows the estimated viscosity of unplasticized CA and the viscosity curves of the four CA/DEP blends.

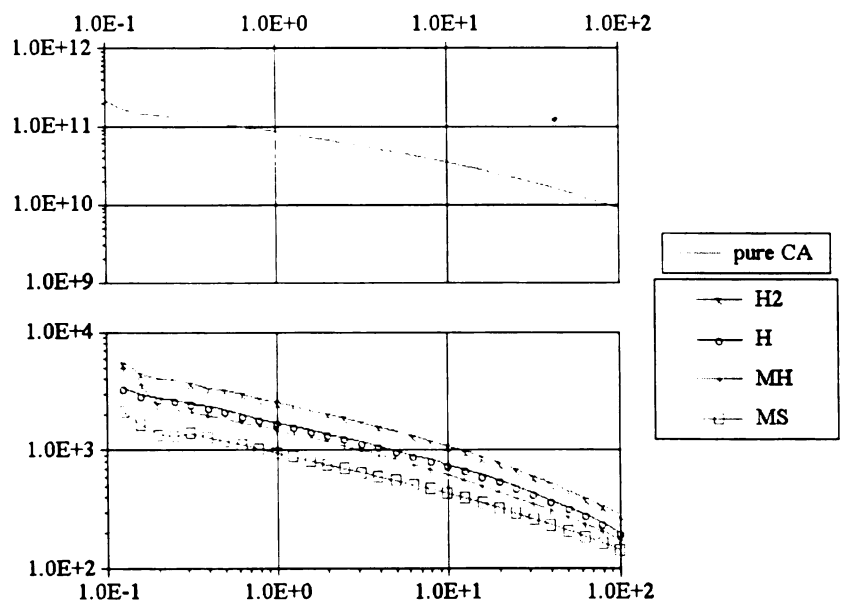

Figure 6.10: Viscosity curve of pure CA estimated by the Kelly and Bueche equation.

CA/PET Blends

Blends of Cellulose Acetate with two kinds of poly(ethylene terephthalate) were made without adding any catalyst for compatibilization. Blends were made by extrusion in the microtruder as well as the twin screw extruder. Rate of crystallinity studies were done on CA blends with highly crystalline PET as the high rate of crystallization was found to make extrusion difficult. Blends of CA with an amorphous grade of PET (EKX-105) were successfully extruded and characterized by thermal analysis and mechanical testing. The morphology of blends extruded both in the microtruder and in the twin screw extruder was studied by Scanning Electron Microscopy.

7.1 Crystallization - Background

A majority of engineering plastics like PET, PAT, PC, Nylon 66, PPS etc are semicrystalline. The crystallinity dictates the mechanical and thermal properties and the processing conditions of the polymers and their blends with other polymers and fillers. A review of the published literature on the crystallization of polymers in blends and alloys clearly indicates that the crystallization behavior and morphology of the component polymers are significantly modified by the presence of the other component [Nadkarni & Jog , 1989 (a)].

In a polymer blend, both the components may be crystalline or one may be crystalline and the other amorphous. In addition, the blends may be miscible or immiscible. In the case of immiscible blends, if there is a large difference in melting points of the polymers, the component with the higher melting point will crystallize in the molten phase of the other component which will affect the crystallization process through the effect of its viscosity on the mobility of the crystallizing polymer chains. On the other hand the lower melting polymer will crystallize in the presence of the solidified particles of the other component which may act as nucleating agents.

In the case of miscible blends, the presence of a single T_g widens or narrows down the temperature range of crystallization of the constituent polymers. If the T_g shifts nearer to the melting point of a polymer, both the degree and rate are seen to be reduced. The molecules of the crystallizing polymer may be hindered by those of the second component and in some rare cases co-crystallinity is observed. In such co-crystalline blends the components are mixed in the crystalline as well a the amorphous regions, for instance, a blend of low density polyethylene with a copolymer of ethylene, polypropylene and 1-4, hexadiene [Starkweather, 1982].

Due to the interplay of these factors, the morphology of a blend is more sensitive to the processing conditions and this can be utilized effectively to obtain a broader range of property combinations from a single blend composition.

Crystallinity behavior has been studied with DSC, DMA, dilatometry, density measurements, Wide Angle X-Ray Spectroscopy, X-Ray diffractometry, Infrared Spectroscopy and depolarized light-intensity measurements. As far as the effect of blending on the crystal structure is concerned, the published literature is limited, yet generally the crystal structure of the constituent polymer does not change appreciably by blending.

7.2 PET Blends and Alloys

PET is semi-crystalline polymer with a melting point of about 250°C. The crystallization of PET with other polymers has been widely studied due to its commercial importance.

Blends of PET with Crystalline Polymers

Wilfong et al [Wilfong, 1986] blends of PET and polyolefins (LLDPE, HDPE, PP etc). In these the crystallization of PET takes place in the melt of the other polymer and the rate of crystallization is reduced. A miscible blend of PET/PAT is reported by Escala and Stein [Escala, 1979] The T_g of PET is lowered resulting in an increase in crystallization rate of PET and a corresponding decrease in crystallinity for PAT. The rate of crystallization of PET is increased by the addition of polyphenyl sulphide (PPS) [Shingankuli] indicating enhanced nucleation due the presence of solidified PPS.

Blends of PET with Amorphous Polymers

Partially or completely miscible blends that have been studied are PET/PC [Nassar,1979], PET/polyarylate [Robeson, 1985] and PET/polyester carbonate blends [Ahroni, 1983] All of them exhibited a slower crystallization rate and a lower degree of crystallinity of PET in the blend due to an increase in the T_g of PET. An immiscible blend of PET/PMMA has been studied by Nadkarni and Jog [Nadkarni, 1987]. PET in the blend exhibited a lower degree of crystallinity, although the rate of crystallization was increased.

The effect of inorganic nucleating agents on crystallization of PET has also been investigated [Pryzgocki, 1975].

7.3 Crystallization of PET with Cellulose Acetate

The poly(ethylene terephthalate) used for these experiments was 'bottle regrind'. The isothermal crystallization kinetics of pure PET and two blends of PET with Cellulose Acetate was studied with the help of DSC. Blends of 90% PET/10% CA and 70% PET/30% CA (by weight) were prepared in the twin screw extruder. A 20 mg sample of the extrudate was then subjected to the heating program in a closed DSC pan. The temperature was raised above the melting point of PET and held there isothermal for 10 minutes to ensure that all crystallites melted. Then the temperature was brought down manually as fast as possible to the temperature required and held isothermal. After the crystallization was complete the sample was melted again and the enthalpy of melting was recorded. This was done at three temperatures (200°C, 210°C and 220°C) for the three blends (0%, 10% and 30% CA content).

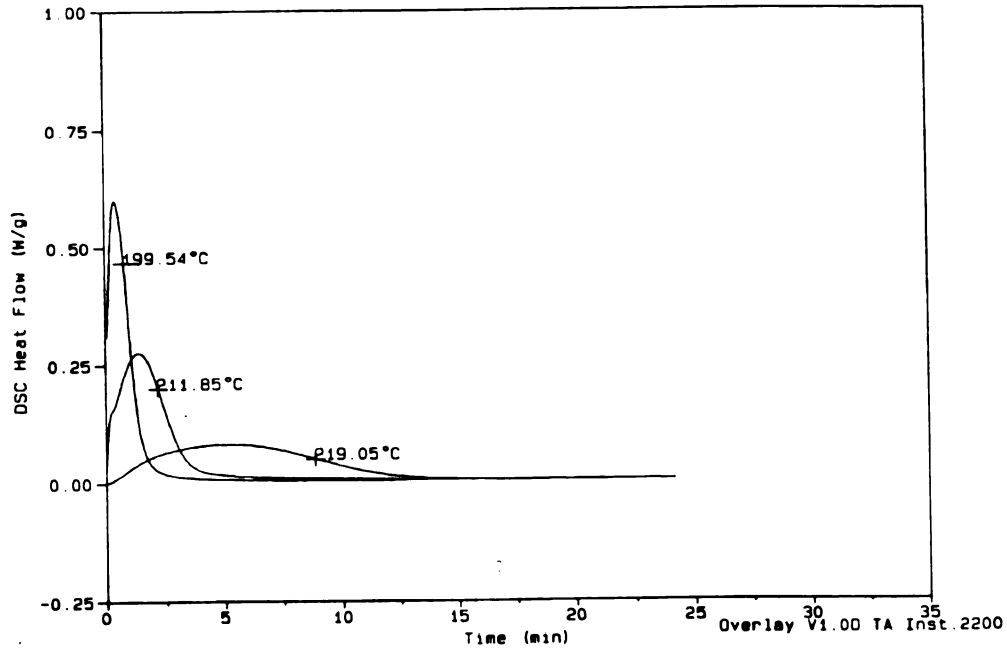

Figure 7.1: Crystallization exotherms of 100% PET.

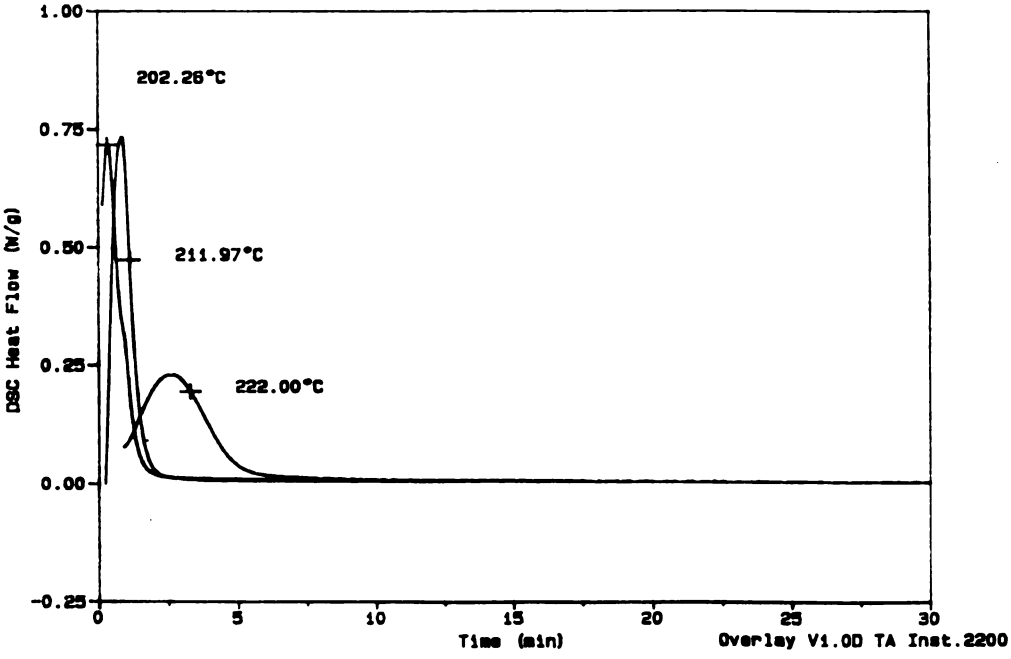

Figure 7.2: Crystallization exotherms of 90% PET/10% CA.

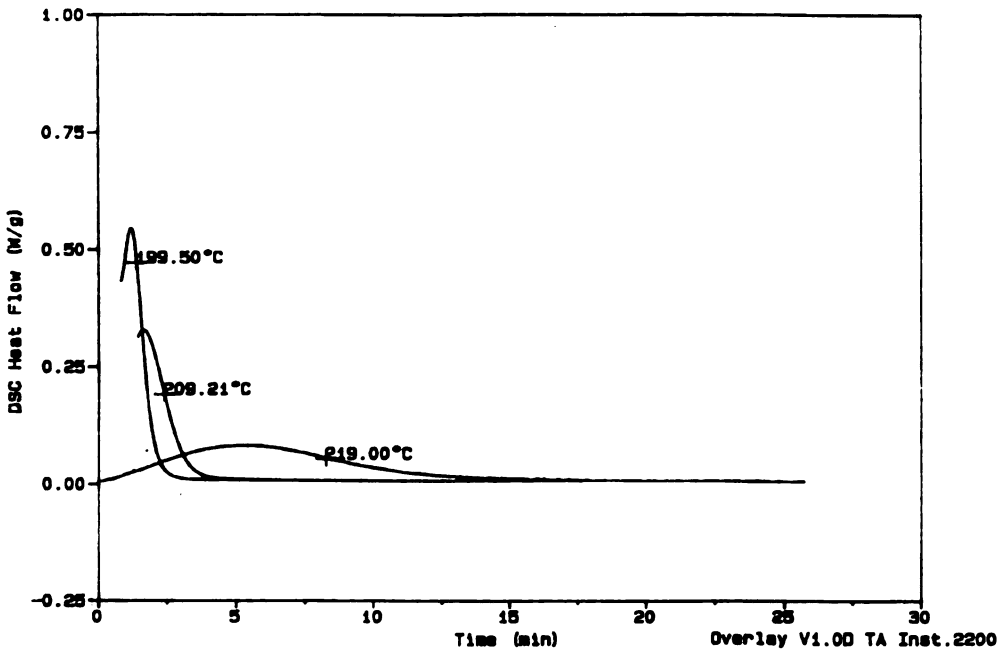

Figure 7.3: Crystallization exotherms of 70% PET/30% CA.

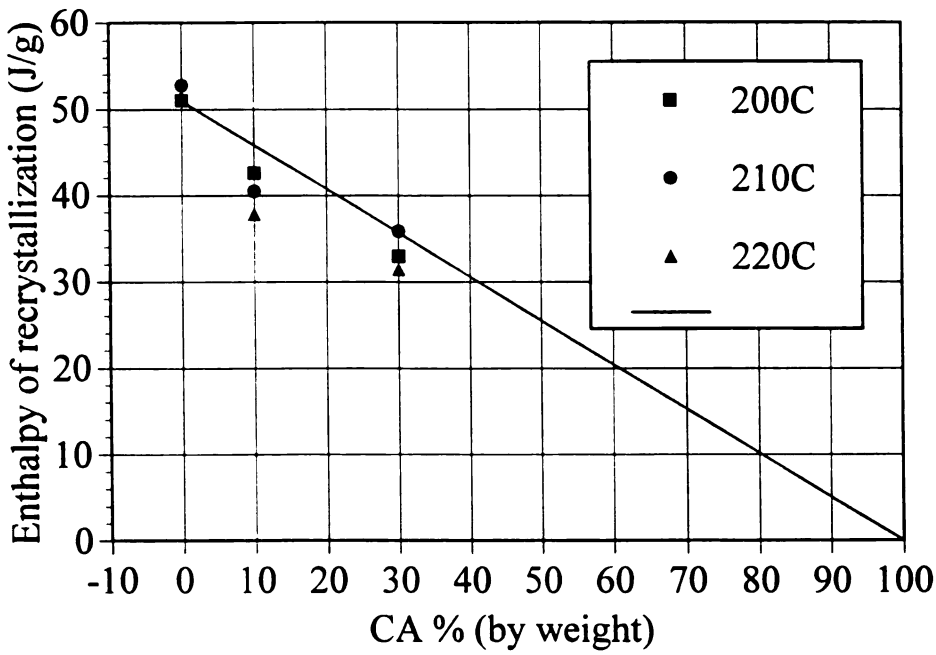

Figure 7.4: Enthalpy of recrystallization of CA/PET blends.

The rate of crystallization as seen is to be quite fast and therefore crystallization at temperatures less than 200°C could not be studied. It is seen that the rate of crystallization decreases with increasing percentage of CA even though 10% CA seems to aid in crystallization perhaps by providing sites of nucleation. Figure 7.4 shows the enthalpy of melting plotted as a function of CA percentage. A reduction in the extent of crystallization of PET is seen. Again for 10%CA at 220°C the reduction is not much. The following table summarizes the results. The rate of crystallization is characterized by a "characteristic time" (T') defined as the time taken for the crystallization to complete after the maxima in the crystallization exotherm is observed.

Table 7.1: Crystallization in CA/PET blends.

CA/PET Blend	Temp(°C)	T'(s)	H_m(J/g)	T_m(°C)
0 % CA	200	128	50.98	250.33
	210	184	52.68	249.01
	220	1218	51.43	248.58
10 % CA	200	92	42.48	251.57
	210	111	40.41	247.44
	220	151	37.69	250.78
30 % CA	200	90	32.85	252.62
	210	156	35.74	246.58
	220	1252	31.67	244.70

The fast rate of crystallization and high melting point of PET made extrusion difficult due to the following reasons

1. The Cellulose Acetate degrades during processing at temperatures above 260°C.
2. If the temperature is kept low (~ 260°C), the PET starts crystallizing in the cold spots of the extruder clogging up the barrel and die.

Because of these reasons an amorphous grade of PET (EKX-105) supplied by Hoechst-Celanese was investigated. Copolymerization with a second component (neo-pentyl glycol) reduces both the crystallinity and the melting point to ~ 220°C. This was found suitable to extrude with Cellulose Acetate.

To extrude CA with PET bottle recycle, cold spots and high residence times in the die and barrel of the extruder should be avoided. It was later realized that blends with high CA content could be extruded as the CA matrix helped in the flow of PET even if it had crystallized. A 80% CA/ 20% PET blend was extruded without much degradation. the properties have been included in Chapter 8 along with other compatibilized blends of the same composition.

7.4 CA/EKX blends

Blends of Cellulose Acetate and "TRANSPET EKX-105" grade PET were extruded in the twin screw extruder in composition ranging from 0-95% CA content by weight. Blends with higher CA content had to be extruded without a die as explained in Section 4.3. The temperatures used are given in Table 4.1. Only 95% CA/5% EKX blend showed some discoloration and blends with higher CA content showed unacceptable degradation.

7.4.1 Mechanical Properties

Figures 7.5 to 7.8 show the strength at break, tensile modulus, elongation at break and Izod impact strength respectively of the CA/EKX blends. Due to technical difficulties, enough material could not be extruded for the mechanical testing of 80% EKX/20% CA blend though we can expect that it's properties would follow the general trends.

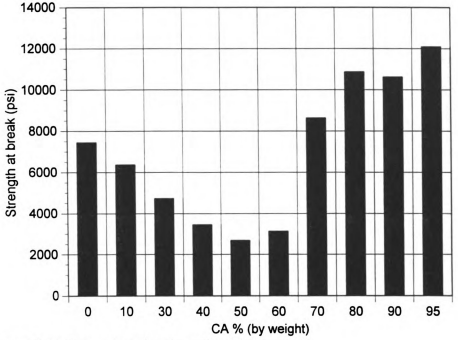

Figure 7.5: Strength at break of CA/EKX blends.

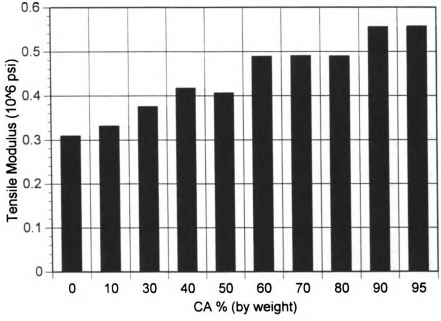

Figure 7.6: Tensile modulus of CA/EKX blends.

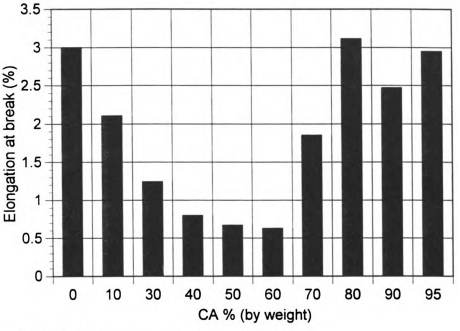

Figure 7.7: Elongation at break of CA/EKX blends.

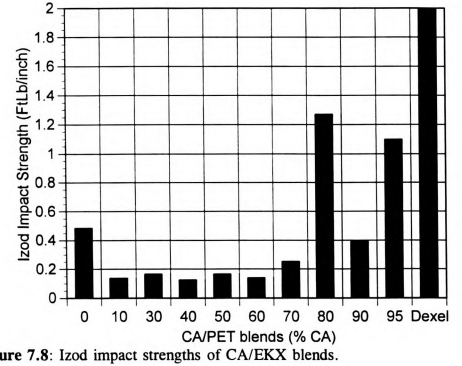

Figure 7.8: Izod impact strengths of CA/EKX blends.

It is seen that the modulus increases consistently with increasing CA content whereas there is a dip in strength and elongation at break around 50% CA content. This is due to the morphology of the blend. The phase size of the dispersed phase becomes quite large and there is no well defined continuous phase at intermediate concentrations. At higher concentrations the CA phase becomes the matrix resulting in an increase in properties. At 70% and 80 % CA content, the morphology is fibrillar and it seems that fiber-pull and fiber elongation are important energy absorbing mechanisms and result in an increase in impact strength (also see Section 8.7). The morphology of the blends will.be discussed in more detail later. These results show that the excellent inherent properties of CA can be recovered by avoiding the use of monomeric plasticizers like DEP and DOP. This increase in mechanical properties is at the cost of clarity and impact strength (2 ft lb/in of notch for CA with 33% DEP).

There is a large decrease in Izod impact strength due to blending. This is most probably due to the large interfacial stress between the two phases. Compatibilization of the two phases generally increases the impact strength of a composite due to better stress transfer at the interface. There is usually an optimum for the dispersed phase size which gives he highest impact strength. Compatibilization should also reduce the phase size of the dispersed phase which could also result in an increase in strength and elongation. Another possible advantage of reduction in dispersed phase size (below the wavelength of light) could be increased transparency of the blend, specially thin films. The effect of reaction on the properties and morphology of the blends is discussed in Chapter 8.

7.4.2 Thermal Analysis

Thermal tests were performed on the extruded samples to check for any changes in glass transition temperatures, melting point, crystallinity etc. A reduction in melting points, or a change in glass transition temperatures can be taken as indicative of miscibility of the two phases. Co-crystallinity is also desirable in a composite as it results in a high strength and modulus. Figure 7.9 show the glass transition temperatures of the two phases as measured by DSC and DMA.

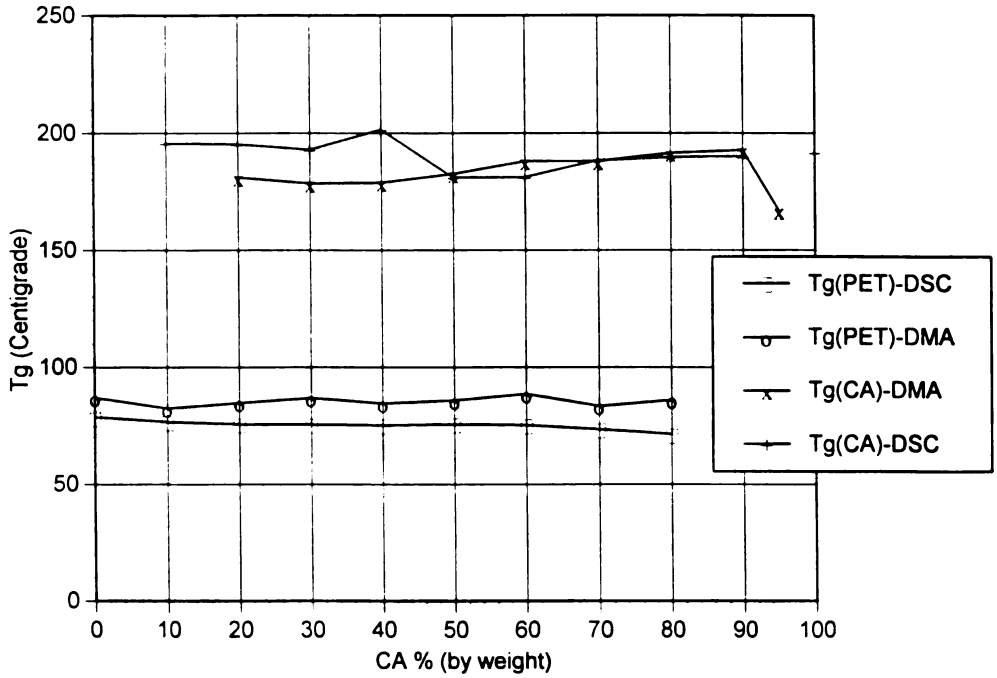

Figure 7.9: Glass transition temperatures of CA/EKX blends.

The data does not suggest any signs of miscibility. The DSC consistently shows T_g of EKX as 5-10°C lower than that measured by the DMA. The T_g of CA does not show any such regular trend.

Figure 7.10 shows the melting points of the CA/EKX blends from DSC endotherms. Since the melting points of both CA and EKX phases are quite close, separate melting endotherms are not observed but rather a composite peak is observed. Thus it is not possible to tell the extent of crystallization of each phase.

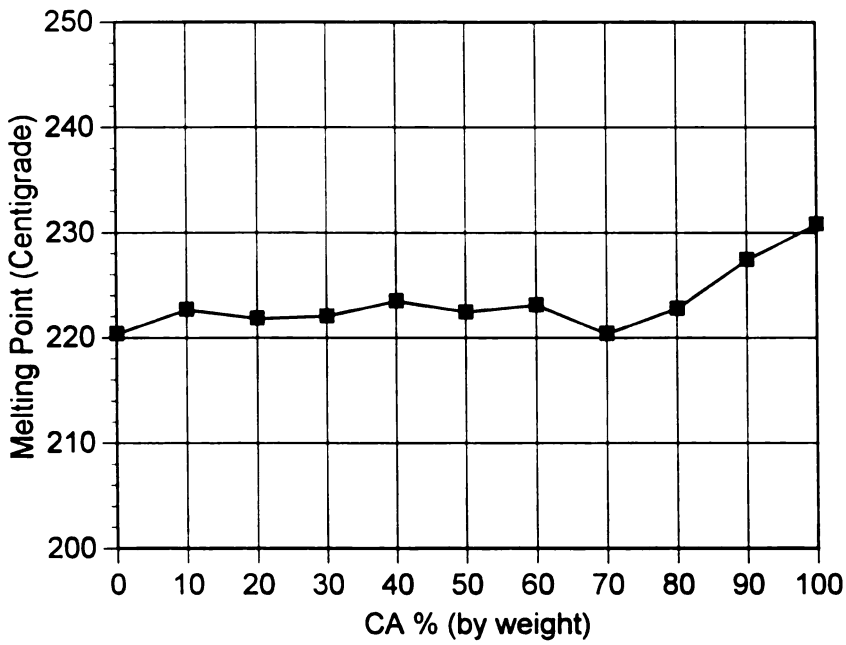

Figure 7.10: Melting points of CA/EKX blends.

The melting point observed is quite constant. Thus it can be said that blending is not causing a change in the structure of crystallites of either phase otherwise some change in melting point would be observed. Figure 7.11 shows the enthalpies of melting of the CA/EKX blends. It is seen that the crystallization of the CA phase is suppressed (otherwise the enthalpy data would have been along the upper dashed line instead of the bold line). For the same reason, it can be said that the crystallinity of EKX is not

affected by the presence of the CA phase. Another explanation can be that the reduction in crystallinity of EKX is offset by the crystallinity of CA phase so as to give enthalpy data along the full line (which assumes only EKX crystallinity from 0 to 100%).

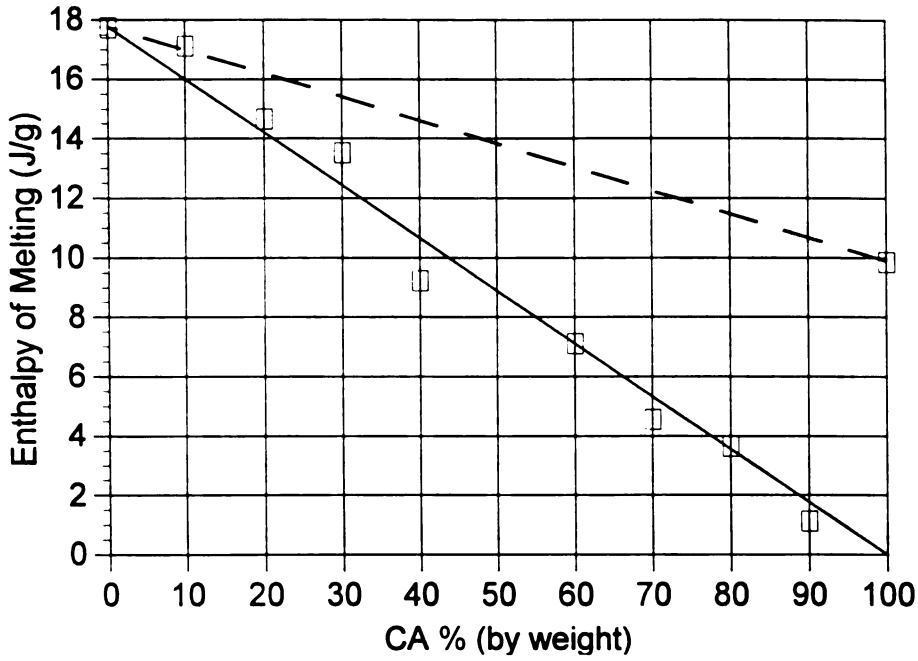

Figure 7.11: Enthalpy of melting of CA/EKX blends.

7.4.3 Morphology of CA/EKX blends

The morphology of the blends was studied by looking at the extruded material with a Scanning Electron Microscope. The samples were fractured in directions parallel (longitudinal) and perpendicular (transverse) to the direction of flow after freezing under liquid Nitrogen. Only the areas representative of the blend were photographed. The dimensions mentioned are approximate and read directly off the photographs. The average diameter was calculated by averaging the diameters of 10-40 particles.

In general, the twin screw extruder gave more homogenous blends, had better dispersion and distribution of the minor phase than the Microtruder. In blends with less CA content, the CA was dispersed in the form of spherical particles. The particle size increased with increasing CA content and at around 40% CA the particles start to coalesce and get elongated. In the Microtruded 50/50 blend there is no well defined matrix. In blends with more than 50% CA, the EKX phase gets elongated into a fibrilla morphology consisting of long thin fibrils with diameter 0.5-10 microns and lengths more than 100 microns. The Microtruded blends had thinner fibrils than those extruder in the twin screw extruder but the was more variation in the size of the fibrils. At 90% CA, the EKX phase was in the shape of droplets with some particles elongated into fibrils.

Figure 7.12 shows a longitudinal section of Microtruded 10% CA/90% EKX blend. This morphology is typical of low CA content blends where the CA phase is in the shape of spherical particles. The dispersion is not very homogenous in this blend and there is no evidence of interfacial adhesion between the two phases (there is an annular space between the CA particles and the EKX matrix which arises due to the difference in extent of contraction of the materials upon cooling).

Figure 7.13 shows a section of a Microtruded 40% CA/60% EKX blend. In this blend (as well as in Microtruded 30% CA/70% EKX blend), the CA phase is present in the form of elongated relatively thick, rod like structures of varying cross-sectional shapes and sizes. The EKX is clearly the matrix and again the blend is non-homogenous. The corresponding blends extruded in the twin screw extruder are homogenous and the CA phase is present in the form of spherical particles 1 to 10 microns in diameter.

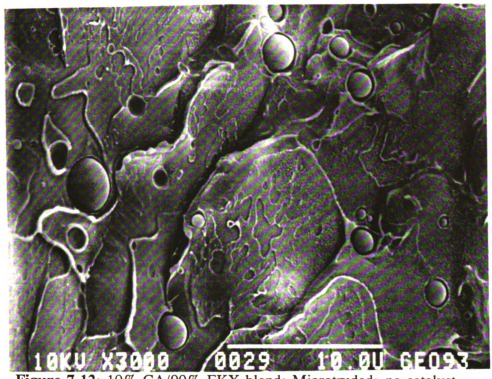

Figure 7.12: 10% CA/90% EKX blend; Microtruded; no catalyst. Sectioning parallel to direction of flow.

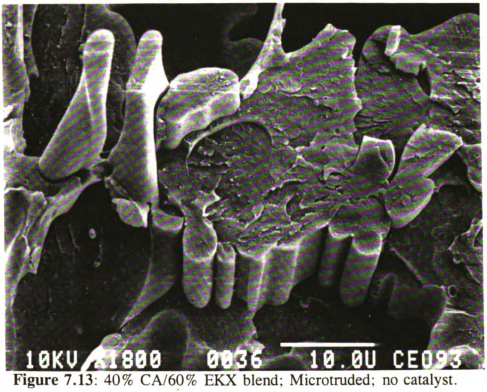

Figure 7.13: 40% CA/60% EKX blend; Microtruded; no catalyst. Sectioning parallel to direction of flow.

Figure 7.14 shows a longitudinal section of Microtruded 50% CA/50% EKX blend. There is no well defined matrix and a mechanically interlocking morphology of two phases can be seen (the fractured surface of the CA phase has a smoother texture than the EKX phase). Figure 7.15 shows a transverse section of the corresponding twin screw extruded blend. The EKX is again the matrix and the CA particles are spherical with diameters ranging from 2 to 15 microns.

Figure 7.16 shows a longitudinal section of a Microtruded 60% CA/40% EKX blend. The EKX phase is now elongated with phase size ranging from 0.25 to 10 microns in diameter and upto 100 microns long. These fibrils are aligned in the direction of flow. The corresponding twin screw extruded blend is more homogenous and the EKX fibrils are shorter with a diameter of about 10 microns.

Figure 7.17 shows a longitudinal section of a Microtruded 70% CA/30% EKX blend. the blend is now quite homogenous. The EKX phase can clearly be seen as long and thin fibrils (only the channels from where the fibrils were pulled out can be seen , though one fibril is seen on the right hand side of the micrograph) with diameter of about 0.4 microns.

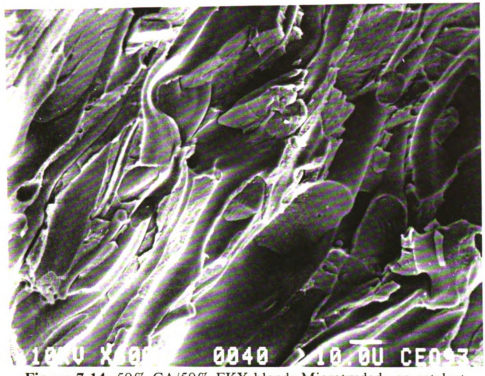

Figure 7.14: 50% CA/50% EKX blend; Microtruded; no catalyst. Sectioning parallel to direction of flow.

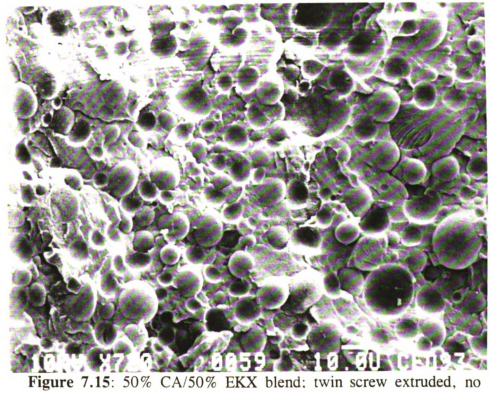

Figure 7.15: 50% CA/50% EKX blend; twin screw extruded, no catalyst. Sectioning perpendicular to direction of flow.

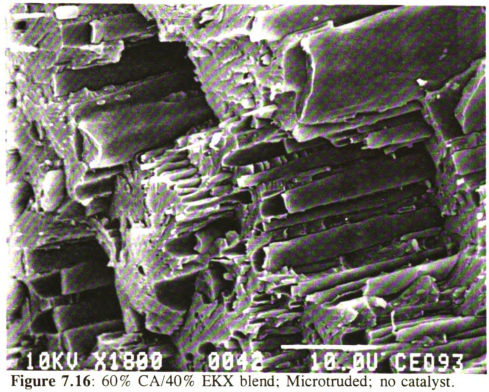

Figure 7.16: 60% CA/40% EKX blend; Microtruded; no catalyst. Sectioning parallel to direction of flow.

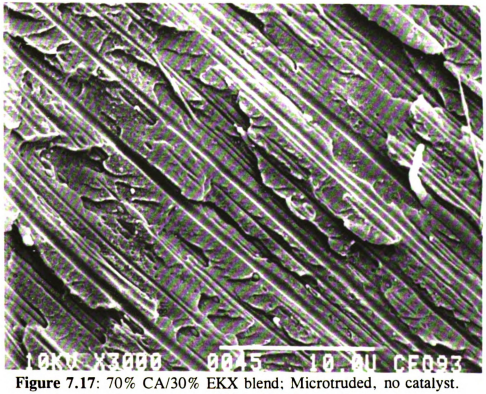

Figure 7.17: 70% CA/30% EKX blend; Microtruded, no catalyst. Sectioning parallel to direction of flow.

Figure 7.18 shows a low magnification micrograph of a twin screw extruded 70% CA/30% EKX blend. The EKX fibrils are seen to be several hundred microns in length and have an average diameter of about 2 microns. the fibers are excellently aligned along the direction of flow. This may be due to the uniaxial strain due to the pelletizer. Instead of the screw pushing the blend out through the die, in this case, the blend was pulled out of the extruder by the pelletizer and this would have caused the EKX dispersed phase to be pulled into fibers and highly aligned in the direction of flow.

Figure 7.19 shows the longitudinal section of a twin screw extruded 80% CA/20% EKX blend in which the EKX fibers have not been pulled out and can be clearly seen the micrograph. Again, the fibers are quite thin (diameter $\sim$ 1 micron), as can be seen in the transverse section of the same blend in Figure 7.20.

In the 90% CA/10% EKX blend most of the EKX is dispersed as droplets though some droplets have been elongated. The blend extruded in the twin screw extruder (Figure 7.21) is homogenous whereas the microtruded is blend is non-homogenous (there is a large difference in the sizes of the dispersed droplets and the elongated EKX phase).

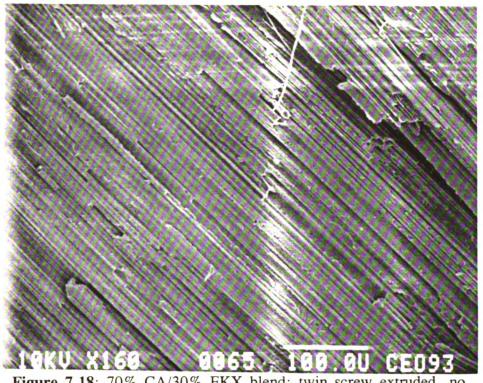

Figure 7.18: 70% CA/30% EKX blend; twin screw extruded, no catalyst. Sectioning parallel to direction of flow.

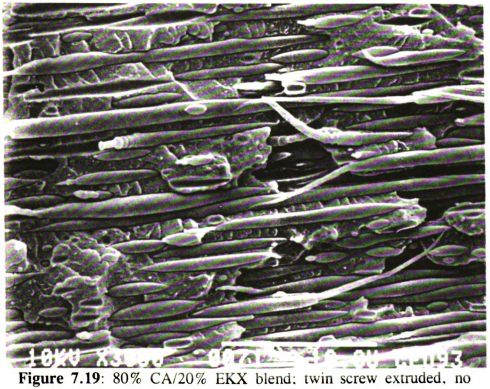

Figure 7.19: 80% CA/20% EKX blend; twin screw extruded, no catalyst. Sectioning parallel to direction of flow.

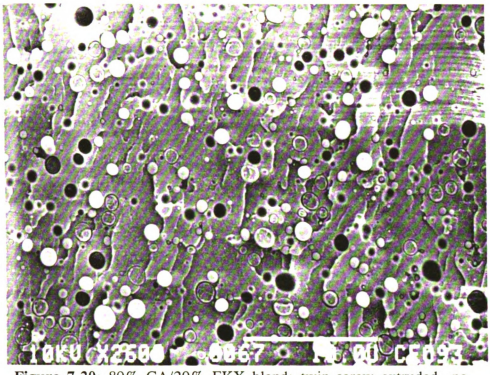

Figure 7.20: 80% CA/20% EKX blend; twin screw extruded, no catalyst. Sectioning perpendicular to direction of flow.

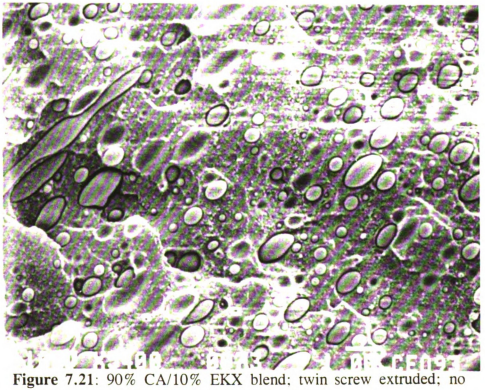

Figure 7.21: 90% CA/10% EKX blend; twin screw extruded; no catalyst. Sectioning parallel to direction of flow

In all these micrographs the CA is seen as a distinct phase than EKX with no sign of adhesion between the two phases. They also illustrate the phenomenon of 'in situ' fiber formation in polymer blends. By removing the die and pulling the strand by the pelletizer, the fibrillation is seen to be enhanced. According to Elemendorf and Van der Vegt [Elemendorf, 1991] the continuous elongation of droplets does not cause enough instability so as to cause break up of the fiber. According to Vinogradov [Vinogradov, 1974], the fibrillar structure in an elongation flow may break up if the residence time in the capillary is longer than the break up time for fiber-like domains. Removing the die, (which has got a converging flow followed by a short capillary (see Figure 4.2), thus also prevents the fibers from breaking up.

Table 7.2 summarizes the morphology of CA/EKX blends extruded in the Microtruder and the twin screw extruder.

Table 7.2: Morphology of CA/EKX blends.

CA % (by weight)	Microtruded	Twin screw extruded
10	CA spherical, not homogenous; particle diameter ~1.5 microns.	CA spherical, homogenous; particle diameter ~1 micron.
20	CA spherical, not homogenous; particle diameter ~1.5 microns.	CA spherical, homogenous; particle diameter ~2 microns
30	CA elongated, not homogenous; d ~7 microns, l > 30 microns.	CA spherical, homogenous; particle diameter ~3 microns.
40	CA elongated, homogenous; d ~ 2-10 microns	CA particles spherical, some fused together; d ~ 6 microns.
50	No well defined matrix.	CA dispersed phase, large particles; d ~ 10 microns.
60	EKX elongated,homogenous; d ~2 microns, l > 50 microns.	EKX elongated, relatively thicker; d ~ 10 microns.
70	EKX fibrillar, long, thin; d ~ 0.4 microns, l > 50 microns.	EKX fibrils highly aligned, long; d ~ 2 microns,
80	EKX fibrillar, long, thin; d ~ 0.4 microns.	EKX fibrillar, thin, some breakup; d ~ 1 micron.
90	Some EKX particles elongated, very non-homogenous.	CA spherical, little elongation, homogenous d ~ 1 micron.

7.4.4 Viscosity

The zero shear viscosity, η_0, of liquid mixtures has been described by a number of simple relations called the additivity rules one of which is [Utracki, 1983]

$$\ln \eta_o = \Sigma X_i \ln \eta_i$$

where X_i and η_i are the weight fraction and viscosity of component i. These additivity rules are followed by ideal mixtures, devoid of any large thermodynamic interactions. Polymer blends usually do not follow these equations and generally show positive, negative or both positive and negative deviations from the log additivity rule [Utracki, 1982]. Figure 7.22 shows the complex viscosities of CA/EKX blends as a function of composition for four different frequencies (in rad/s).

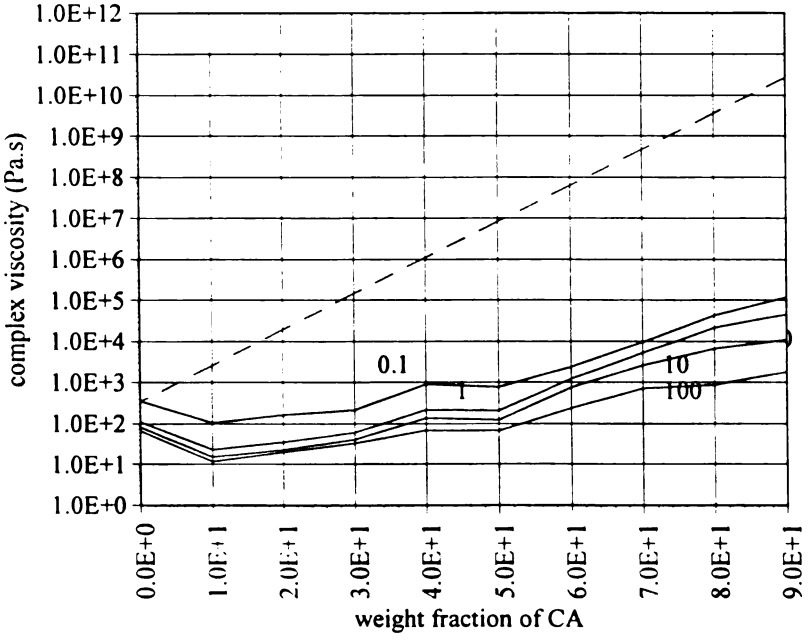

Figure 7.22: Complex viscosities of CA/EKX blends.

The CA/EKX blends are seen to have a negative deviation from the log additivity rule (shown by the dashed line). The predictions by log additivity rule were calculated by using the estimated viscosity of CA (see section 6.6) of 2.09 X 10^{11} Pa.s and 352 Pa.s for EKX, both at 0.1 rad/s. This negative-deviation type behavior is typical of immiscible blends and other blends like Polyamide-6/PET, LDPE/PS etc. also are negative - deviation blends [Utracki, 1983]. One of the proposed explanations for this behavior is that due to lack of adhesion between the domains of the two polymers, there is slippage. For such systems with slippage, it should be expected that viscosity would be dependent on the morphology and type of strain. It is interesting to note that the drop in viscosity corresponds to the drop in properties such as Izod impact strength, strength at break and elongation at break.

7.5 Theoretical prediction of modulus

Several theories exist to predict the elastic properties of multiphase polymers as a function of composition and temperature. For a heterogeneous blends of two polymers, a broad range of responses to mechanical deformations is possible, depending o blend morphology, on the degree of molecular mixing or interpenetration, compatibility at the interfaces and on the size of the phase separated regions- as well as on the properties of blend constituents [Dickie, 1978].

There are three principle groups of models that have been applied to the problem of predicting modulus-composition dependence:

1. Mechanical Coupling Models: These are empirical mechanical models used to predict modulus. They are not however, morphologically or mechanically realistic models of blend structure and response. The models of Takayanagi, Kraus and Rollman and Fujino fall in this category. They employ various arrangements of the familiar spring and dashpot models to describe the dynamic mechanical response of a heterogenous system.
2. Self-Consistent Models: In these models, the mechanical response of an idealized representative composite structure (comprising of a dispersed phase particle embedded in a matrix) is compared with that of a homogenous body having the properties of the composite. the Kerner model [Kerner, 1956], modified Kerner models and van der Poel's derivation [C, van der Poel, 1958] fall in this category.
3. Bounds on the modulus: In these the strategy is to calculate upper and lower

bounds on the composite moduli. The models of Paul [Paul, 1960], Hashin [Hashin, 1962] and Hashin and Shtrikman [Hashin, 1963] fall in this category. Often the bounds are too widely separated to provide an useful prediction of the response but coincide for a few special cases [Hill, 1963].

In the following figures, the prediction of three models have been compared with the experimental data. Similar analysis for poly(urethane-urea) blends has been done by Ryan et al [Ryan, 1991] and for SAN/PC blend by Kodama [Kodama, 1993]. The Kerner equation

$$G_c = G_1 \frac{\phi_1/\nu' + \phi_2 G_2/G_1'}{\phi_1/\nu' + \phi_2 G_1/G_1'} \qquad (7.1)$$

requires that the materials be isotropic, that the dispersed phase is spherical and there is good adhesion at the interface. Here $\nu = 1(1\text{-}\nu_1)$ and $G' = (7\text{-}5\nu_1)G_1 + (8\text{-}10\nu_1)G_2$, where G_c is the composite shear modulus, ϕ is the volume fraction and ν is the Poisson's ratio. Subscripts 1 and 2 refer to the matrix and filler respectively.

The Davies model [Davies, 1971]

$$G_c^{1/5} = \phi_1 G_1^{1/5} + (1 - \phi_1) G_2^{1/5} \qquad (7.2)$$

has been derived for two incompressible interpenetrating continuous phases with perfect bonding at the interface.

For materials without a well defined morphology, Budiansky [Budiansky, 1965] has modified Kerner's equation. The model assumes that both components are continuous but the material is isotropic and macroscopically homogenous. The composite modulus

is obtained from a solution to the quadratic equation

$$\phi_1(G_1 - G_c)(G_c + \alpha G_2) + \phi_2(G_2 - G_c)(G_c + \alpha G_1) = 0 \qquad (7.3)$$

where $\alpha = 2(5-4\nu_c)/(7-5\nu_c)$ and ν_c is the Poisson's ratio of the composite and in this case is taken to be the weighted average of the Poisson's ratio of the two components.

For all calculations, the Poisson's ratio have been taken as 0.44 for both EKX and CA. Pure CA complex shear modulus is taken as 1.305 MPa and Young's modulus is taken as 5.665 X 10^5 psi. The Davies equation requires the materials to be incompressible, i.e. Poisson's ratio = 0.5 but the error introduced is negligible. Figure 7.22 is a semi-log plot of complex shear modulus (measured by DMA) versus volume fraction of CA and Figure 7.23 is a semi-log plot of Young's modulus (measured by Tensile tests) versus volume fraction of CA. In these figures the boxes are experimental data; the upper full curve is the prediction of Kerner equation for a blend with CA as the matrix; the lower chain curve is the prediction of Budiansky equation; the upper chain curve is the prediction of the Davies equation and the lower full curve is the prediction of Kerner equation with EKX as the matrix.

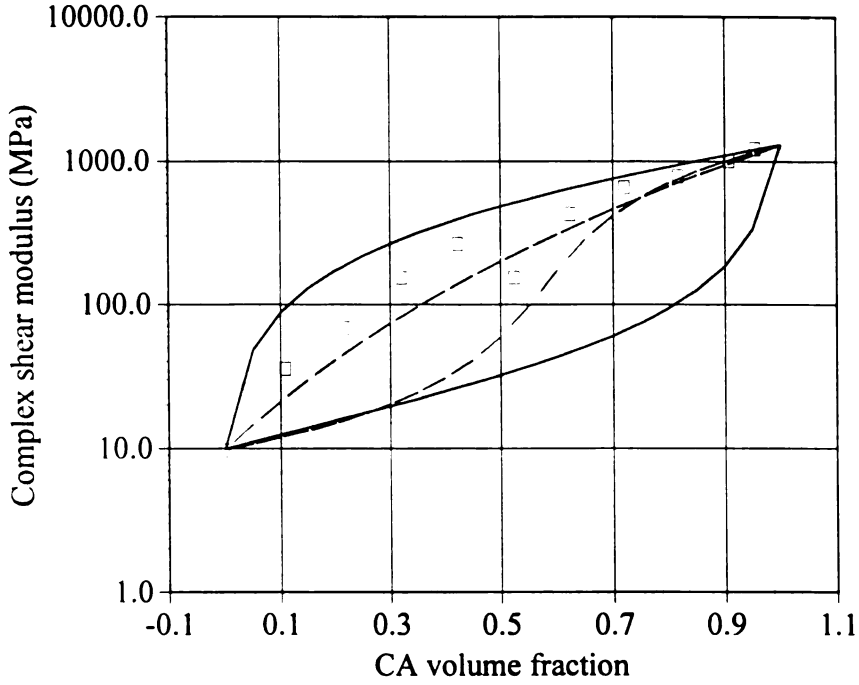

Figure 7.23: Prediction of complex shear modulus for CA/EKX blends.

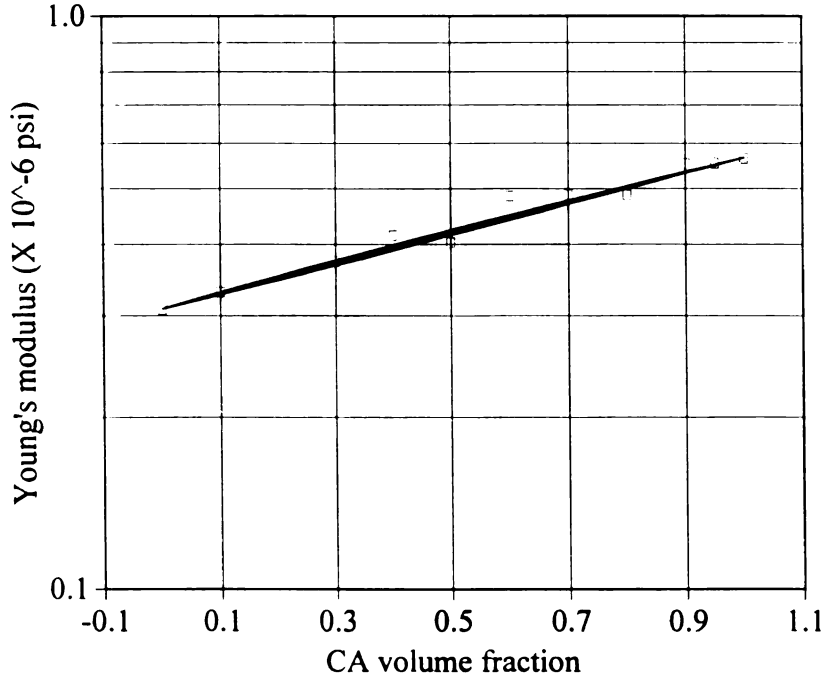

Figure 7.24: Prediction of Young's modulus for CA/EKX blends.

It can be seen that the observed modulus is consistent with the prediction of the models. Indeed, the experimental data obtained seems to be on the higher side of the predicted range. This could be interpreted as an indication of good interfacial adhesion since the models used are derived with this assumption [Allen et al, 1974]. However here, modulus values for 100% CA have been estimated. Actual values could be much higher which would predict higher values for the blends. The decrease in impact strength could also be indicative of poor interfacial adhesion.

Reactive Compatibilization

The Scanning Electron Micrographs and low impact strengths of uncompatibilized blends of CA and PET suggested poor interfacial adhesion. Advantage is taken of the ester groups in the polymer backbone of PET and the ester groups of CA to form a compatibilizing copolymer via trans-esterification reaction. It was attempted to characterize the extent of the reaction and the compatibilizing effect with extraction, mechanical tests, thermal analysis and Scanning Electron Microscopy.

8.1 Trans-esterification

Condensation polymers normally have potentially reactive groups inherent in the backbone and at the chain ends. For instance polyamides have carboxylic acid and amine endgroups and amide groups in the backbone. PET has ester groups in the backbone and hydroxyl and carboxylic acid end groups. The ester groups of Cellulose Acetate are also potentially reactive. Therefore it was attempted to form a copolymer of CA and PET via trans-esterification which could act as a compatibilizer for the two phases. Interchange reactions involving chain end groups, ester groups and hydroxyl groups of CA are also possible. Trans-esterification would result in a copolymer consisting of a CA backbone with PET side chains. the breaking of the ester bond in the PET backbone would result

in shorter chain lengths (Figure 8.1). On the other hand a reaction between the end groups of PET and the hydroxyl and/or the ester groups on the glucopyranosyl units would give longer PET side chains.

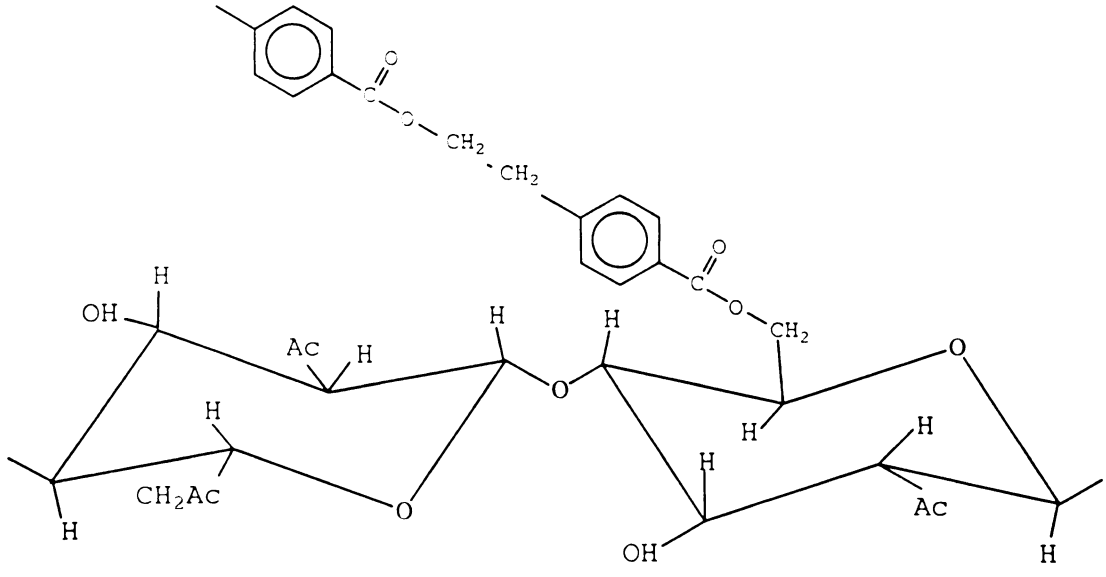

Figure 8.1: CA backbone grafted with PET.

Three types of interchange reactions are theoretically possible:

$$R_1CO\text{-}OR_2 + R_3OH \rightleftharpoons R_1CO\text{-}OR_3 + R_2OH$$

$$R_1CO\text{-}OR_2 + R_3COOH \rightleftharpoons R_3CO\text{-}OR_2 + R_1COOH$$

$$R_1CO\text{-}OR_2 + R_3CO\text{-}OR_4 \rightleftharpoons R_1CO\text{-}OR_4 + R_3CO\text{-}OR_2$$

Since the end-group concentration is very small compared to the ester groups, trans-esterification would be the more predominant reaction.

In recent years considerable interest has arisen in the study of blending of polyesters and in the exchange reaction which may occur during the melt mixing process. Montaudo et al [Montoudo, 1992] have investigated interchange reaction between poly(thylene adipate) and PET. Dröscher [Dröscher, 1981] investigated the ester interchange between PET and an oligoester with di(oxyethylene) units. Tranesterification between poly(butylene terephthalate) and Polyarylate led to reduced crystallinity and melting points [Miley & Runt, 1992; Espinoza, 1993] and for PET/Polyarylate systems increased miscibility led to a slight densification [Robeson, 1985]. The PET/Polycarbonate system has been investigated by many authors [Pilati, 1985; Dewaux, 1982; Nassar, 1979]. The difference between these systems and the CA/PET system is that in CA the ester groups are not in the backbone and so the CA chain remains intact. Unlike the other systems in which the final result of a very high degree of interchange reaction would be a random copolymer, in the CA/PET system, small PET segments would be grafted at many places along the CA chain.

8.2 Characterization of the reaction

For miscible blends factors determining T_g and Melting Point change, viz., interchain versus intrachain interaction, crystallites formed etc. So thermal analysis provides an easy method to monitor the progress of the reaction. IR and NMR spectroscopies are preferred among the few direct and quantitative analysis methods, despite their lack of sensitivity at low reaction levels [Espinoza, 1993].

Cellulosic graft copolymer are somewhat easier to separate from their homopolymers than other systems due to greater solubility differences. Extraction procedures and solution followed by fractional precipitation have both been used. A density gradient ultracentrifugation technique has also been used [Krassig, 1965]. Another advantage of cellulosic grafts is that the cellulose (or it's derivative) backbone can be destroyed by acid hydrolysis and the side chain isolated for studying the molecular weight distribution and other properties.

It was decided to use extraction with a Soxhlet tube to characterize the reaction since a small extent in reaction would translate as a much larger change in the amount that could be extracted. Acetone was used a the solvent to extract the CA phase. The transesterification catalyst was added to a 80/20 (by weight) feed of CA/EKX blend. The extrudate obtained was dissolved in phenol (common solvent) and reprecipitated in Methanol. The precipitate was filtered out and washed with methanol and then with water. The precipitate was then dried in a vacuum oven. By this method it was hoped to get a porous and "loose" structure was obtained in all the CA phase was easily accessible to the solvent. Unfortunately it was difficult to get consistent results by this method and it was decided to perform extraction of powdered (or rather "shredded" since the blend was fibrous) samples.

About 10 g of the dried shredded sample thus obtained was added to a (dried) extraction thimble and the CA phase was extracted with Acetone in a Soxhlet apparatus for 24 hours at the end of which the thimble was again dried and weighed giving the weight of the residue. The difference between the original weight of the precipitate and

the residue gave the weight of the extract. The samples and the thimble were dried in a vacuum oven at 60°C for at least 5 hours. Table 8.1 shows the results obtained. Extraction was also carried out on a physical mixture of 80% CA and 20% EKX to compare with other blends.

Table 8.1: Extraction results.

S. no.	Catalyst (by weight)	weight % of total extracted.
1	Physical mixture	27.4
2	No catalyst	13.1
3	0.05% FASCAT 4201	11.4
4	0.2% FASCAT 4202	9.0
5	0.05% DMAP	9.1
6	0.05% Sn. Oc.	17.3
7	0.9% $Ti.BuO_4$	7.5

These results indicate that less material can be extracted with more compatibilization. It is assumed that in all the blends, the extractable phase is equally accessible to Acetone, though this may not be entirely true in the case of the physical blend (which was not extruded like the rest of the blends). It is also interesting to see that

even without adding catalyst, there is some evidence of compatibilization. This may be due to the esterification catalyst(s) already present in the EKX which are known to promote transesterification or simply due to hydrogen bonding.

8.3 Processing of CA with PET-bottle recycle

With the isothermal crystallization studies on CA/PET blends, it was realized that, crystallization of PET, it was necessary that long residence times and cool spots in the extruder and die should be avoided. However, to minimize degradation of CA, the temperatures have be kept as low as possible. Low die temperatures also help in the processing of the extrudate as PET has a very low melt strength. Another phenomenon that was making processing difficult was the strain induced crystallization of PET. PET molecules are known to orient during elongational flows and crystallize even at temperatures very near it's melting point [Van der vegt, 1967].

In view of the above limitations on the processing conditions, it was decided to extrude a 80% CA/20% PET blend without the die to prevent elongational flow. The high percentage of CA would also help in the transportation of any PET which had crystallized.

Table 8.2 shows the temperatures used for extrusion of CA/PET blend. The RPM was 200 as before and the feed rate was 10%. The conditions for injection molding are shown in Table 9.3

Table 8.2: Temperatures used for extrusion of CA/PET.

Zone	Set Temperature (°C)	Melt temperature (°C)
feed zone	210	154
1	280	283
2	275	274
Die	225	239

Very slight discoloration was observed. The strand could be directly pulled out from the screw end by the pelletizer roll and pelletized.

Table 8.3: Temperatures used for injection molding CA/PET.

Zone	Temperature (°C)
1	250
2	268
nozzle	235

The injection time was 1.8 s, the holding time 5 s and the cooling time was 18 s for a water cooled die. The mechanical properties of 80% CA/ 20% PET blend are included in the next section for comparison with other blends of similar composition.

8.4 Mechanical Properties

Figures 8.2-8.5 show the strength at break, tensile modulus, elongation at break and Izod impact strength respectively for CA/EKX blends with and without catalysts and also for a CA/PET blend all containing 80% by weight of CA.

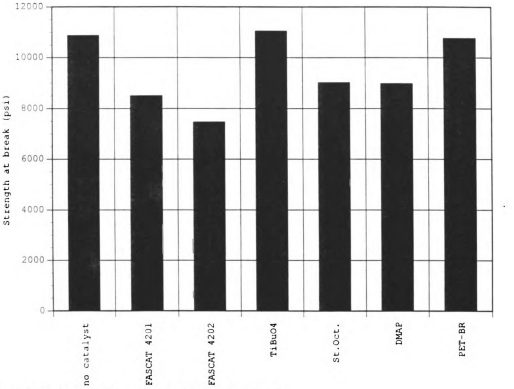

Figure 8.2: Strength at break for 80/20 blends.

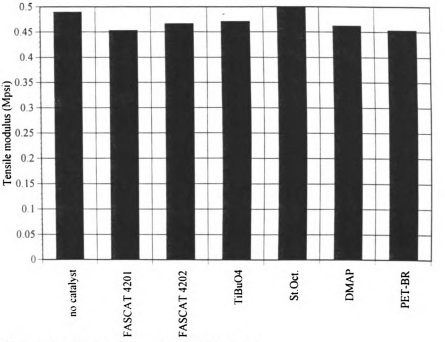

Figure 8.3: Tensile modulus for 80/20 blends.

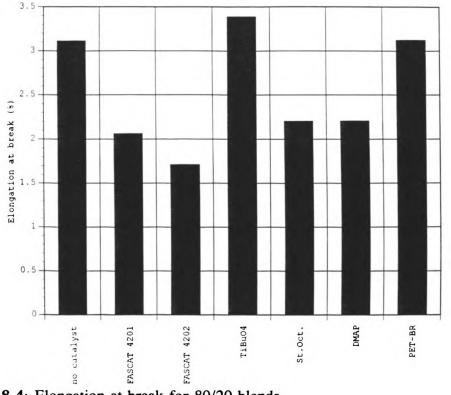

Figure 8.4: Elongation at break for 80/20 blends.

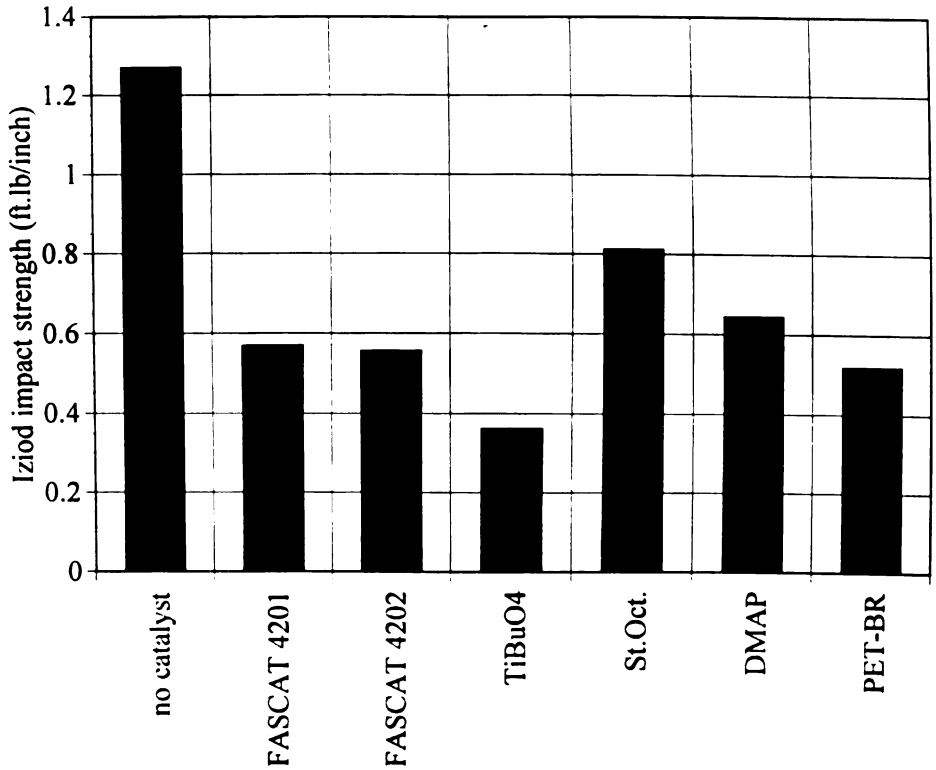

Figure 8.5: Izod impact strength of 80/20 blends.

8.5 Thermal Analysis

Figure 8.6 shows the glass transition temperatures of the 80/20 blends as measured by DSC and DMA. It is seen that there is not much change in T_g of CA phase, but there is a decrease in the T_g of EKX phase. This result would be expected as a result of tranesterification as the chains of EKX are being broken and grafted onto the CA backbone. If reduction in the T_g of EKX phase is taken as a measure of the extent of reaction, it is seen that the FASCAT catalysts and DMAP are more effective than the others. This also agrees with the extraction results where a decrease in weight percentage extracted was observed with the FASCAT catalysts and DMAP. Addition of Titanium

butoxide ($TiBuO_4$), however, causes little change in the T_g of EKX phase, while resulting in a large decrease in weight percentage extracted.

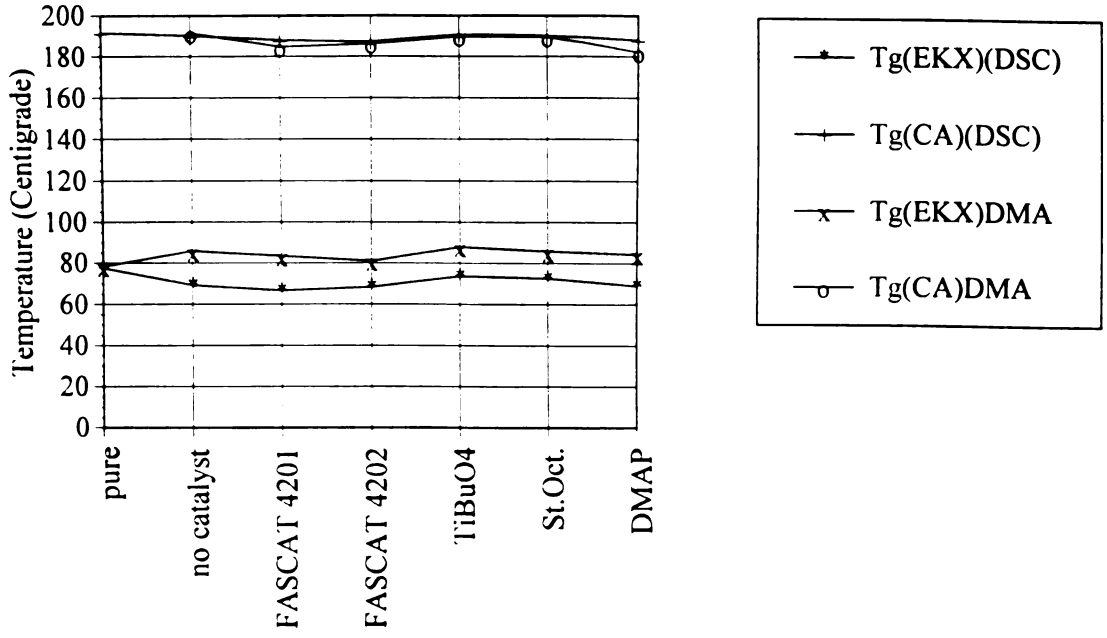

Figure 8.6: T_gs of 80/20 CA/EKX blends.

Figure 8.7 shows the melting points for the 80/20 compatibilized and uncompatibilized blends. There is hardly any change in the melting point, and obviously, this parameter cannot be used as an indication of the extent of the reaction. It seems that the grafted CA chains are not hindering or modifying the crystalline structure of EKX (it was concluded in Section 7.3 that CA phase was not crystallizing in the presence of EKX; see Figure 7.11).

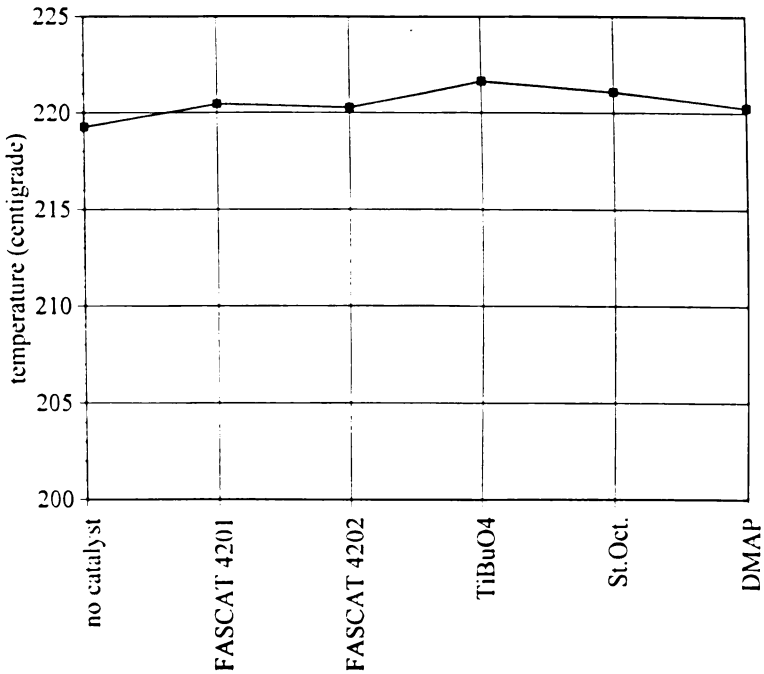

Figure 8.7: Melting points of 80/20 blends.

Figure 8.8 shows the enthalpy of melting of the 80/20 blends. It is seen that with except for blends containing $TiBuO_4$ or DMAP, the extent of crystallization actually increase as compared to that of pure EKX. This may be due to morphological reasons and due to increased orientation of the EKX molecules during extrusion. This effect of morphology will be discussed later.

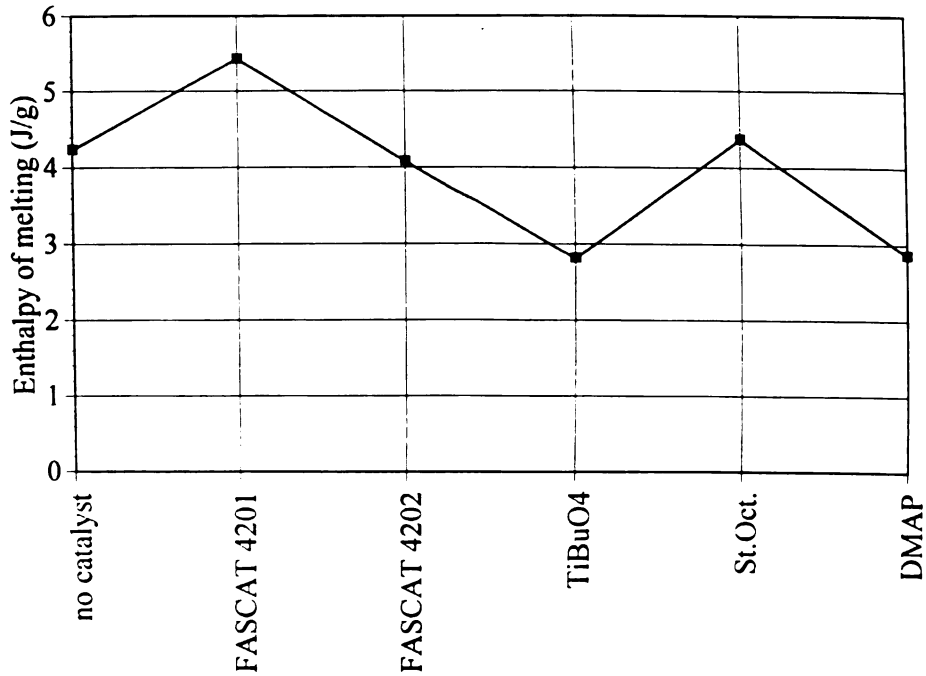

Figure 8.8: Enthalpy of melting of 80/20 CA/EKX blends.

8.6 Morphology

Figures 8.9 and Figure 8.10 show the twin screw extruded 80/20 CA/EKX blends without any catalyst to compare with the blends with catalysts. These are the same as Figure 7.19 and Figure 7.20 respectively. The EKX phase is elongated into fibers of diameter ~ 1 micron and quite homogeneously distributed.

Figures 8.11 and 8.12 show the morphology of 80/20 CA/EKX blend with 0.05% FASCAT 4201 catalyst. The dispersion and phase size of the EKX phase is the same as that without any catalyst. The morphology is still fibrillar.

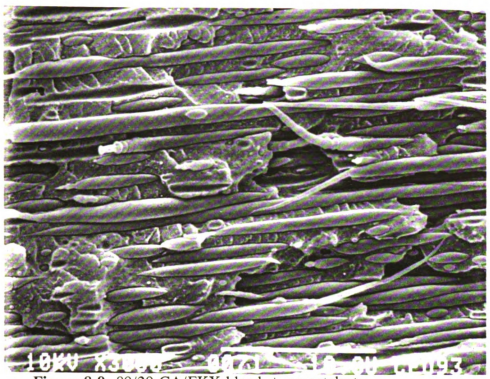

Figure 8.9: 80/20 CA/EKX blend + no catalyst;
Sectioning parallel to direction of flow.

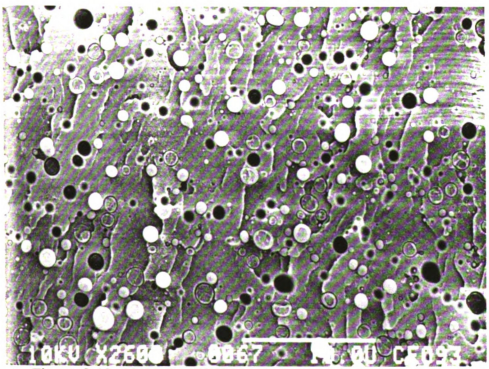

Figure 8.10: 80/20 CA/EKX blend + no catalyst;
Sectioning perpendicular to direction of flow.

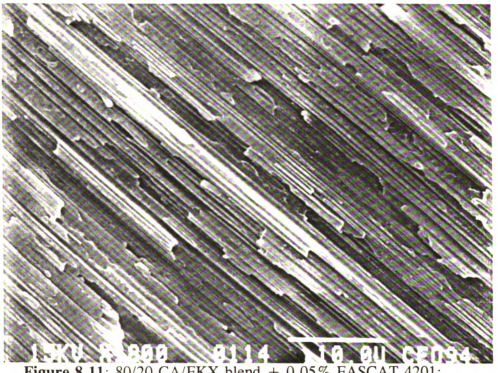

Figure 8.11: 80/20 CA/EKX blend + 0.05% FASCAT 4201; Sectioning parallel to direction of flow.

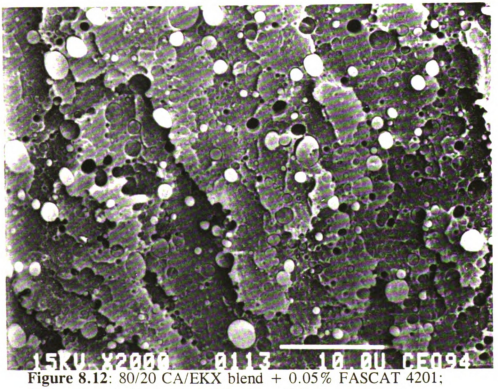

Figure 8.12: 80/20 CA/EKX blend + 0.05% FASCAT 4201; Sectioning perpendicular to direction of flow.

Figure 8.13 and Figure 8.14 show the SEM micrographs of 80/20 CA/EKX blends in which 0.2% by weight of FASCAT 4202 catalyst was added. It is seen in the longitudinal section that the particles are elongated but there are many small dispersed droplets visible. The transverse section shows that the EKX phase is now very well dispersed with a phase size of less than a micron (Compare Figure 8.14 with Figure 8.12 which are at the same magnification.

Figure 8.15 shows the transverse section of 80/20 CA/EKX blend with 0.05% of DMAP as catalyst. The dispersion is better as compared to the blend with no catalyst or that with FASCAT 4201. There was difficulty in pelletizing this blend and also there was color of the extrudate was dark brown. This is possibly due to the degradation of the catalyst itself and not due to the degradation of CA, as it is observed that the mechanical properties are not effected to a large extent. Also, the discoloration was reduced when the blend was dissolved in phenol to reprecipitate for extraction.

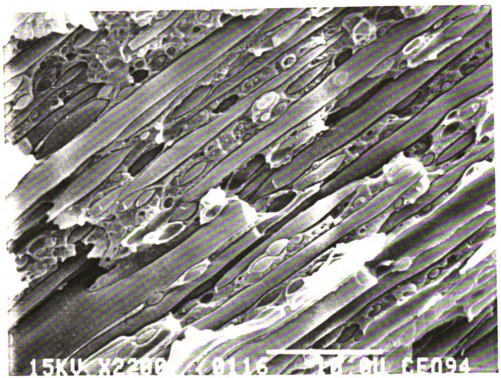

Figure 8.13: 80/20 CA/EKX blend + 0.2% FASCAT 4202; Sectioning parallel to direction of flow.

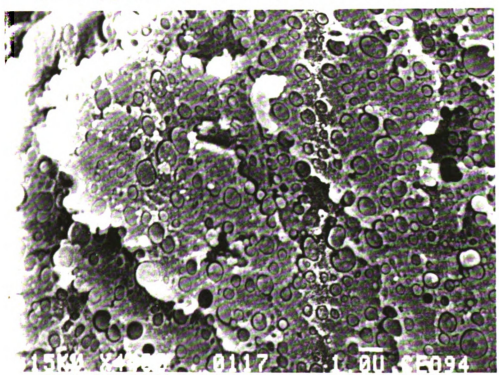

Figure 8.14: 80/20 CA/EKX blend + 0.2% FASCAT 4202; Sectioning perpendicular to direction of flow.

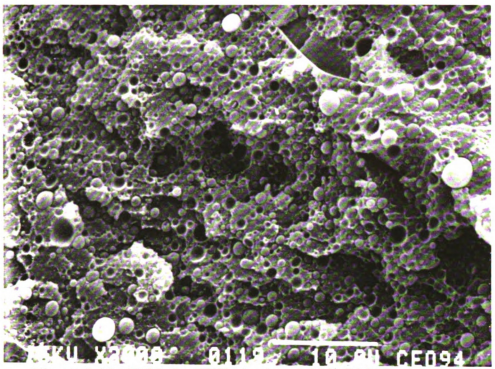

Figure 8.15: 80/20 CA/EKX blend + 0.05% DMAP
Sectioning perpendicular to direction of flow.

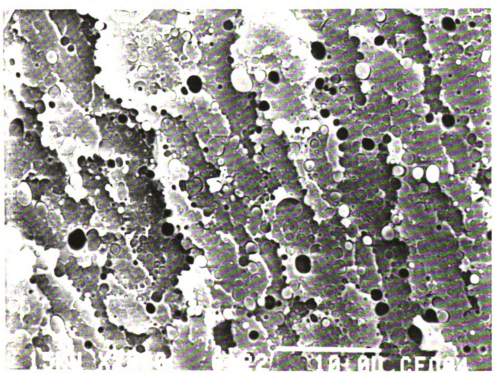

Figure 8.16: 80/20 CA/EKX blend + 0.05% Stannous Octoate
Sectioning perpendicular to direction of flow.

Figure 8.16 shows the transverse section of 80/20 CA/EKX blend with 0.05% of Stannous Octoate. The dispersion is the same as that for the blend with no catalyst. the particles have been elongated into fibers as can be seen in the longitudinal section (Figure 8.17). The thin white strands are an artifact due to improper fracture causing the pulling out of EKX fibers from the CA matrix.

Figure 8.18 shows the longitudinal section of 80/20 blend with 0.9% by weight of Titanium butoxide. The morphology has been completely changed. There are a large number of very fine particles of less than a micron size but also some elongated large particles with diameters of ~ 10 microns.

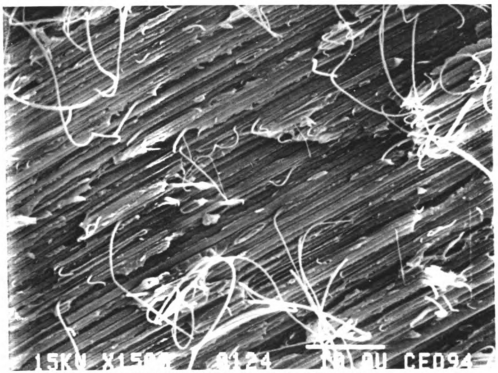

Figure 8.17: 80/20 CA/EKX blend + 0.05% Stannous Octoate; Sectioning parallel to direction of flow.

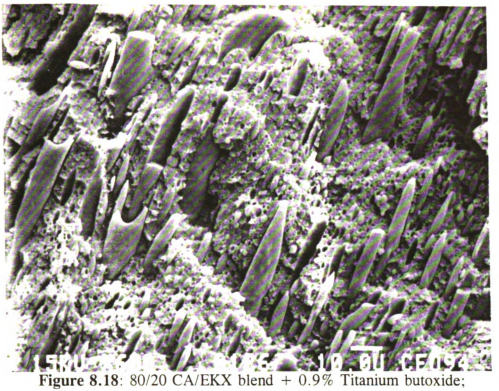

Figure 8.18: 80/20 CA/EKX blend + 0.9% Titanium butoxide; Sectioning parallel to direction of flow.

Figure 8.19 shows the transverse section of a 60% EKX/40% CA blend with 0.1% DMAP extruded three times in the microtruder. The catalyst was added in the first run. This micrograph clearly shows good adhesion between the two phases. The dispersed phase (CA) looks like it is coated with EKX and the fracture has not taken place along the interface.

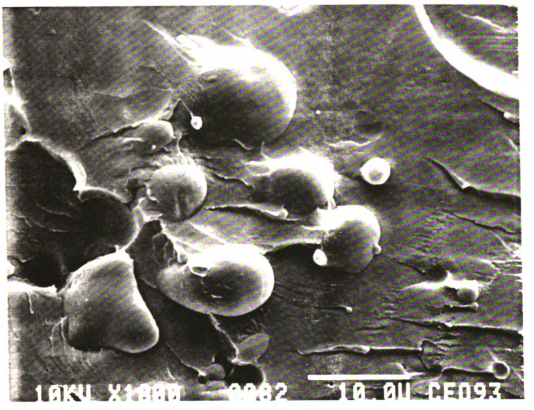

Figure 8.19: 40/60 CA/EKX blend + 0.1% DMAP; Microtruded three times. Transverse section.

8.7 Discussion

The extraction results coupled with thermal analysis and change in morphology and mechanical properties strongly suggests that a compatibilization reaction is occuring between the two phases. The FASCAT catalysts, DMAP and Titanium butoxide are seen to be effective as compatibilizing agents. It is interesting to study the relationship between the extent of compatibilization, morphology and properties of the blends (Figure 8.19).

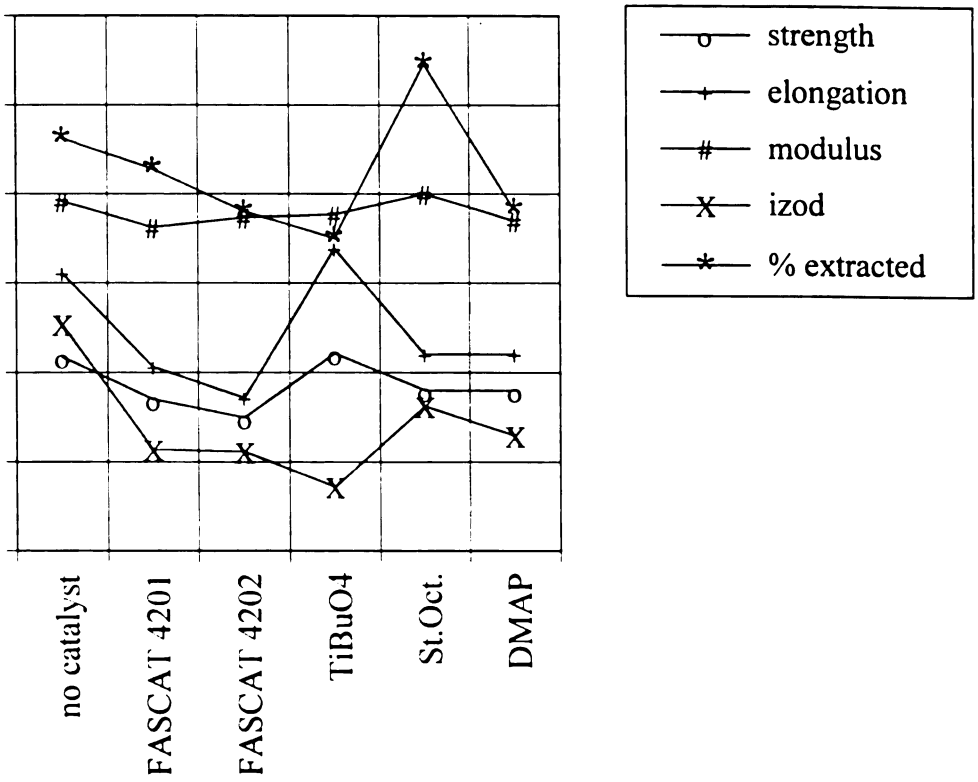

Figure 8.19: Variation of 80/20 CA/EKX blend properties.

Except for Stannous octaoate, all the rest of the catalysts effect the morphology. The phase size is seen to be reduced. This is very characterisitic of a compatibilizing reaction and similar results have been reported earlier [Tanaka, 1992; Willis, 1991; Gleinser, 1994, Xanthos, 1990]. The morphology is dictated by two driving forces - 1) unfavorable thermodynamics which drives the morphology towards phase separation and 2) the compatibilizing reaction which tends to reduce the interfacial tension and thus the tendency to phase separate. When the phase separation proceeds much faster than the chemical reaction, a domain structure is first formed, then the chemical reaction proceeds mainly on the domain surface and helps in compatibilizing the blend. On the other hand, when the chemical reaction is much faster than the phase separation, the reaction

proceeds homogeneously throughout the melt and a large concentration fluctuation is never established. As a distinct and much finely dispersed domain structure is seen, it is the former process which is occuring in CA/PET blends.

It is seen that reduction in the diameter of fibrils has an adverse effect on the properties of the blend. This suggests that fibre pull out and possible yielding of the EKX phase before failure are important energy absorbing mechanisms. When there is good adhesion between the two phases and the fiber diameter is $>$ 1 micron, only shear yielding can occur. The fiber is not pulled out and the crack proceeds to go through the fiber. This results in properties which are a little less than that which would be expected if both the energy absorbing mechanisms were occuring. This is the mode of fracture in the blend compatibilized with Stannous octoate. When there is good adhesion and the fiber is thinner and possibly crystallized due to orientation, both of the above two cannot take place and there is a large decrease in properties. This seems to be the mode of fracture of the blends compatibilized by FASCAT 4201, FASCAT 4202 and DMAP. The morphology of the blend compatibilized with Titanium butoxide is very different. Due to good adhesion (as indicated by extraction) and lack of long fibers, there is a large decrease in impact strength. But there are some thick fibers of about 10 micron diameter present. These are not contributing towards the energy absorption by fiber pull out but are absorbing energy during tensile elongation due to yielding. This results in an increase in elongation before failure and compensates for the energy not absorbed due to fiber pull out.

It can be concluded that fibers and particles less than 1 micron are not effective as crack inhibitors and cannot effectively absorb energy by yielding. Long fibers are effective only when they can be pulled out of the CA matrix. This requires sharp interface and poor adhesion. This is a very surprising result since generally much improvement in mechanical properties is observed with better adhesion. This also suggests that CA fails by crazing and particles smaller than a critical size ($\sim$ 1 micron) are not effective in either terminating or initiating crazes. For PVC the critical size is less than 0.1 micron and for PS, the critical size is about 1 micron. This suggests that the critical particle size for every individual polymer is different.

Morphology of CA/PET Blends

The morphology of CA/PET blends were studied as a function of volume ratio and viscosity ratio. A novel method was employed to vary the viscosity ratio. Standard curve of viscosity anf glass transition temperature were drawn as a function of plasticer content for the pure polymers. The equation of Kelly & Bueche was used for this purpose (see Section 6.6). The glass transition temperatures of the two phases in the blends were then used to calculate the viscosity and thus the viscosity ratio of the phases.

9.1 Background

Physical properties of immiscible polymer blends have been shown to be closely related to the size and shape of the deformable minor phase. Most investigations generally discuss phase morphology variations in terms of shear stresses, composition ratios, shear rate and effect of compatibilization. Very few papers are found in which the effect of viscosity ratio has been studied exclusively.

Starita [Starita,1972] studied the blend of five polystyrenes (of different molecular weights) and five polyethylenes (of different molecular weights) over a range of compostion ratios in an extruder. The type of microstructure in the blended systems were determined by solvent leaching, electron microscopy and DTA studies. He concluded that

when the ratio of viscosity of minor dispersed phase to the viscosity of matrix (p) is > 1, the minor component is coarsely dispersed. When this ratio is < 1 or ~ 1, the minor phase is finely dispersed. However in this paper, the effect of compatibilization on the phase morphology has not been studied.

Favis & Therrien [Favis, 1991] have done a similar study using Polycarbonate and Polypropylene of various molecular weights. It was found that proximity to the die wall also effected the morphology in the strands. The influence of viscosity ratio becomes more pronounced at higher composition. It was also found that over a wide range, the effect of screw speed and volumetric flow rate on the phase size was not significant (these parameters have more effect on highly elastc dispersed phases such as elastomers).

Min & White [Min, 1984] have studied PE (three molecular weights) and PS at two different temperatures and one of the PE with Nylon-6 and polycarbonate. The polarity of the phases was found to effect the morphology of the blends. It is concluded that when $0.7 < p < 1.7$, the droplets are elongated by the shear stress and form fibrils, increases in shear stress decreases the domain size of the dispersed phase and when $p > 2.2$, undeformed droplets are observed.

Willis et al [Willis, 1991] have studied the effect of compatibilization on PE/Polyamide and PE/PA blends. They blended three grades of each polymer but have not reported the effect of change in viscosity of the components. Their main conclusion is that the effect of interfacial modification on morphology predominates over that of composition and viscosity ratio. A narrowing of the region of dual phase continuity was observed due to the addition of the compatibilizer.

Tsebrenko et al [Tsebrenko, 1980] have investigated the formation of fibres in polyoxymethylene and a copolymer of ethylene and vinyl acetate. Here p varied from 0.35 to 27.7. Fibres are formed at viscosity ratios close to unity. Fibre formation is also governed by extrusion shear stress.

No paper can be found in which both the viscosity ratio and composition of the blend is varied and subsequently the effect of compatibilizer on the phase morphology is studied. The easiest way to vary the viscosity of the component(s) in the blend is to vary the molecular weight of the component. The effect of varying shear stress (RPM) or temperature in the extruder is difficult to characterize and moreover do not seem to influence the phase morphology much [Favis, 1991].

9.2 Experimental

To study the morphology of CA/EKX blends as a function of volume ratio and viscosity ratio, samples of Cellulose Acetate or EKX grade PET of different molecular weight could not be obtained. It was decided to follow a novel appraoch to vary the viscosity ratio. Diethyl pthalate was found to be miscible with both CA and EKX Moreover, diehyl pthalate is commercially the most popular plasticizer for CA. It was envisioned that when plasticized samples of CA were blended with EKX, the plasticizer would get redistributed in the two phases changing the viscosity of the two phases. The plasticizer would also change the glass transition temperature T_g of the phase . By measuring the T_gs of both the phases, it would be possible to calculate the volume

fraction of plasticizer present in the phase this would make calclation of the viscosity of the phase possible. This approach makes the assumption that both the phases are completely immiscible and there is no reaction between the two components.

The equation of Kelly and Bueche (section 6.6) was found suitable to model the variation in viscosity as a function of volume fraction of polymer. The variation of T_g with volume fraction polymer also follows from the same equation [Kelly, 1961]. Since, at T_g, the system is assumed to have reached a critical free volume fraction A = 0.025,

$$.025 = c[.025 + 4.8\ X\ 10^{-4}\ (T - T_g)] + (1 - c)[.025 + \alpha_s(T - T_g')] \qquad \textbf{(9.1)}$$

and since $T = T_g$ of the system:

$$T_g\ (system) = \frac{[4.8\ X\ 10^{-4} + \alpha_s(1 - c)T_g']}{[4.8\ X\ 10^{-4}c + \alpha_s(1 - c)]} \qquad \textbf{(9.2)}$$

Four blends of CA/DEP were obtained from Rotuba extruders (grades MS, MH, H and H2). Samples for viscosity measurement on the RMS were compression molded and the weight fraction of DEP was found out by TGA. Samples for DMA were also cut from the same compression molded slab and these were used to measure the T_gs of the blends. Blends of EKX with different amounts of DEP were extruded in a twin screw extruder and similar measurements were made on these also. The viscosity and T_g models were obtained by fitting the data to equations 6.30 and 9.2 respectively.

Blends of the plasticized CA were blended with EKX in different weight ratios. The morpholgy was studied with SEM and the T_gs were measured by DMA.

9.3 Results

Figure 9.1 shows the variation of $T_g$of CA as a function of volume fraction of CA.

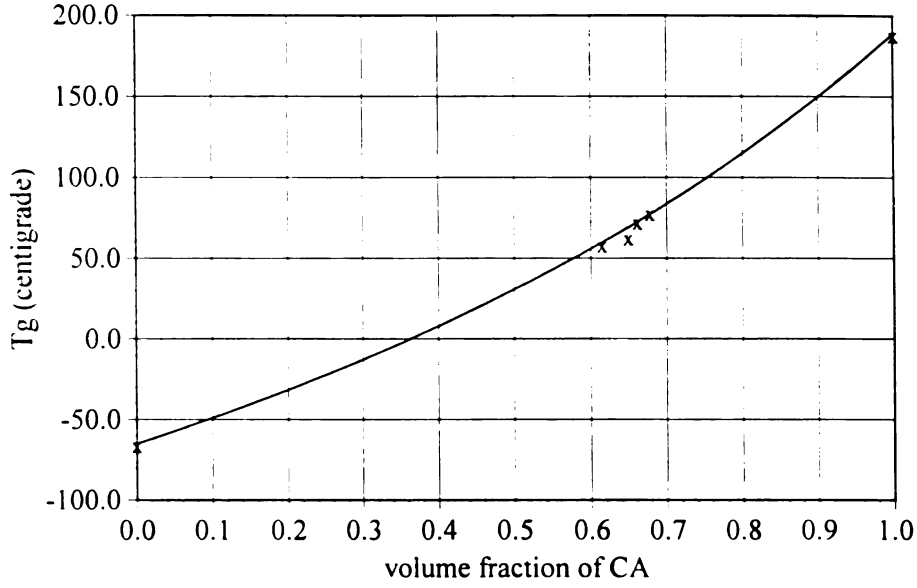

Figure 9.1: Estmation of T_g for CA/DEP blends.

The value of α_s used was 7.91 X 10^{-4}. Viscosity fit for CA is shown in Figures 6.9 and 6.10. Figure 9.2 shows the measured complex viscosities for six EKX/DEP blends (the polymer volume fractions are indicated on the figure). Figure 9.3 shows the Kelly and Bueche equation fitted to the viscosity data at 100 rad/s for EKX/DEP blends. The values of K and α_s used were 0.0374 and 0.001 respectively. Figure 9.4 shows the estimation of T_gs of the EKX/DEP blends as a function of EKX volume fraction. It seems that at more than 15% DEP, there is some phase seperation and so only the values for concentrated solutions were used to optimize the parameters.

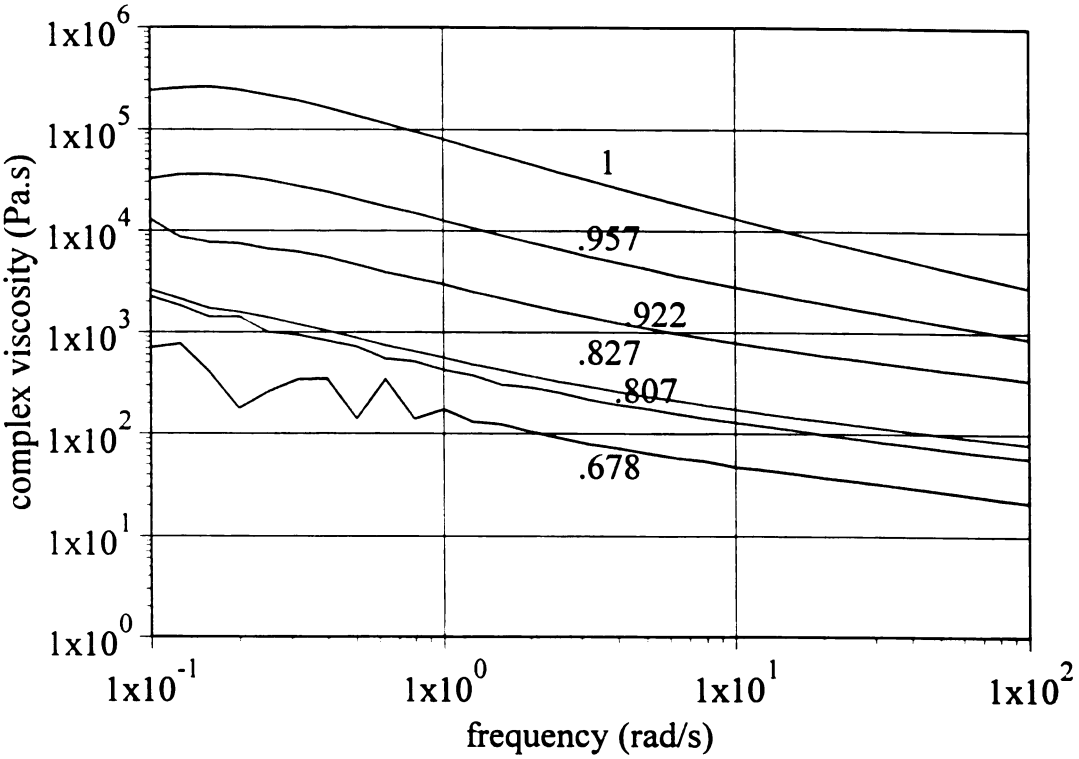

Figure 9.2: Viscosities of EKX/DEP blends.

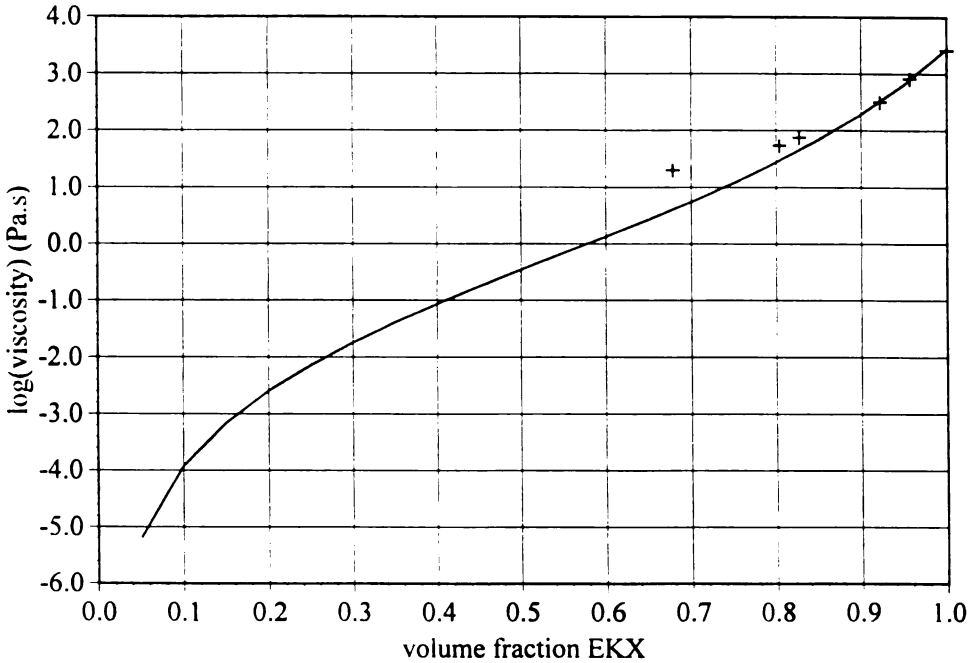

Figure 9.3: Estimation of viscosity for EKX/DEP blend.

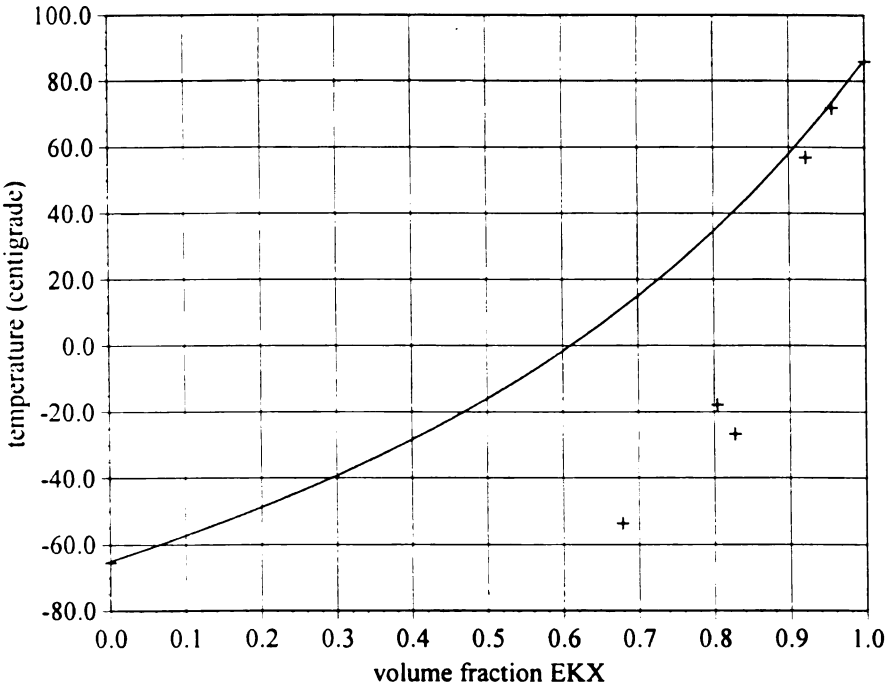

Figure 9.4: Estimation of T_gs for the EKX/DEP blends.

With the help of these equations it was thus possible to calculate the viscosity of each phase if the glass transition temperature of the phase was known. Subsequently eight blends of CA/EKX/DEP were extruded (ratios by weight)

CA(MS)/ EKX blends -30/70, 40/60 and 50/50.

CA(H)/EKX blends - 30/70 and 40/60.

CA(H2)/EKX blends- 30/70, 40/60 and 50/50.

Figure 9.5 shows the T_gs of the CA/DEP phase and the EKX/DEP phase for these blends as measured by DMA. These values of T_g were now used to calculate the volume fraction DEP and the viscosity of the two phases and thus the volume and viscosity ratio. The estimated viscosity values for 100 rad/s were used for this purpose.

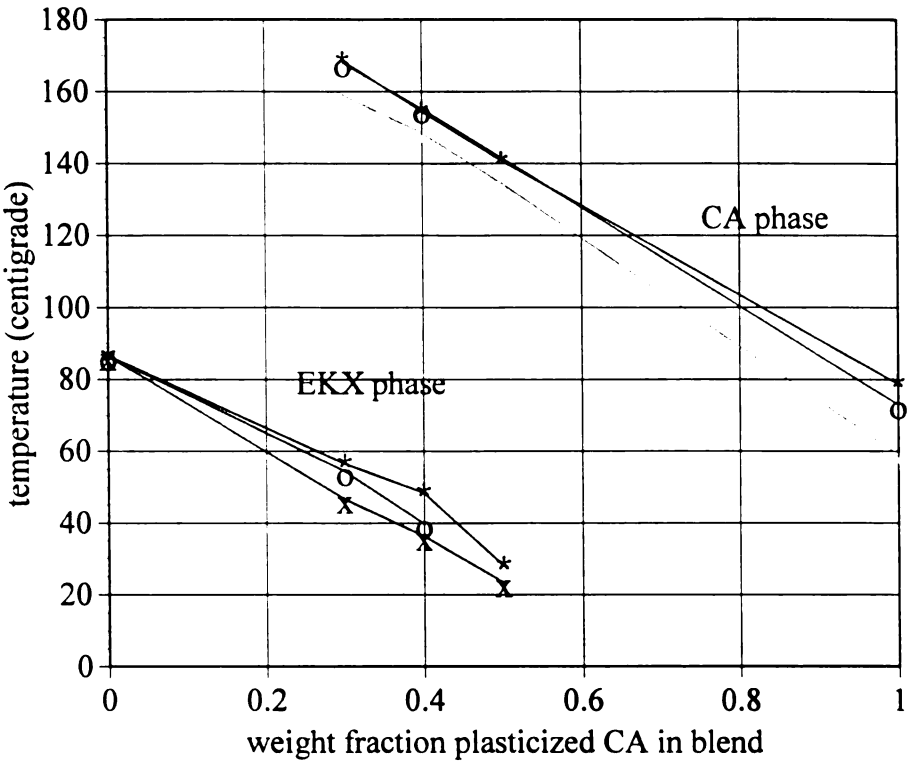

Figure 9.5: T_gs of the two phases in the EKX/CA+DEP blends; "*" EKX/CA(H2) blends; "o"EKX/CA(H) blends; "x" EKX/CA(MS) blends.

Table 9.1 shows the values calculated for the EKX/plasticized CA blends using the estimated viscosities at 100 rad/s. The addition of DEP to the blend changes the viscosity ratio by an order of two but unfortunately viscosity ratios ~ 1 are not obtained. Also, in the blends in which DEP volume fraction is more than 15%, there may be some phase seperation in which case, that T_g readings and the estimated viscosities would not be dependable. Due to these reasons and unavailablity of more plasticized CA samples, more blends were not made.

Table 9.1: Calculated vis

Table 9.1: Calculated viscosity ratios for plasticized CA/EKX blends.

Blend No.	grade of CA used	weight fraction in blend	T_g of CA/DEP phase	T_g of EKX/DEP phase	Viscosity of CA/DEP phase	Viscosity of EKX/DEP phase	Viscosity ratio
1	pure CA	.3, .4 or .5	189.0	86.5	8.77E+9	2.80E+3	3.13E+6
2	H2	.3	168.5	56.44	3.61E+7	1.72E+2	2.11E+5
3	H2	.4	154.5	48.43	2.27E+6	8.66E+2	2.61E+4
4	H2	.5	140.7	28.0	2.44E+5	1.61E+1	1.52E+4
5	H	.3	168.0	54.45	3.24E+7	1.45E+2	2.24E+5
6	H	.4	155.2	39.86	2.57E+6	4.24E+1	6.05E+4
7	MS	.3	159.0	46.59	5.17E+6	7.42E+1	6.97E+4
8	MS	.4	148.4	36.29	8.58E+5	3.16E+1	2.71E+4
9	MS	.5	134.3	23.27	9.88E+4	1.09E+1	9.04E+3

Figure 9.6 shows the transverse section of blend 5 and Figure 9.7 shows the transverse section of blend 9. In these two blends and blend numbers 1, 2, 3, 6, 7 and 8, the CA phase is dispersed in the EKX matrix in the form of spherical particles. The change in viscosity ratio has apparently had not much effect on the distribution or the domain size of CA phase. However, in blend 4, the two phases are co-continuous (Figure 9.8) as opposed to dispersed CA morphology for blend 1(Figure 7.15).

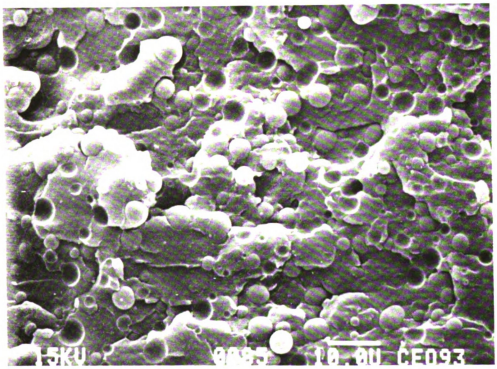

Figure 9.6: 30/70 CA(H)/EKX blend; 1000X
Sectioning perpendicular to direction of flow.

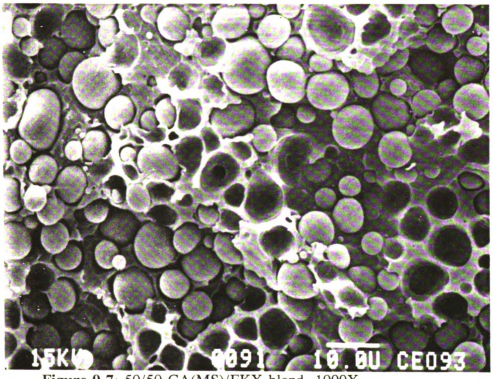

Figure 9.7: 50/50 CA(MS)/EKX blend. 1000X
Sectioning perpendicular to direction of flow.

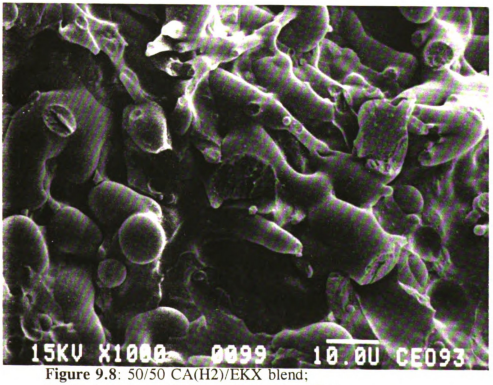

Figure 9.8: 50/50 CA(H2)/EKX blend;
Sectioning perpendicular to direction of flow.

Conclusions and Recommendations

10.1 Extrusion

Cellulose Acetate has a high shear viscosity, of the order of 10^{11} Pa.s as estimated in Chapter 6. The extent of degradation of CA was observed to be highly dependent on the amount of shear. There was considerably less degradation even at high temperatures in the Micsrotruder. Therefore, high shear rates and long residence times should be avoided while extruding CA. The self-wiping twin screws configuration elimainates stagnant zones where degradation could occur. The mixing elements impart high shear to the melt and so only as many as that required for good dispersion should be used. Twin screw extruders can be designed for very little axial mixing by using either very low helix angle screws or straight segments which impose no axial forwarding. The straight segments have the advantages of greater free path for vapor evolution, and of increased surface generation without proportionate reduction in residence times [Todd, 1975]. To enhance mixing and avoid product overheating, the application of successive kneading zones is feasible in short axial length due to excellent pressure generating capability of the screw elements [Eise, 1983].

PET bottle recycle was found to crystallize faster than even virgin PET, perhaps due to impurities present in it (Section 7.3). To extrude blends with high PET content,

it is necessary to avoid any cold spots in the die and barrel where PET could start to crystallize. PET could also crystallize due to the orientation of molecules and this may be fascilated by elongationaal flow in the barrel or die. Blends of CA/PET-bottle recycle were successfully extruded without the use of the die which used to clog due to crystallization of PET. The use of higher temperatures in the die resulted in low melt strength. Extrusion of PET bottle recycle was easier with a higher content of CA as the CA matrix helped to transport the dispersed PET phase.

Another method that could prove feasable is the use of an extruder with two feed ports. The PET could be fed from the first port along with some CA and melted at higher temperatures. The rest of the CA could be added downstream where the temperature would be lower. This setup could possibly reduce the thermal degradation of CA.

10.2 Trans-esterification

The use of trans-estrification reaction to compatibilize CA/PET or CA/EKX blends has been shon to be a simple and effective method with the use of reactive extrusion. The reaction is intrinsically difficult to characterize due to the lack of formation of any new types of functional groups which could be easily detected by techniques such as FTIR spectroscopy. Recourse had to be taked to indirect methods to characterize the reaction. Soxhlet extraction of the CA phase with Acetone was found more sensitive to the reaction, since the reaction involves species of high molecular

weights and so a relatively small extent of reaction translates as a much greater change in the weight of CA that could be extracted. The amount of PET chains in the extracted phase was still an unknown and this could be found out by FTIR spectroscopy (if the amount of PET is greater than the senstivity of the instrument) or CHN analysis. Another way to do this would be to destroy the CA backbone by acid hydrolysis and titrating for the amount of glucose units formed.

Scanning Electron Microscopy also provided strong evidence of transesterification. Due to compatibilization, the particle size of the dispersed PET phase is seen to be reduced. An increase in adhesion between the two phases is seen in Figure 8.19 where the sample was extruded three times with a catalyst.

10.3 CA/EKX blends

CA blends could be easily extruded with a glycol modified grade of PET called Transpet EKX-105 (supplied by Hoechst Celanese). EKX had a low degree of crystallinity and a melting point nearer to that of CA, so higher temperatures were not necessary during processing.

Thermal analysis of CA/EKX blends, both compatibilized and uncompatibilized, showed no evidence of miscibility. The mechanical properties of the blends were found to be highly dependent on morphology of the blends. Dispersed particles of EKX in CA, helped in increasing the impact strength of the blend. By analyzing the morphology-property dependence of compatibilized blends, it was concluded that the critical size of

EKX particles necerssary to impart impact toughening was ~ 1 micron (section 8.7). A dispersed phase elongated into fibrils helped to increase the tensile properties of the blends. Blends with intermediate compositions gave a large dispersed phase particle size or a co-continous morphology. Both of these had an inverse effect on the mechanical properties (Figures 7.4-7.8). The tensile properties of uncompatibilized CA/EKX blend were found to agree with those predicted by models. This could be due to the presence of transesterification catalysts present in EKX or due to hyrogen bonding between CA and EKX. Further compatibilization by adding more catalysts had an adverse effect on mechanical properties. It was concluded that pull-out of EKX fibrils was an important energy absorbing mechanism and is thus a desirable morphology for CA/EKX blends. Addition of plasticier should increase the impact strength and make processing easier.

10.4 Plasticized CA/EKX blends

Diethyl pthalate was found to be compatible with both CA and EKX (Chapter 9). DEP was redistributed in the two phases lowering the T_g and the viscosity of the two phases. However, the change in the viscosity ratio was not much and thus this teqnique could not be used to study the dependence of morphology on viscosity and volume ratios. Addition of 25 % by weight of DEP to the EKX reduces the T_g to room temperature and this phase dispersed in CA could increase the impact strength.

A plasticizer more compatible with CA and relatively incompatible with PET (or EKX) would decrease the viscosity of CA only. This would change the viscosity ratio

and could make the technique used in Chapter 9 more useful in studying the morphology of CA/PET blends. On the other hand, a plasticizer for EKX, which is incompatible with CA would reduce the T_g of EKX phase only. This would provide impact toughening to the blend without sacrificing properties such as modulus, strength and service temperature.

10.5 Achievements and Prospects

The excellent properties of CA/PET blends places them in the category of "engineering grade resins" like nylons, ABS, PMMA etc. Significant improvement in properties such as tensile modulus and strength has been achieved by elimination of the use of plasticizers such as DEP. However, due to blending with another polymer, the transparency and impact strength asssociated with plasticized CA have been lost. The impact strength of CA/PET blends could be improved by addition of plasticizers or a toughening rubbery phase (like rubber modified PS, Polybutyl acrylate modified PMMA). Such an impact modified grade of CA/PET blend could have hugh commercial possibilities.

It has been demonstrated that recycled bottle grade PET can be utilized to prepare an engineering grade material when blended with CA. Since CA itself is made from Cellulose, a renewable natural resource and is possible biodegradable, this blend can also be termed as "environment friendly".

Currently CA is an underutilized polymer with limited uses when plasticized with DEP. It is also facing increasing competition from styrenic polymers which are cheaper. It is thus an oppurtune time to find new uses for CA. Also, recycled PET is much cheaper than either glycol modified PET or virgin PET. These factors and the ease of blending and compatibilizing CA/PET blends would make them commercially attractive alternative to both suppliers of raw materials and compounders.

CA/PET blends could be potential alternatives to nylons in structural applications, in household articled such as haircombs, in extrusion operations where the low melt viscosity of nylons is a disadvantage and in applications where the lower cost of CA/PET blends would compensate for any loss in propereties.

Glass filled Polyphenyl sulphide articles such as molded bulb sockets, motor housings, switch components are also potential uses for CA/PET blends due to the high cost of PPS.

Due to better processibility and heat distortion temperature, another possible application could be in tiles and laminates where PMMA and epoxy are currently used.

CA/PET could compete with currently available cellulosics (CA, CAB and CAP, all use monomeric plasticizers) in applications where transparency is not of importance and greater dimensional stability and heat resistance is required. Potential uses include tool handles, safety goggles, steering wheels, tabulator keys, and telephone housings.

BIBLIOGRAPHY

Bibliography

- Ahroni, S. M., *J. Macromol. Sci. (B)*, **22**, 813 (1983).
- Allen, G. et al, *Polymer*, **15**, 28 (1974).
- Berry, G. C. and Fox T. G., *Adv Polymer Sci.*,**5**, 261 (1968).
- Berry, G. C. V. C. Long, and L. M. Hobbs, *Polymer*, **5**, 31 (1964).
- Bikales, N. M. and L. Segal, eds., ***Cellulose and Celulose derivatives***, Wiley Interscience, NY, 1971, Part IV, page 151.
- Brandrup, J., and E. H. Immergut, eds., ***Polymer Handbook***, Third ed., Wiley-Interscience, New York (1989).
- Brydson, J. A., ***Plastic Materials -5th edition***, Butterworths, London (1989).
- Bueche, F., *J. Appl. Phys.*, **24**, 423 (1953).
- Bueche, F., *J. Appl. Phys.*, **26**, 738 (1955).
- Bueche, F. J., *J Chem. Phys.*, **25**, 599 (1956).
- Bueche, F., *J. Appl. Phys.*, **30**, 1114 (1959).
- Burke, J. J. and Weiss V., ed., ***Characterisation of Materials in Research***, Syracuse Univ. Press, Syracuse (1975).
- Burkhardte, K. H. Hermann, and S. Jakopin, *SPE ANTEC Tech. Papers*, **36**, 498 (1978).
- Chaffey, C. E. et al, *Rheol. Acta*, **4**, 56 (1965).

- Cheung, P. D. Suwanda and S. T. Balke, *Polymer Engg. and Sci.*, **30** (17), 103 (1990).
- Chia, L. and Ricketts S., ***Basic Techniques and Experiments in Infrared and FT-IR Spectroscopy***, Perkin Elmer publication 0993-8420, March 1988.
- Cohen, M. H., and D. Turnbull, *J. Chem. Phys.*, **31**, 1164 (1959).
- C. van der Poel, *Rheol Acta*, **1**, 198 (1958).
- Davies, W. E. A., *J. Appl.Phys.*, **4**, 1176 (1971).
- Dickie, R. A. in ***Polymer Blends Vol. 1***, Academic press, 1978, Chapter 8.
- Doolitle, A. K., *J. Appl. Phys.*, **22**, 1471 (1951).
- Eise, K., J. Curry, and J. F. Nangeroni, *Polym. Eng. Sci.*, **23**, 642 (1983).
- Elemndorf, J. J. and A. K. van der Vegt, in ***Progress in Polymer Processing, Vol 2,*** Utracki, L. A., ed., (1991).
- Escala, A. and R. S. Stein, *Adv. Chem. Ser.*, 176 (1979).
- Favis, B. D. and D. Therrien, *Polymer*, **32**, 8, 1474 (1991).
- Fixman, M. and J. M. Peterson., *J. Am. Chem. Soc.*, **86**, 3524 (1964).
- Fox, T. G. and Allen V. R., *Polymer*, **3**, 111 (1962).
- Fox, T. G. and Allen V. R., *J. Chem Phy.*,**41**, 344 (1964).
- Fujita, H. and Kushimoto A., *J. of Chemical Physics*, **34** (2), 393 (1961).
- Gauthier F. et al., *Tran. Soc. Rheol.*, **15**, 297 (1971).
- Gleinser, W., et al, *Polymer*, **35**, 128 (1994).
- Goldsmith, H. L. and S. G.Mason, *J. Colloid Sci.*, **17**, 448 (1962).
- Graessley, W.W., ***Viscoelasticity and flow in Polymer Melts and Concentrated Solutions,*** American Chemical Society, 1984.
- Han, C. D., ***Multiphase flow in Polymer Processing***, Academic Press, New York (1981).

- Hanrahan, B. D., S. R. Angeli, and J. Runt, *Polym. Bull.*, **15**, 455 (1986).
- Hashin, Z. *J. Appl. Mech.*, **29**, 143 (1962).
- Hashin, Z., and S. Shtrikman, *J. Mech. Phys. Solids*, **11**, 127 (1963).
- Hetsroni G et al., ***Progess in Heat and Mass Transfer***, G Hestroni, S. Sideman, and J. P. Hartnett, eds., Vol. 6, p 591, Pergamon, London (1972).
- Hill, R., *J. Mech. Phys. Solids*, **11**, 357, (1963).
- Hirschfeld, T. B., *Anal. Chem.*, **48**, 721 (1976).
- Hyun, M. E., and S. C. Kim, *Polymer Engg. and Sci.*, **28** (11), 743 (1988).
- Johnson, M.F., W. W. Evans, I. Jordan, and J. D. Ferry, *J. Coll. Sci.*, **7**, 498 (1952).
- Kelly, F. N. and F. Bueche, *J Polmer Sci.*,**50**, 549 (1961).
- Kerner, E. H. , *Proc. Phys. Soc. Lond.* (B), **69**, 808 (1956).
- Kirk-Othmer (eds.), ***Encyclopeia of Chemical tehnology, Third Ed.***, Wiley Interscience, New York, **23** (1983).
- Kodama, M., *Polym. Engg.Sci.*, **33** (17), 1141 (1993).
- Koenig, J. L. et al, *Appl. Spectrosc.*, **.31**, 292 (1977).
- Koenig, J. L., *Adv. Polym. Sci.*, **54**, 101 (1983).
- Kraus G. and J. T. Gruver, *J Polmer Sci.*,**A2**, 797 (1964).
- Kuleznev V. N. et al., *European Pol. J.*, **14**, 455-461 (1978).
- Lee W. K., Ph. D. Thesis (Chem. Eng.), Univ. of Houston, Houston, Texas, (1972).
- Lodge, A. S., *Rheologica Acta*, **2**, 158 (1958).
- Lyons, P. F., and A. V. Tobolsky, Polym. Eng. Sci., 10, 1 (1970).
- Markowitz, H., and D. R. Brown, *Trans. Soc. Rheol.*, **7**, 125 (1963).

- Michigan Dept. of Nat. Res., *Statewide Market Study for Recyclable Plastics*, Feb. (1987).
- Min K. et al, *Pol. Engg. Sci.*, **24** (17), 1327 (1984).
- Modern Plastics Encylopedia '90, McGraw Hill (1990).
- Nadkarni, V. M., and J. P. Jog, ***Handbook of Polymer Science and Technology Vol.4,*** ed. N. P. Cheremisinoff, Marcel Dekker, Inc., New York, (1989).
- Nadkarni, V. M., and J. P. Jog, *Polym. Eng. Sci.*, **27**, 451 (1987).
- Narayan, Ramani, ***Rationale and Design of Environmentally Degradable Plastics: Recycling back to nature***, 83rd Annual Meeting, Air and Waste Management Asso., Pittsburgh, Pennsylvania, June 24-29 (1990).
- Narayan Ramani, in ASC Symposium Series 476, 1 (1991).
- Nassar, T. R., D. R. Paul and J. W. Barlow, *J. Appl. Polym. Sci.*,**23**, 85 (1979).
- Nichols, Kevin, PhD. thesis, Department of Chemical Engineering, Michigan State University (1991).
- Nielson, L. E., ***Mechanical Properties of Polymers and Composites Vol. 1,*** Marcel Dekker Inc., New York (1974).
- Paul, B., *Trans. AIME*, **218**, 36 (1960).
- Paul, D. R., and Newman S., eds., ***Polymer Blends Vol.1***, Academic Press, New York (1978).
- Paul, D. R., and Newman S., eds., ***Polymer Blends Vol.2***, Academic Press, New York (1978).
- Peterlin, A., *J. Polymer Sci.*, **12**, 45 (1954).
- Peticolas, W. L., *Rubber Chem. Technol.*, **36**, 1422 (1963).
- Porter, R. S., and J. F. Johnson, *Chem Rev.*, **66**, 1 (1966)
- Pryzgocki, W and A. Wlochowicz, *J Appl. Polym. Sci.*, **19**, 2683 (1975).
- ***Recycling Sourcebook***, Thomas J Cickonski and Karen Hill, eds., Gale Research Inc., Detroit (1993).

- Ryan, A. J., J. L. Stanford and R. H. Still, *Polymer*, 32 (8), 1426 (1991).
- Rumscheidt, F. D., and S. G. Mason, *J. Colloid Sci.*, **16**, 238 (1961).
- Sakellarides, S. L., and A. J. McHugh, *Polym. Engg. Sci.*, **27** (22), 1662 (1987).
- Sheridan, L. A., *Chem. Eng. Progress*, **71** (2) (1975).
- Shingankuli, V. L., J. P. Jog, and V. M. Nadkarni (submitted).
- Simha, R. and J. L. Zakin, *J. Chem. Phys.*, **33,** 1791 (1960).
- Simha, R. and J. L. Zakin., *J. Colloid Sci.*, **17**, 270 (1962).
- Starita, J. M., *Trans. Soc. Rheol.*, **16** (2), 339 (1972).
- Starkweather, H. W. Jr, ***Polymer Compatibility and Incompatibility***, ed. Karel Solc, Harwood Academic Publ., Chur (1982).
- Tanaka, H., *Macromolecules*, **25**, 4453 (1992).
- Tavgac, T., Ph. D. Thesis (Chem. Eng.), Univ. of Houston, Houston, Texas (1972).
- Taylor, G. I., *Proc. R. Soc. Lon, Ser. A*, **146**, 501 (1934).
- Todd, D. B., *Chem. Eng. Progress*, **71** (2), 81 (1975).
- Torza, S. et al., *J. Colloid Interface Sci.*, **38**, 395 (1972).
- Tsebrenko, M. V., M. Rezanova, and G. V. Vinogrodov., *Polym. Engg. Sci.*, **20** (15), 1023 (1980).
- Tucker, C. S., in *Plastics Engg.*, pg 27-30, May (1987).
- Utracki, L. A., and M. R. Kamal, *Polym. Eng. Sci.*, **22**, 96 (1982).
- Utracki, L. A., *Polym. Eng. Sci.*, **23**, 602 (1983).
- Utracki, L. A., *J. Rheol.*, **35**, 1615 (1991).
- Utracki, L. and Simha R., *J. Polymer Sci.*, **A1**, 1089 (1963).
- Van der Vegt, A. K., and P. P. A. Smit, *S. C. I. Monograph*, **26**, 313 (1967).

- Van Oene, H., *J. Colloid Interface Sci.*, **40**, 448 (1972).
- Vinogradov, G. V. et al, *Int. J. Polym. Metals*, **3**, 99, 1974.
- Wilfong, D. L. et al, *J. Mater. Sci.*, **21**, 2014 (1986).
- Williams, M. L., R. F. Landel, and J. D. Ferry, *J. Am. Chem. Soc.*, **77**, 3701 (1955).
- Willis, J. M. et al, *J. Mat. Sci.*, **26**, 4742 (1991).
- Wood, L. A., in ***Synthetic Rubber***, G. S. Whitby, ed., John Wiley and Sons, New York (1954).
- Wu, S., ***Polymer Blends Vol. 1***, Academic press, p. 243 (1978).
- Wu, S., *Polym Eng. Sci.*, **27**, 335 (1987).
- Xanthos M., M. W. Young, and J. A. Biesenberger, *Polym. Eng. Sci.*, **30**, 355 (1990).